MoDOT

Research, Development and Technology

University of Missouri-Rolla

RDT 03-002

Automated Pavement Analysis in Missouri Using Ground Penetrating Radar

RI 98-002
RI 98-002B

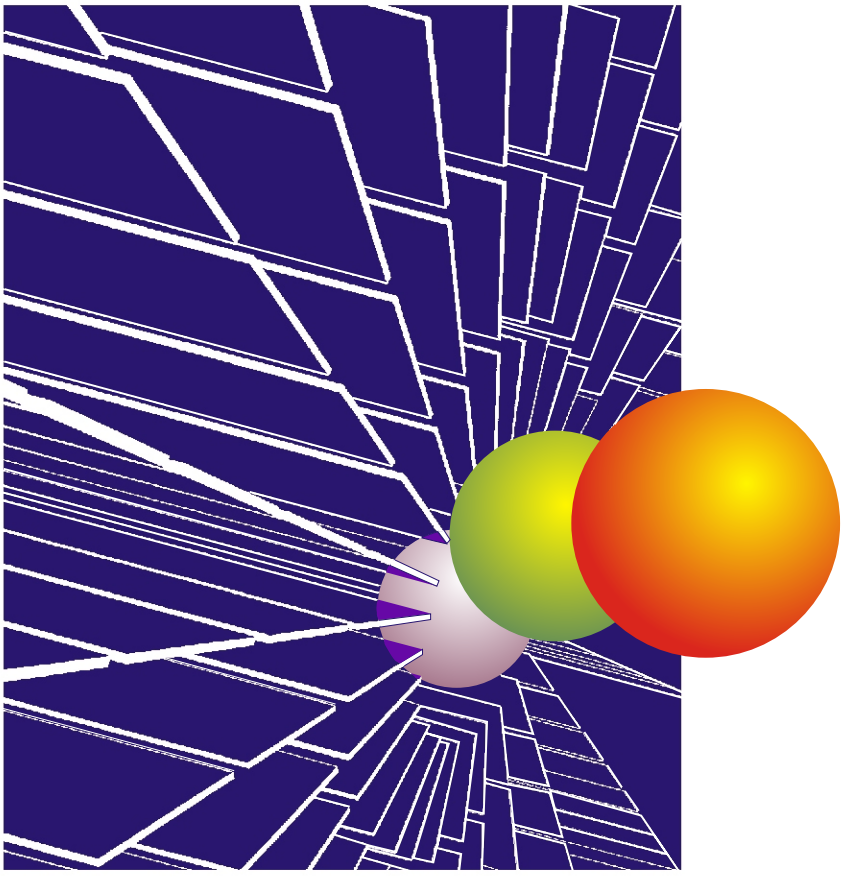

February, 2003

TECHNICAL REPORT DOCUMENTATION PAGE

1. Report No. RDT03-002	2. Government Accession No.	3. Recipient's Catalog No.
4. Title and Subtitle **Automated Pavement Analysis In Missouri Using Ground Penetrating Radar**		5. Report Date February, 2003 6. Performing Organization Code
7. Author(s) Steve Cardimona, Brent Willeford, Doyle Webb, Shane Hickman, John Wenzlick, Neil Anderson		8. Performing Organization Report No. RI98-002 & RI98-002B
9. Performing Organization Name and Address University of Missouri – Rolla Department of Geology and Geophysics, B-43 McNutt Hall 1870 Miner Circle, Rolla, MO 65409-0410		10. Work Unit No. 11. Contract or Grant No.
12. Sponsoring Agency Name and Address Missouri Department of Transportation Research, Development and Technology P. O. Box 270-Jefferson City, MO 65102		13. Type of Report and Period Covered Final Report 14. Sponsoring Agency Code

15. Supplementary Notes
The investigation was conducted in cooperation with the U. S. Department of Transportation, Federal Highway Administration.

16. Abstract

Current geotechnical procedures for monitoring the condition of roadways are time consuming and can be disruptive to traffic, often requiring extensive invasive procedures (e.g., coring). Ground penetrating radar (GPR) technology offers a methodology to perform detailed condition assessment of existing roadways, with the added advantage over other techniques of being rapid and cost-effective. This project and report were split into four different sections based on the type of roadway being surveyed.

The first section presents the results of a GPR survey over portions of Interstate 44 near Springfield, Missouri. The goal of this survey was to evaluate concrete pavement layer thickness and continuity within the specific study regions. The second section applies GPR techniques to a survey along Interstate 70 across the state of Missouri. Goals of this survey were threefold: 1) determine layer thicknesses every tenth mile; 2) update history information related to types of pavements that make up I70 across Missouri; and 3) note regions where the radar signal appears anomalous. The third section applies GPR techniques to 35 test pavements of the Strategic Highways Research Program LTTP sites across the state of Missouri. The result is a correlation of GPR reflection character and GPR-derived layer thickness estimates with design information for each test pavement. In the last section of the report, GPR surveys were performed over 42 miles of secondary highways to determine the thickness of the asphalt pavement and also to determine if indications of potential maintenance problem areas could be identified.

Asphalt surface layering proved to be the easiest to image, creating a strong signal in the GPR data. Not as consistently clear is the concrete-to-baserock interface where the dielectric contrast between these two media is not always strong enough to create a high amplitude reflected signal. It was also determined by correlation of GPR data and coring that anomalous areas could be characterized, especially to recognize pavement where the asphaltic cement was stripping from the aggregate

17. Key Words Ground Penetrating Radar, pavement, thickness, stripping	18. Distribution Statement No restrictions. This document is available to the public through National Technical Information Center, Springfield, Virginia 22161

19. Security Classification (of this report) Unclassified	20. Security Classification (of this page) Unclassified	21. No. of Pages 157 w/o Addendum	22. Price

Form DOT F 1700.7 (06/98)

Final Report

RI98-002

Automated Pavement Analysis in Missouri Utilizing Ground Penetrating Radar

Steve Cardimona[*], Brent Willeford[*], Doyle Webb[*], John Wenzlick[+], Neil Anderson[*]

[*]The University of Missouri-Rolla, Department of Geology and Geophysics

[+]The Missouri Department of Transportation

And

RI98-002B

Automated Pavement Analysis of Collector Routes Using Ground Penetrating Radar

BY: Steve Cardimona, Shane Hickman

The University of Missouri-Rolla, Department of Geology and Geophysics

MISSOURI DEPARTMENT OF TRANSPORTATION
RESEARCH, DEVELOPMENT AND TECHNOLOGY

JEFFERSON CITY, MISSOURI
DATE SUBMITTED: February 2003

EXECUTIVE SUMMARY

Current geotechnical procedures for monitoring the condition of roadways are time consuming and can be disruptive to traffic, often requiring extensive invasive procedures (e.g., coring). Ground penetrating radar (GPR) technology offers a methodology to perform detailed condition assessment of existing roadways, with the added advantage over other techniques of being rapid and cost-effective. This project and report were split into four different sections based on the type of roadway being surveyed.

The first section presents the results of a GPR survey over portions of Interstate 44 near Springfield, Missouri. The goal of this survey was to evaluate concrete pavement layer thickness and continuity within the specific study regions. The second section applies GPR techniques to a survey along Interstate 70 across the state of Missouri. Goals of this survey were threefold: 1) determine layer thicknesses every tenth mile; 2) update history information related to types of pavements that make up I70 across Missouri; and 3) note regions where the radar signal appears anomalous. The third section applies GPR techniques to 35 test pavements of the Strategic Highways Research Program Long Term Pavement Performance sites across the state of Missouri. The result is a correlation of GPR reflection character and GPR-derived layer thickness estimates with design information for each test pavement. In the last section of the report, GPR surveys were performed over 42 miles of secondary highways to determine the thickness of the asphalt pavement and also to determine if indications of potential maintenance problem areas could be identified.

Overall, the studies showed GPR was a good tool for determining pavement layer thicknesses. Asphalt surface layering proved to be the easiest to image, creating a strong signal in the GPR data. Not as consistently clear is the concrete-to-baserock interface

where the dielectric contrast between these two media is not always strong enough to create a high amplitude reflected signal. On the Interstate GPR would be a good tool to clarify breaks in historical data and supply an accurate pavement layer and thickness inventory. It was also determined by correlation of GPR data and coring that anomalous areas could be characterized in areas where the concrete appeared excessively thick or thin relative to the design values and especially in asphalt pavement to recognize where the asphaltic cement was stripping from the aggregate.

TABLE OF CONTENTS

Ground Penetrating Radar Survey of

Portions of Interstate 44 near Springfield, Missouri

Steve Cardimona[*], Brent Willeford[*], John Wenzlick[+], Neil Anderson[*]

[*]The University of Missouri-Rolla, Department of Geology and Geophysics

[+]The Missouri Department of Transportation

Section 1

EXECUTIVE SUMMARY

This paper presents the results of a ground penetrating radar (GPR) survey over portions of Interstate 44 near Springfield, Missouri. The goal of this survey was to evaluate concrete pavement layer thickness and continuity within the specific study regions, and to determine if there are any anomalous areas where the concrete appeared excessively thick or thin relative to the design values. Concrete pavement over gravel base coarse proved to be a difficult roadway to investigate using GPR. The radar signature from the base of the concrete was not distinct over much of the survey, making automated interpretation techniques difficult to use. Interpreter-guided analysis allowed mapping the pavement layers and fulfilled the project goal.

TABLE OF CONTENTS

LIST OF FIGURES

LIST OF TABLES

BACKGROUND AND METHODOLOGY

Ground penetrating radar (Daniels, 1996; Cardimona, et al., 1998) uses a radio wave source to transmit a pulse of electromagnetic energy into the pavement. Reflected energy originating in the pavement at interfaces between materials of different dielectric properties or of differing conductivities is received and recorded for analysis of internal layering within the pavement. GPR data consist of a) changes in reflection strength, b) changes in arrival time of specific reflections, c) source wavelet distortion, and d) signal attenuation. These different GPR signatures can be used as discriminates for detecting poor quality pavements (e.g., insufficient asphalt overlay, variable concrete pavement or base coarse).

Modern antennae for roadway analysis are normally designed as air-launched horn antennae with nominal peak frequencies of around 1.0GHz, offering the ability to obtain high resolution images of pavement layers. Data can be collected using monostatic antennae, which means the same antenna acts both as transmitter and receiver, or with bistatic antennae where the transmitting and receiving antennae are separate. Multichannel recording instrumentation in either monostatic or bistatic modes allow us to collect more than one pass of data along the vehicle traverse. Collection of this data is fast and not disruptive to traffic patterns, with reasonable collection speeds up to 50mph.

The standard methodology for the automatic interpretation of GPR data over pavements (ASTM D 4748-87) measures reflection amplitudes. The contrast in dielectric constant (relative dielectric) across an interface is what produces the reflection in the first place, so the measured reflection amplitudes, scaled with an initial amplitude calibration, can be related directly to the dielectric values for each layer. Once all layer dielectric constants are determined, the layer thicknesses can be calculated using the radar wave

velocities (based also on the dielectric constants) and the measured travel time of each interface reflection.

This automatic interpretation procedure implies that all layer interfaces are represented by distinct reflection peaks in the recorded GPR signal. That all layers are represented means that each reflection coefficient is large enough to produce a returned signal with an amplitude above the noise level. User guided interpretation uses similar concepts to the automated interpretation scheme, but the amplitude of reflection events is not formally used to measure dielectric constants. Instead, after interface reflections (and their associated travel times) are picked from the data, ground truth is used to calibrate the signal. Dielectric constants are determined from this ground truth, and layer thickness estimates along the whole survey are then produced. Where direct ground truth is unavailable, design values for pavement layer thicknesses are used to estimate dielectric constants.

FIELD ACQUISITION PROCEDURES

A ground penetrating radar survey was performed of road pavement along portions of Interstate 44 near Springfield, Missouri (Figure 1). The instruments and the software for analysis of the data are manufactured by Geophysical Survey Systems, Inc. These data were acquired using 1.0GHz air-launched bistatic horn antennae (Geophysical Survey Systems, Incorporated antenna model #4208). All data were collected at 30mph yielding ~5 radar scans/m (1.5 scans/ft, or 1 scan per 8 inches) with a 20 ns time recording window. The scans-per-meter defines the horizontal sampling. The time recording length determines (with the radar velocity) the maximum depth imaging, expected which was on the order of one meter for this survey. The bistatic antennae was mounted behind a pickup truck, acquiring two channels of data resulting in parallel survey passes separated

by three feet. The two channels of data were used together to aid during the interpreter-based analysis. Data was collected in both driving and passing lanes along all six segments of I44 (Figure 1). This gave 24 data sets for a total of almost 600MB of raw data.

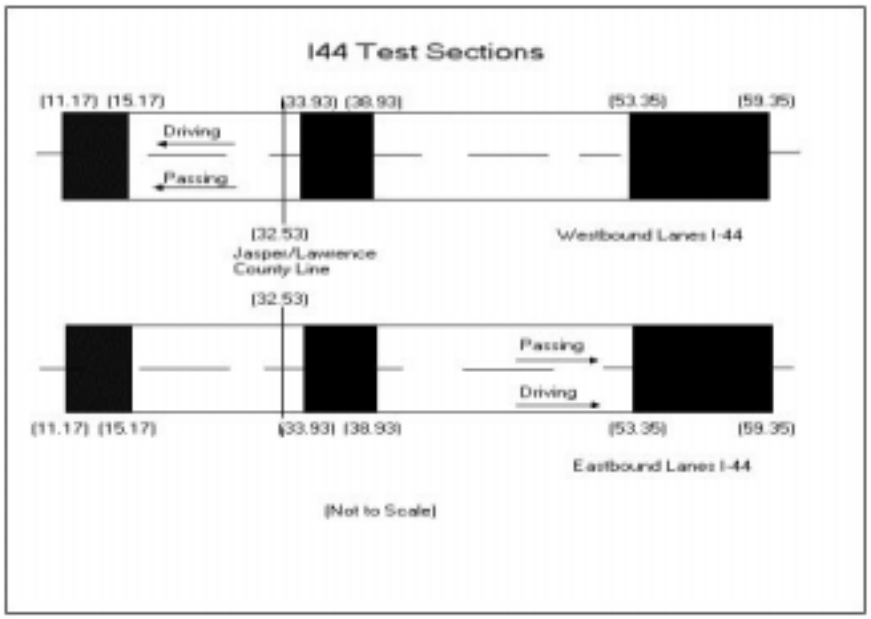

Figure 1. Location of surveyed portions of I44, relative to continuous mile marker.

ANALYSIS AND INTERPRETATION PROCEDURES

Interpreter-based analysis of roadway data to produce layer thickness estimates requires correlation with ground truth. Ideally, the ground truth consists of core information from every different roadway surface; however, in the absence of this, design plans were used to calibrate the radar data in this study, with an associated loss in confidence in the resulting interpretation. The design plans used were from the history information supplied by MoDOT. Of course, care had to be employed when using design thickness as a guide because a main goal of the study was to compare the GPR results with the design information. For this study, a dielectric of 11.7 was used for the concrete,

based on the average two-way radar travel time and design thickness for miles 35-39 eastbound driving lane I44.

In our data from I44, the signal from the base of the concrete pavements was often very weak, meaning the interface between the concrete and the base rock was not distinct. Because the base of the concrete (concrete to base coarse interface) was often difficult to interpret, the use of a calibration file (reflection from a metal reflector) for automated analysis broke down and required constant interpreter input to keep it on track. Using the history information as a guide, we chose to use interpreter guided analysis throughout the study (Willeford et al., 1998). Further analysis and investigation would require core control from numerous points along the surveyed portions of I44.

The analysis procedure involved multiple steps:

1) **Resample data** every second scan (to 1 sample in every 16 to reduce file size)
2) **Layer pick** (Surface, asphalt, concrete) interfaces using both channels of data as a guide for helping to see all layer interfaces. Anomalously low amplitude reflections for each base-of-asphalt and base-of-concrete interface were noted.
3) **Thickness estimation**
   a) used spreadsheet to get 2-way travel time for concrete layer based on GPR travel time picks
   b) used design values to get an average dielectric of 11.7 for the concrete (based on analysis of GPR data from mile 35-39 eastbound driving lane)
   c) used 2-way time and average dielectric to get layer thicknesses in inches
4) **Graphing** and interpretation of data using Microsoft Excel
   a) anomalous data determined (sorted) based on +/-1inch variation in thickness
   b) anomalous amplitude of reflections plotted as different color
5) **Identify and tabulate** areas exhibiting anomalous thickness based on radar.
   a) identify anomalous areas that have lateral continuity
   b) list average anomalous thickness and start/end mile position

SUMMARY OF RESULTS

Figures 2 and 3 show example radar data. Where the interface between the concrete pavement and the base coarse was variable and indistinct (Figure 3), interpretation was more difficult than where this interface was well constrained by the GPR reflection data (Figure 2). The majority of the survey discussed in this report could be described by "bad" areas that were more difficult to interpret. Automated interpretation broke down, however interpreter-guided analysis was performed on all data and allowed the project goals to be met.

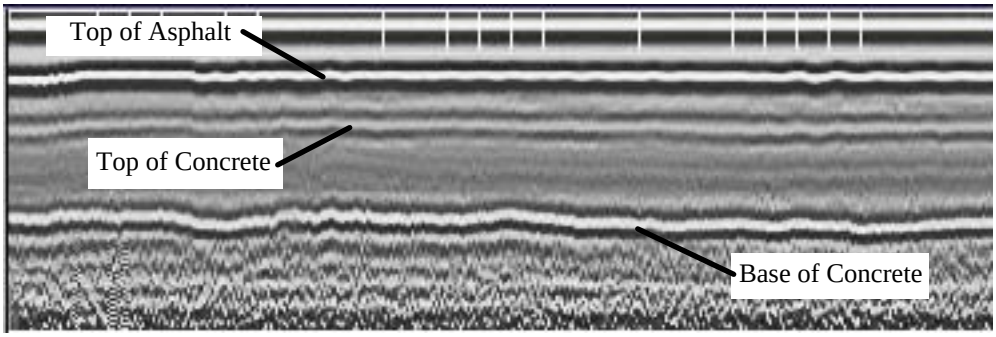

Figure 2. Example of "good" (easy to interpret) data, where the interface designating the base of the concrete layer is quite distinct. Data shown is from mile 32-35.5 eastbound passing lane. This location had asphalt overlay.

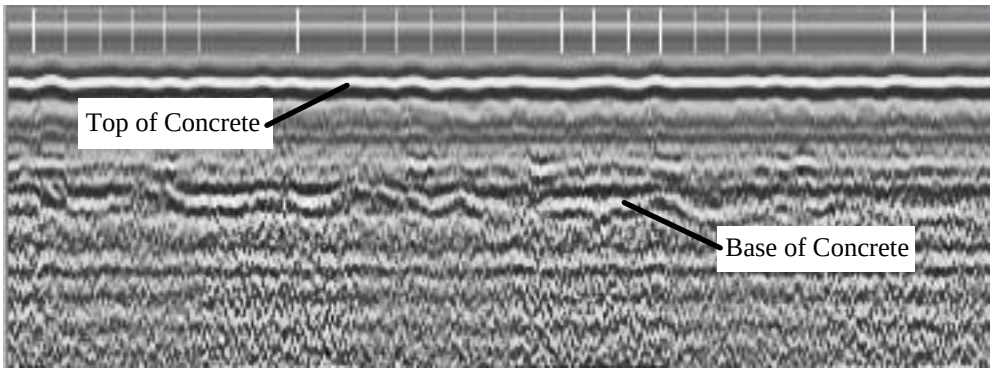

Figure 3. Example of "bad" (more difficult to interpret) data, where the radar image of the interface designating the base of the concrete layer is quite variable in character. Data shown is from mile 52-56 eastbound driving lane.

Figure 4 displays example profiles from the analysis. After creating the layer profile information and storing in spreadsheet format, the data could be sorted to determine areas of the concrete that had anomalous thickness. Tables 1 and 2 summarize the anomalous (thickness) regions (east and west bound) based on a variation of +/- 1 inch from design.

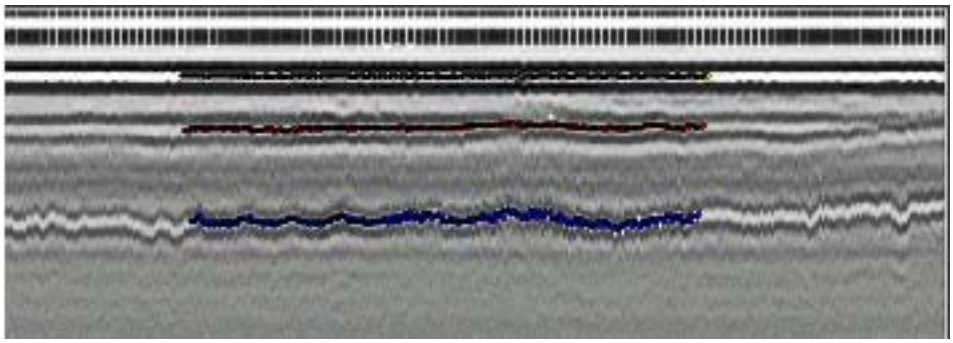

Figure 4a. Example of analysis: Interfaces picked and plotted along with GPR data profile. This location had asphalt overlay.

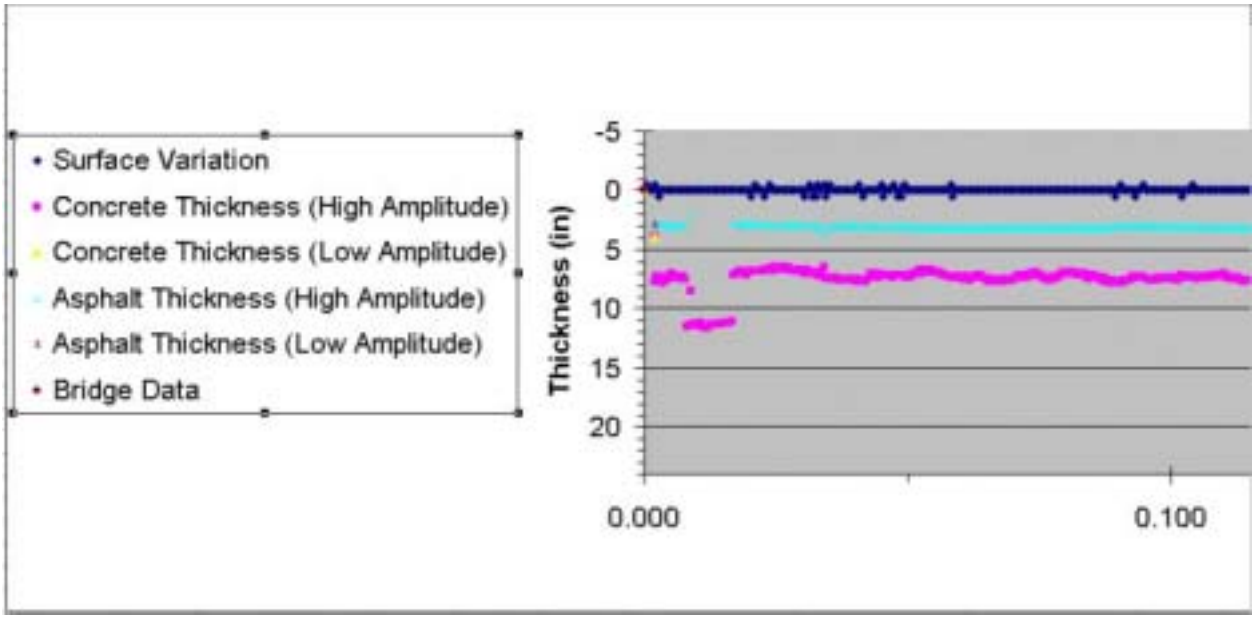

Figure 4b. Example of analysis: Layer thicknesses determined and profiles plotted using spreadsheet.

Table 1a

Eastbound Thickness Anomalies

Driving Lane

Thick

Continuous mile

From	To	Average	Design	Dif
13.283	13.292	9.15	8	1.15
15.434	15.79	9.1	8	1.1
33.395	34.152	10.2	9	1.2
35.061	35.183	10.22	9	1.22
35.688	36.084	10.23	9	1.23
36.404	36.457	10.21	9	1.21
38.527	38.622	10.13	9	1.13
56.007	58.27	9.82	8	1.82
56.145	58.591	10.06	8	2.06
56.559	59.885	9.23	8	1.23

Driving Lane

Thin

Continuous mile

From	To	Average	Design	Dif
10.673	10.683	3.49	8	-4.51
11	11.1	3.8	8	-4.2
12.226	12.241	6.86	8	-1.14
13.19	13.203	6.95	8	-1.05
13.814	13.824	6.9	8	-1.1
15.147	15.218	6.88	8	-1.12
33.034	33.051	7.39	9	-1.61
33.173	33.296	7.85	9	-1.15
37.114	37.151	7.83	9	-1.17

Table 1b

Eastbound Thickness Anomalies

Passing Lane

Thick

Continuous mile

From	To	Average	Design	Dif
10.759	10.766	9.55	8	1.55
33.053	33.172	10.22	9	1.22
33.513	33.734	10.14	9	1.14
34.055	34.209	10.16	9	1.16
34.581	34.76	10.15	9	1.15
35.706	35.814	10.21	9	1.21
35.882	36.084	10.22	9	1.22
36.397	36.457	10.31	9	1.31
36.534	36.605	10.15	9	1.15
37.045	37.057	10.23	9	1.23
37.416	37.475	10.13	9	1.13
37.652	37.763	10.23	9	1.23
38.756	38.892	10.21	9	1.21
55.957	56.058	10.19	9	1.19
58.127	58.371	9.32	8	1.32
58.656	58.972	9.12	8	1.12
59.361	59.692	9.15	8	1.15

Passing Lane

Thin

Continuous mile

From	To	Average	Design	Dif
11.213	11.227	6.94	8	-1.06
13.49	13.545	6.93	8	-1.07
14.006	14.061	6.88	8	-1.12
14.162	14.198	6.85	8	-1.15
14.314	14.377	6.8	8	-1.2
32.537	33.051	7.62	9	-1.38

Table 2a

Westbound Thickness Anomalies

Driving Lane

Thick

Continuous mile

From	To	Average	Design	Dif
10.677	10.781	9.1	8	1.1
11.65	11.694	9.18	8	1.18
11.887	12.02	9.15	8	1.15
12.803	12.932	9.27	8	1.27
13.782	13.902	9.32	8	1.32
14.064	14.112	9.18	8	1.18
14.21	14.278	9.33	8	1.33
14.319	14.349	9.66	8	1.66
14.674	14.699	9.76	8	1.76
15.2	15.36	9.341	8	1.341
15.56	15.7	9.11	8	1.11
38.927	38.959	10.3	9	1.3
52.497	52.499	10.65	9	1.65
52.588	52.617	10.33	9	1.33
56.463	56.494	10.23	9	1.23
58.186	58.45	9.42	8	1.42
59.104	59.133	9.21	8	1.21
59.822	59.855	9.26	8	1.26

Driving Lane

Thin

Continuous mile

From	To	Average	Design	Dif
10.645	10.649	3.7	8	-4.3
12.647	12.657	6.55	8	-1.45
13.562	13.565	6.73	8	-1.27
15.993	15.997	3.97	8	-4.03
32.592	32.844	7.38	9	-1.62
32.85	33.09	5.97	9	-3.03
37.247	37.252	7.53	9	-1.47
38.993	38.995	3.85	9	-5.15
54.912	54.957	7.92	9	-1.08
54.982	55.076	7.81	9	-1.19

Table 2b

Westbound Thickness Anomalies

Passing Lane

Thick

Continuous mile

From	To	Average	Design	dif
11.032	11.086	9.09	8	1.09
13.902	13.914	9.1	8	1.1
33.409	33.496	10.21	9	1.21
35.496	35.512	10.15	9	1.15
38.522	38.531	10.18	9	1.18
53.788	53.822	10.2	9	1.2
58.027	58.22	9.27	8	1.27

Passing Lane

Thin

Continuous mile

From	To	Average	Design	dif
12.464	12.471	6.92	8	-1.08
13.529	13.538	6.56	8	-1.44
13.857	13.897	6.77	8	-1.23
32.586	32.816	7.33	9	-1.67
32.827	33.061	3.88	9	-5.12
54.535	54.559	7.61	9	-1.39
55.806	55.855	7.77	9	-1.23

SUGGESTIONS FOR FUTURE WORK

1) Get core information from various points along the surveyed portions of I44 in order to adjust dielectric constants accordingly.

2) Collect data over a small portion of the previously surveyed area (in area untouched by MoDOT maintenance) in which good and bad areas exist (areas easy to interpret and areas more difficult to interpret). With an associated calibration file carefully acquired, compare results of automated technique (desired) and interpreter-based technique (as used in this study) for more definitive investigation of when/where the automated technique breaks down in order to help determine how to improve automated techniques for pavement analysis.

CONCLUSIONS

In this report the ground penetrating radar technique was applied to high resolution roadway pavement analysis along portions of Interstate 44 near Springfield, Missouri. Through a comparison with history information, the utility of the tool for determining pavement layer thickness estimates in a rapid fashion was demonstrated. The result is a quantitative display of layer profiles, with the ability to determine regions of anomalous concrete thickness based on an interpreter-guided cut-off value. Although this project was successful in meeting the original goal, there was difficulty investigating the concrete pavement of I44. There was an associated loss of confidence in the resulting concrete layer profiles, since the concrete to gravel base interface did not have clearly defined reflectivity throughout the survey. Interpreter input was necessary (in lieu of completely automated techniques) to help guide the analysis, allowing concrete layer thickness to be estimated and anomalous thick/thin zones to be determined.

REFERENCES CITED

ASTM Designation D 4748 - 87 (1995), Standard Test Method for Determining the Thickness of Bound Pavement Layers Using Short-Pulse Radar.

Cardimona, S., M. Roark, D. J. Webb and T. Lippincott, 1998. Ground penetrating radar, *Highway Applications of Engineering Geophysics with an Emphasis on Previously Mined Ground*, pp. 41-56.

Daniels, D., 1996. Surface-penetrating radar, Inst. Electr. Eng.

Willeford, B., N. Anderson and S. Cardimona, 1998. Evaluation of selected sections of U.S. Interstate 44 using ground penetrating radar techniques, report for the Missouri Department of Transportation, UMR Department of Geology and Geophysics contribution November 1998.

Ground Penetrating Radar Survey of

Interstate 70 Across Missouri

Steve Cardimona[*], Brent Willeford[*], Doyle Webb[*], John Wenzlick[+], Neil Anderson[*]

[*]The University of Missouri-Rolla, Department of Geology and Geophysics

[+]The Missouri Department of Transportation

Section 2

EXECUTIVE SUMMARY

Current geotechnical procedures for monitoring the condition of roadways are time consuming and can be disruptive to traffic, often requiring extensive invasive procedures (e.g., coring). Ground penetrating radar (GPR) technology offers a methodology to perform detailed condition assessment of existing roadways, with the added advantage over other techniques of being rapid and cost-effective. This study applies GPR techniques to a survey along Interstate 70 across the state of Missouri. Because of the deterioration of this forty-year-old pavement strategies needed to be developed to rehabilitate the entire length of I-70. It was hoped that GPR would tell what condition the pavement structure was in, the concrete pavement under the asphalt overlaid areas and what kind of condition the base and subbase were like under the concrete sections. Goals of this survey were threefold: 1) determine layer thicknesses every tenth mile (primarily asphalt and concrete, with base coarse information secondary); 2) update history information related to types of pavements that make up I70 across Missouri; and 3) note regions where the radar signal appears anomalous. Goals (1) and (2) are related and were the primary goals. Goal (3) required visually interpreting the full data set and was done as a guide for further investigation. The result is an extensive data set allowing the user to visualize the east and westbound pavement profiles in comparison to design history information, view a table of surface types and anomalous regions associated with those profiles, and cross-reference this information with the actual GPR data in a book form.

TABLE OF CONTENTS

LIST OF FIGURES

LIST OF TABLES

BACKGROUND AND METHODOLOGY

Ground penetrating radar (Daniels, 1996; Cardimona, et al., 1998) uses a radio wave source to transmit a pulse of electromagnetic energy into a nonmagnetic body. The reflected energy, originating within the body at interfaces between materials of different dielectric properties or of differing conductivities, is received and recorded for analysis of internal structure of the body. GPR data consist of a) changes in reflection strength, b) changes in arrival time of specific reflections, c) source wavelet distortion, and d) signal attenuation. When applied to the analysis of roadways, these different GPR signatures can be used as discriminates for detecting poor quality pavements (e.g., insufficient asphalt overlay, variable concrete pavement or base coarse).

Ground penetrating radar techniques applied to roadway assessment are relatively new. Only recently has the instrumentation been improved so that interpretable high resolution data can be obtained regarding pavement condition. Various GPR tools and methodologies exist (e.g., ASTM D 4748-87), some with more potential than others. Modern antennae for roadway analysis are normally designed as air-launched horn antennae with nominal peak frequencies of around 1.0GHz, offering the ability to obtain high-resolution images of pavement layers. Data can be collected by monostatic antennae, which means the same antennae acts both as transmitter and receiver, or with bistatic antennae where the transmitting and receiving antennae are separate. Bistatic horn antennae designed for high speed road pavement imaging are normally mounted behind a truck in a transverse configuration (radar antennae transverse to vehicle motion), and they offer more rapid data collection and thus more samples per distance than does the monostatic tool. Multichannel recording instrumentation in either monostatic or bistatic modes allow us to collect more than one pass of data along the vehicle traverse. Collection of

this data is fast and not disruptive to traffic patterns, with reasonable collection speeds up to 50mph.

The standard methodology for the automatic interpretation of GPR data over pavements (ASTM D 4748-87) measures reflection amplitudes. These reflection amplitudes, scaled with an initial amplitude calibration, allow for the determination of layer dielectric constants. The contrast in dielectric constant (relative dielectric) across an interface is what produces the reflection in the first place, so the reflection amplitudes can be related to the dielectric values with a layer-stripping technique; i.e., the relative dielectric of the first layer is determined, then it is used to determine the relative dielectric of the next layer, and so on. Once all layer dielectric constants are determined, the layer thicknesses can be calculated using the radar wave velocities (based also on the dielectric constants) and the measured travel time of each interface reflection.

This interpretation procedure implies that all layer interfaces are represented by distinct reflection peaks in the recorded GPR signal. That all layers are represented means that each reflection coefficient is large enough to produce a returned signal with an amplitude above the noise level. That all reflection peaks be distinct relates to the vertical resolution of the GPR tool. This resolution will be most related to the peak frequency of transmission, because the wave velocity divided by the wave frequency determines the wavelength of the radar in the pavement layers. For an antenna with nominal frequency of 1.0GHz, the wavelength would be on the order of a tenth of a meter for a medium with a dielectric constant of 9 (corresponding to a radar velocity of 0.1m/ns). The slower the medium (the larger the dielectric constant) or the larger the source frequency, the better the resolution (smaller the wavelength).

User guided interpretation uses similar concepts to the automated interpretation scheme, but the amplitude of reflection events is not formally used to measure dielectric constants. Instead,

after interface reflections (and their associated travel times) are picked from the data, ground truth is used to calibrate the signal. Dielectric constants are determined from this ground truth, and layer thickness estimates along the whole survey are then produced.

FIELD ACQUISITION PROCEDURES

We have performed an extensive ground penetrating radar survey of road pavement along Interstate 70 across Missouri. The instruments and the software for analysis of the data are manufactured by Geophysical Survey Systems, Inc. In Summer 1998, the Department of Geology and Geophysics at UMR acquired GPR data along both east and westbound I70 from Mile marker 20 (Kansas City) to 210 (St. Louis) in Missouri. These data were acquired using 1.0GHz air-launched horn antennae (Geophysical Survey Systems, Incorporated antenna model #4208). All data were collected at 30mph yielding ~5 radar scans/m (1.5 scans/ft, or 1 scan per 8 inches) with a 20 ns time recording window. The scans-per-meter defines the horizontal sampling. The time recording length determines (with the radar velocity) the maximum depth imaging expected which was on the order of one meter for this survey. We mounted the bistatic antennae behind a pickup truck, acquiring two channels of data resulting in parallel survey passes separated by three feet.

For calibration, we collected radar data over core locations near to the start of the survey (on I70 near Columbia, MO). In addition, a calibration file was acquired each new day of the survey, consisting of data recorded in place over a metal (perfect) reflector.

The difficult logistics of acquisition required that data be collected in four mile sections to keep the file sizes manageable (just under 32MB). Starting and stopping every four miles introduced a horizontal error during acquisition of on average 19 feet over four miles, for about

4.75 ft/mile position error. From approximately mile 144-180 eastbound, acquisition was undersampled relative to the rest of the survey at 5scans/m. This was due to incorrect acquisition parameter settings for such a large file size, but could be compensated for during processing with only minimal extra position error. The total data collected amounted to just under 3GB of data, posing yet another logistical problem of storage of the entire data set. Data were stored directly onto 1GB removable media during acquisition and ultimately were stored on CD-ROM for archiving.

ANALYSIS AND INTERPRETATION PROCEDURES

Preliminary qualitative determination of anomalous roadway areas can be done during acquisition or during post-survey assessment of the data. Quantitative interpretation of the roadway data to help produce layer thickness estimates requires correlation with ground truth. Ideally, the ground truth consists of core information from every different roadway surface; however, in the absence of this, design plans were used to calibrate the radar data in this study, with an associated loss in confidence in the resulting interpretation. The design plans we used are from the history information supplied by MoDOT. This history information could only be used as a guide, as it is incomplete and inaccurate. Of course, one of our primary goals was to update and correct this information.

Neither of the calibration techniques was truly effective for analysis of the extensive data set we acquired. Although some of the calibration files were not collected under ideal circumstances and proved less than useful, the use of the calibration file technique for automated analysis of this extensive data was not appropriate. The automated technique requires that all layer interfaces be interpretable (above the noise level and resolvable), and also all layers and numbers of layers

should ideally be consistent. Our data from I70 included patchy and discontinuous roadway for both asphalt and concrete pavements. In addition, the concrete pavements included both non-reinforced and reinforced concrete. The reinforcement essentially puts an additional layer into the pavement analysis. Use of the calibration file for automated analysis broke down and required constant interpreter input to keep it on track through these changes in pavement character. In addition, the base of the concrete (concrete to base coarse interface) was often difficult to interpret and the automated analysis technique using a calibration file requires each interface to be distinct and clear (above the noise level). With such variability across some 400 miles of roadway, the limited core control (one area of concrete and one area of asphalt) was basically useless. Further analysis and investigation would require core control from numerous points along the surveyed portion of I70.

Using the history information as a guide, we chose to use interpreter guided analysis throughout the study. Since we wanted to produce a listing of anomalous areas, this required interpreter involvement through analysis of the entire data set and thus our analysis technique was consistent with meeting our third goal. Our analysis procedure involved multiple steps:

1) **Stacking** 9 scans (to reduce file size and increase signal to noise ratio)
2) **Layer Picking** (Surface, asphalt, concrete) interfaces (using both channels of data as a guide for helping to see all layer interfaces).
3) **Distance Correction** (based on 4 mile) (cut/paste long files to files that ran short)(MS-Excel)
4) **Sorting** of 0.1 Mile data. (Microsoft query to subsample original lay files)
   a) Averaged GPR signal from 20 ft window around each 0.1 mile interval.
5) **Graphing** and interpretation of data (from query) using Microsoft Excel
   a) Distance converted to continuous mile marker (from linear feet to continuous mile)
   b) Dielectric constant determined from design data (thickness estimate) and acquired data (travel time measurement) to get average velocity estimate. We used dielectrics of 4.2 for

the asphalt (based on 172-176 E, 3in design) and 10.5 for concrete (based on 110-114 E, 8in design). Calibration positions were chosen based on regions that had strong, laterally continuous GPR reflections.

c) Thickness estimates based on 2 way travel time between layer events. [i.e. (t2-t1)*Vel/2]

d) Design-history information converted to continuous mile and summarized in spreadsheet information.

e) Data Filtered to throw out No data sections in GPR and design spreadsheet information.

f) Graphs of GPR and design showing calculated thickness for asphalt and concrete compared with design/history thickness information.

6) **Interpretation** of un-stacked data to locate anomalous features and classify surface material type (i.e. asphalt or concrete).

7) **Identify** and tabulate areas exhibiting anomalous radar signatures.

SUMMARY OF RESULTS

Figures 1 and 2 (multi-page) show profile plots for east and west bound driving lane. The radar layer thickness estimates are tabulated in Appendix A. In figures 1 and 2, layer thicknesses are plotted as a function of distance (continuous mile) based on the GPR interpretation and are compared with the design history information. Where the two plots diverge, the design history may be in question. For example, the eastbound asphalt thickness from mile 20 to about 40 is much thicker than the history records indicate, and this extra thickness was confirmed by MoDOT personnel.

Table 1 summarizes surface pavement types along I70 as 1) asphalt, 2) reinforced concrete, 3) reinforced concrete patch, 4) non-reinforced concrete, 5) non-reinforced concrete patch, 6) bridge or 7) unknown. This table should be used in conjunction with Figures 1 and 2 when assessing the roadway. In particular, we note in Table 1 if we have lower confidence in the GPR

interpretation based on the quality of the GPR data (“pd” or “vpd” for “poor data” and “very poor data”).

Table 2 delineates anomalous regions exhibited in the radar data, and Table 3 lists anomalies that correspond to tenth mile positions for correlation with ground truth (e.g., falling weight deflectometer). Radar anomalies are categorized into six different types:

1) increase amplitude	--interface with stronger than surrounding reflectivity (presumably due to greater dielectric contrast)
2) decrease amplitude	--interface with weaker than surrounding reflectivity (presumably due to lower dielectric contrast)
3) thickening	--interface that drops down over a relatively broad region, (indicative of layer that increases in thickness or layer dielectric that increases)
4) thinning	--interface that raises up over a relatively broad region, (indicative of layer that decreases in thickness or layer dielectric that decreases)
5) discontinuous	--interface that is broken up or sharply (vertically) variable
6) washout	--very localized layer thickening presumed to be related to moisture content (slow velocity push-down)

Each of these anomalies can be associated with the base of asphalt, base of concrete (reinforced or non-reinforced), the reinforcement itself, or the base coarse layer. In addition, we note in some places where the surface of the roadway was especially rough and where we interpret pavement patches, since these might be indicative of roadway problems. Figures 3-12 display examples of radar anomalies, labeled at nearest tenth mile mark. Note that the “thickening” and “thinning” areas, and the more localized “washout” areas as well, should show up on the pavement profile data. These areas are designated “anomalous” because they are more localized than variations in layer thickness are expected to be if they are related to pavement

layering put down by MoDOT, although that may prove to be the correct situation. These anomalous regions should be investigated for correlation of ground truth with the radar signatures.

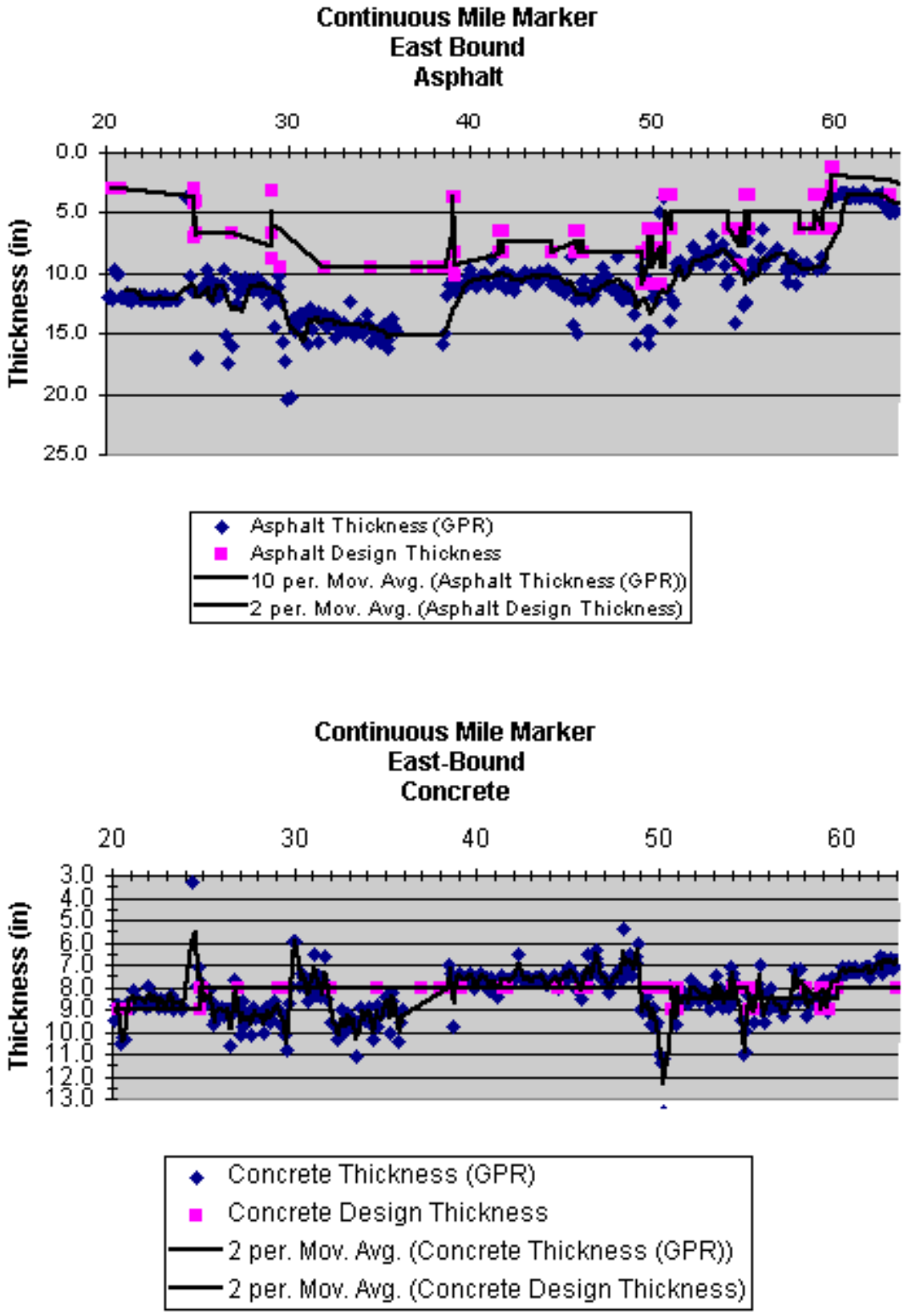

Figure 1. Eastbound pavement layer profiles.

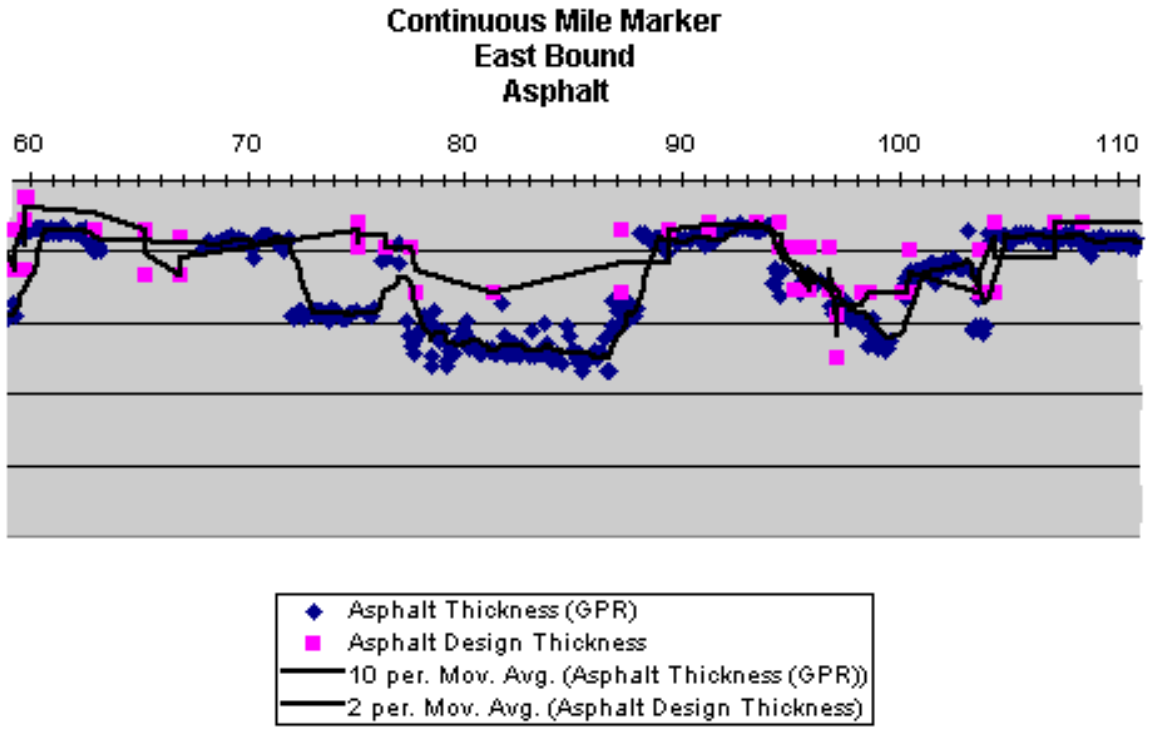

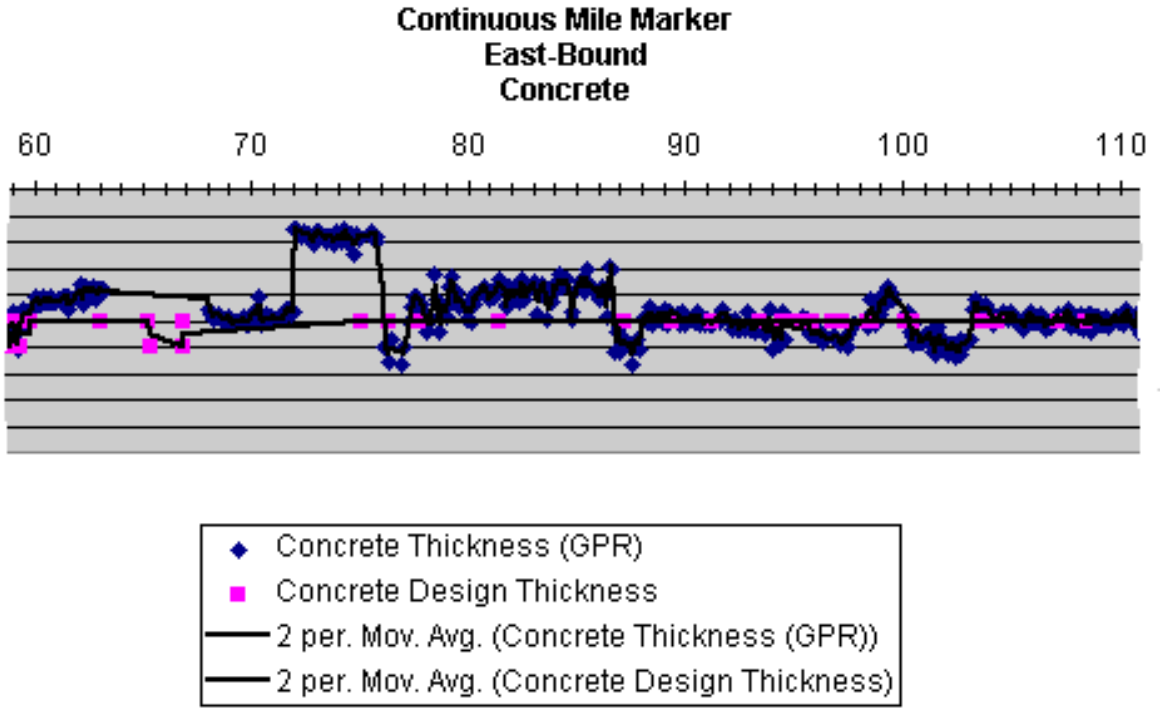

Figure 1 cont. Eastbound pavement layer profiles.

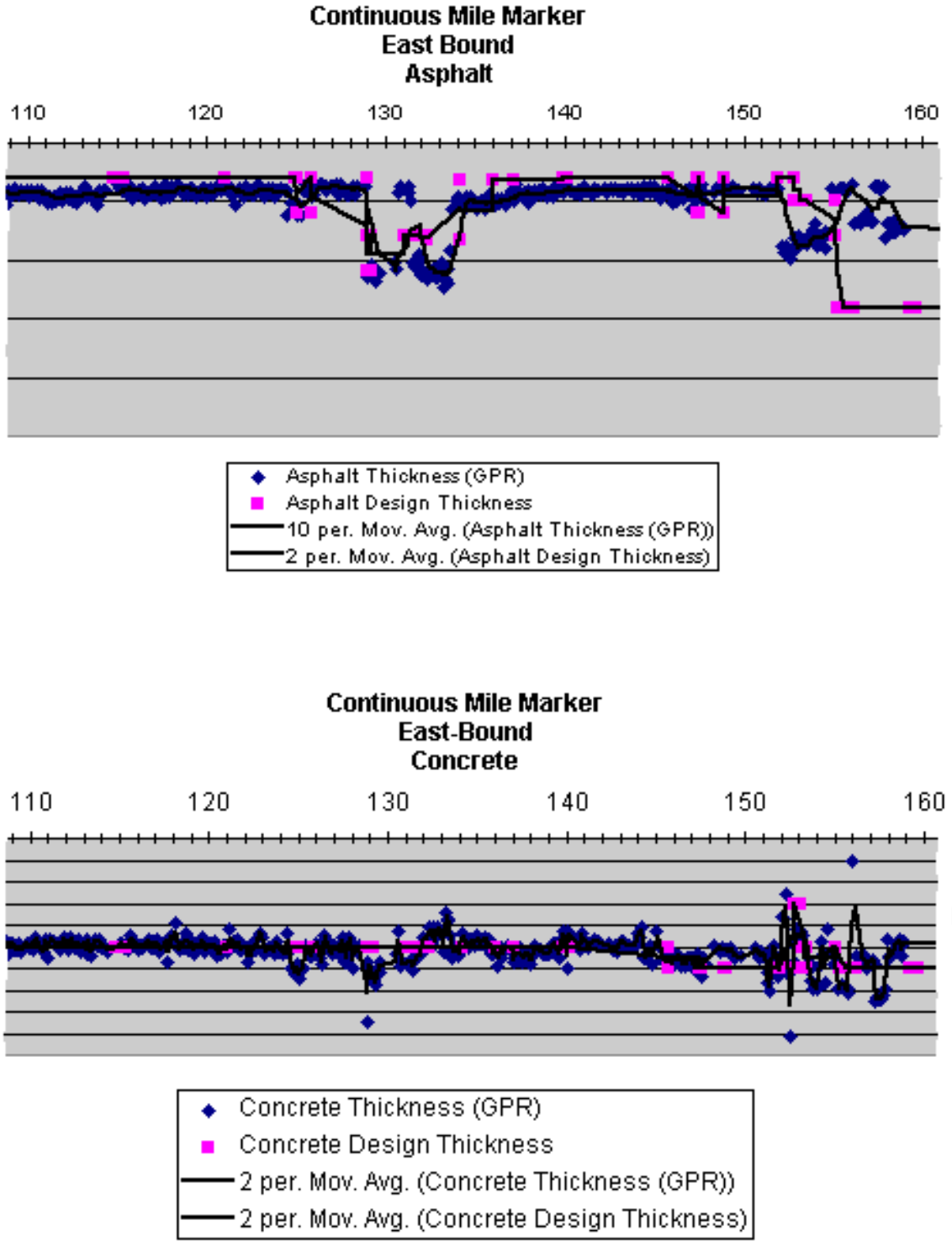

Figure 1 cont. Eastbound pavement layer profiles.

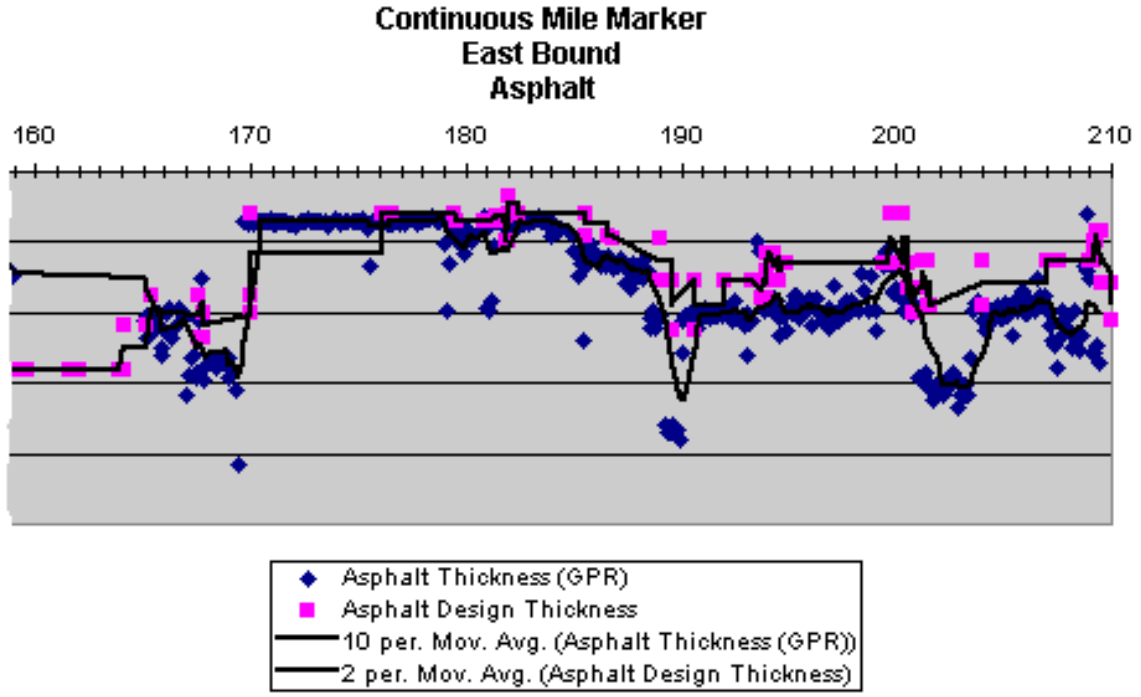

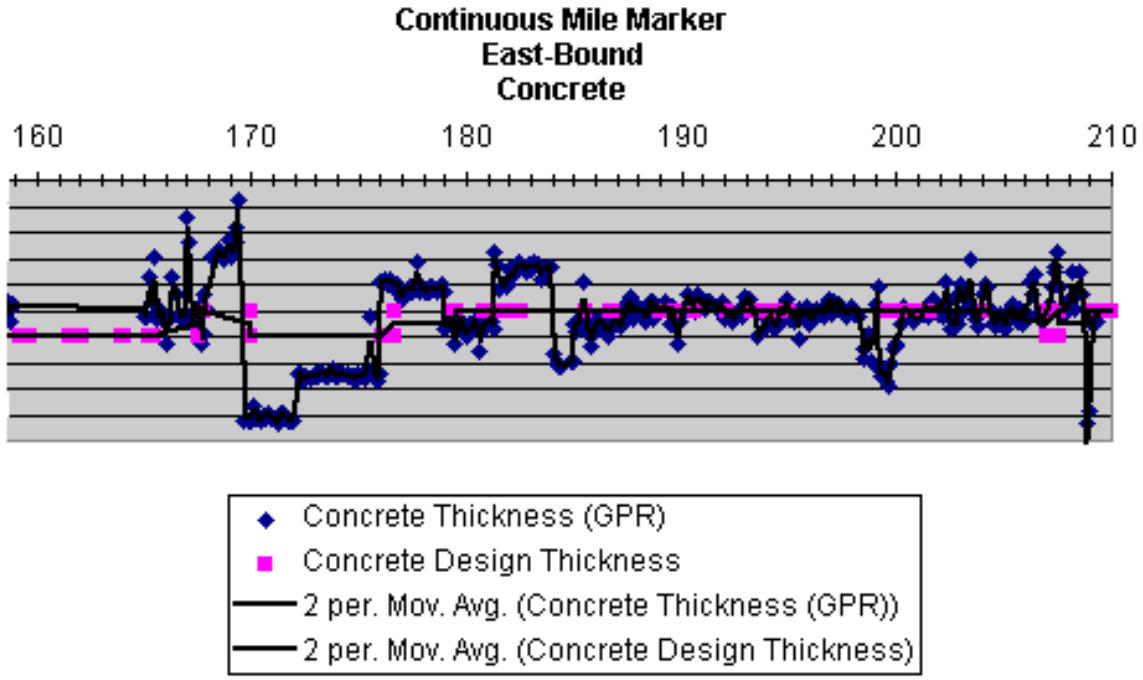

Figure 1 cont. Eastbound pavement layer profiles.

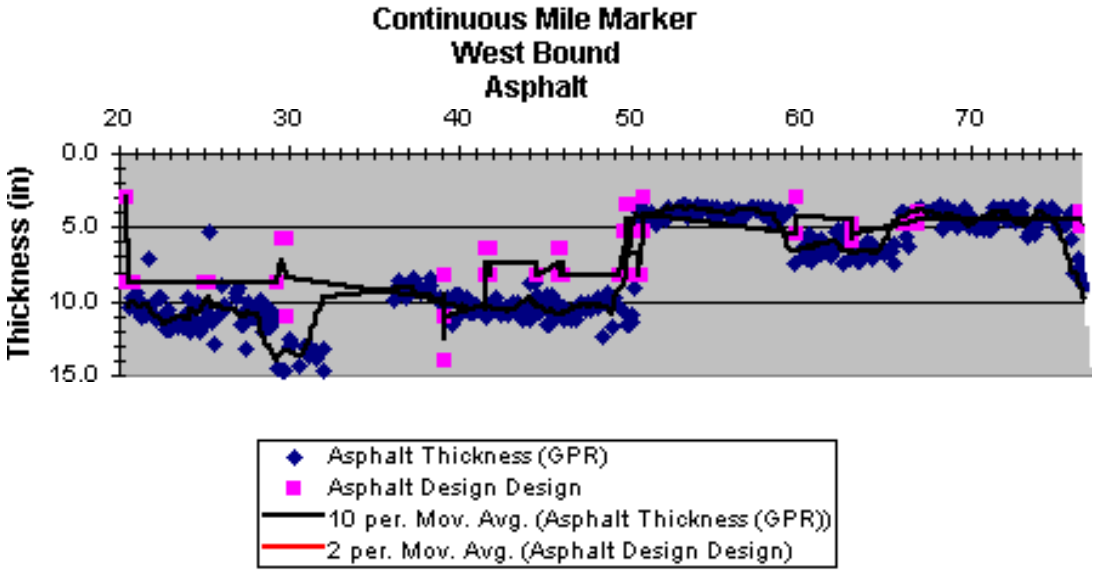

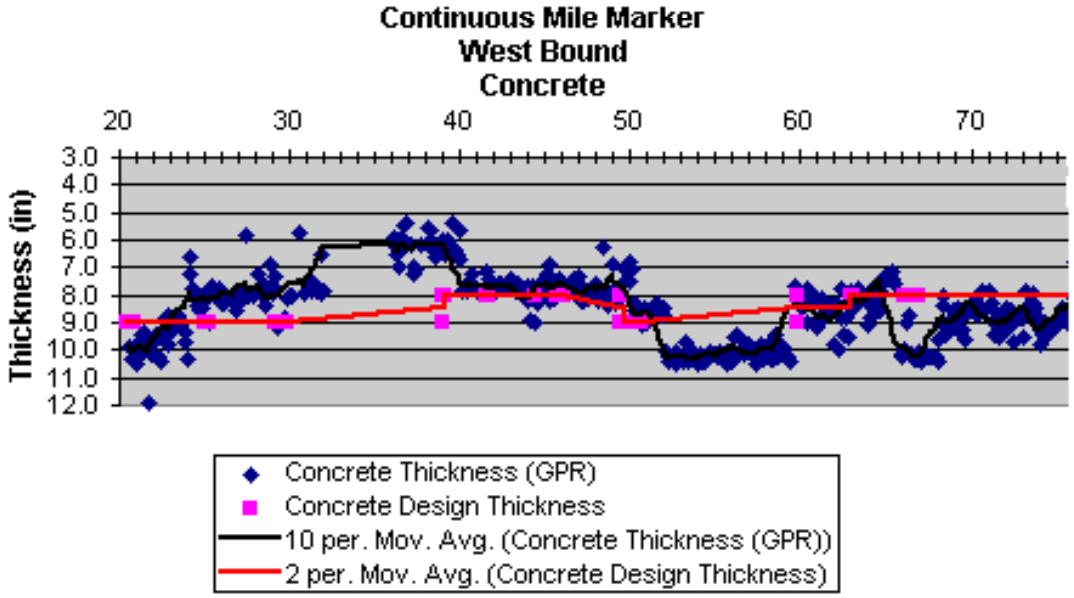

Figure 2. Westbound pavement layer profiles.

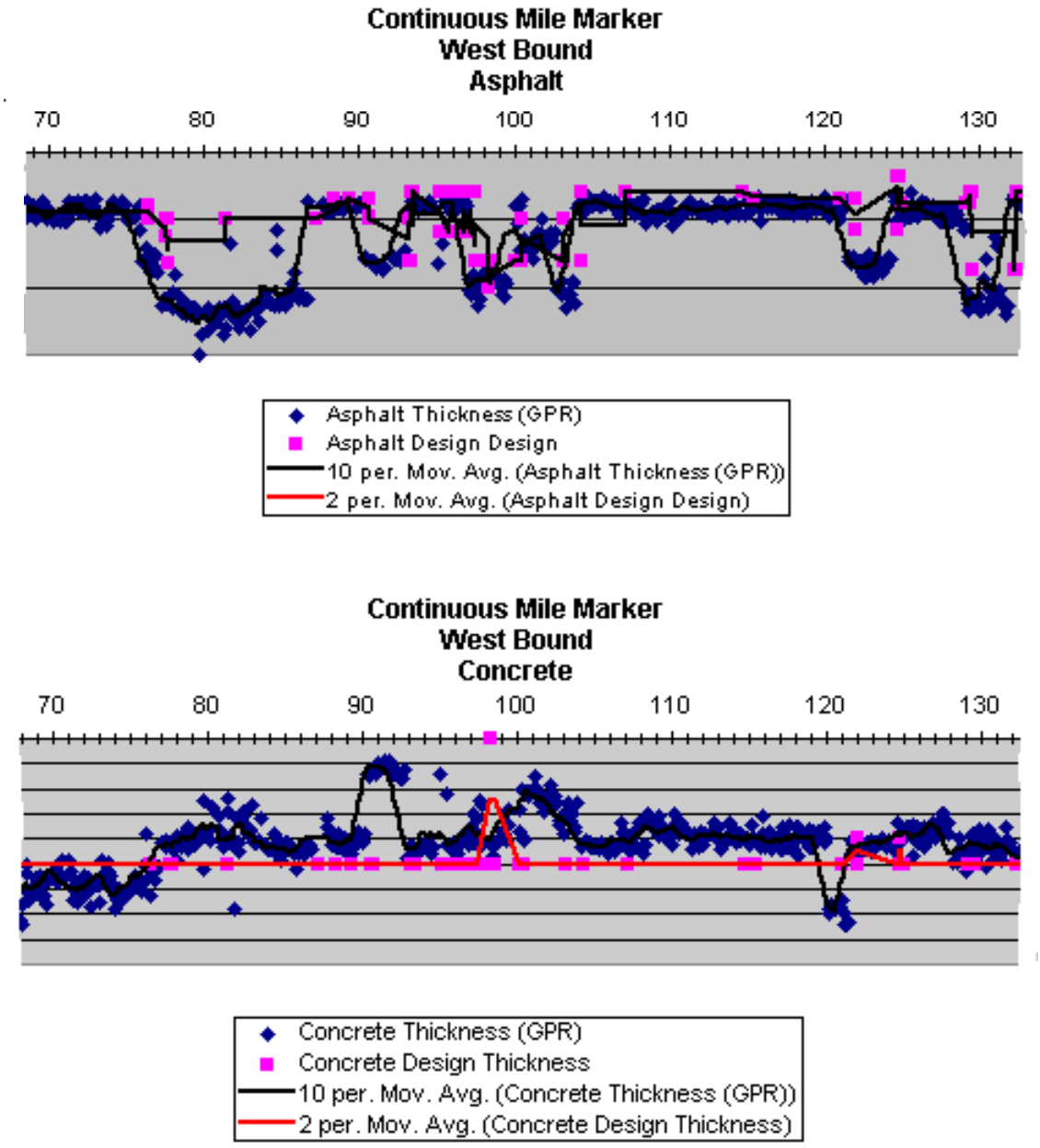

Figure 2 cont. Westbound pavement layer profiles.

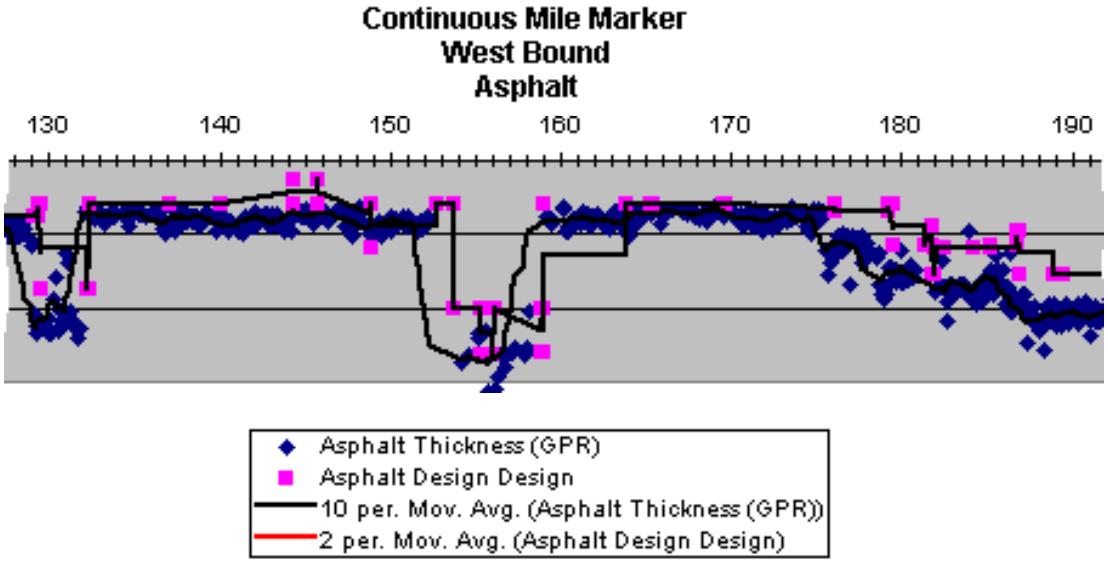

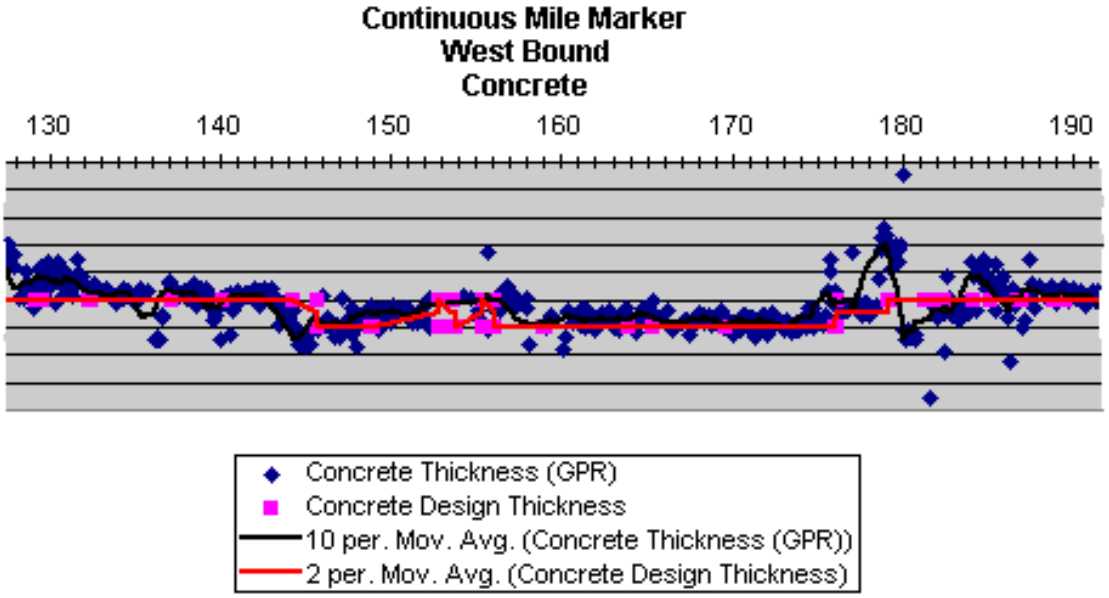

Figure 2 cont. Westbound pavement layer profiles.

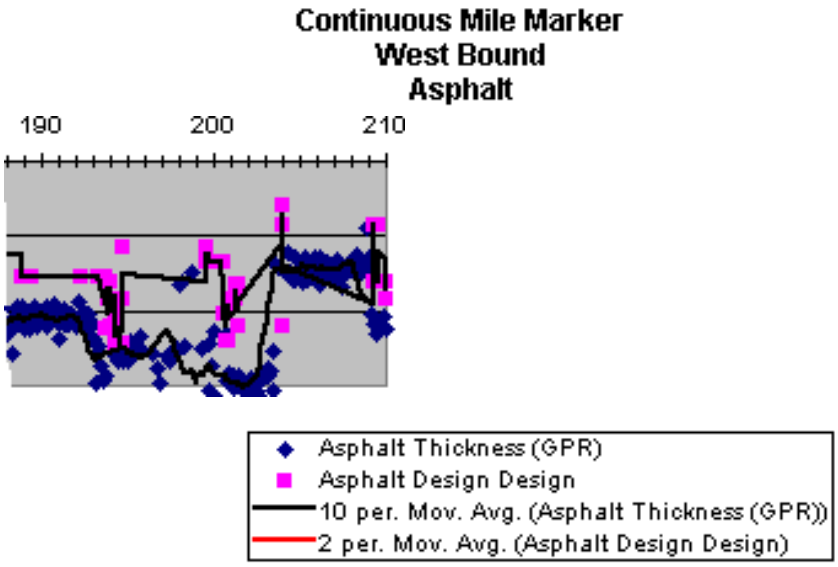

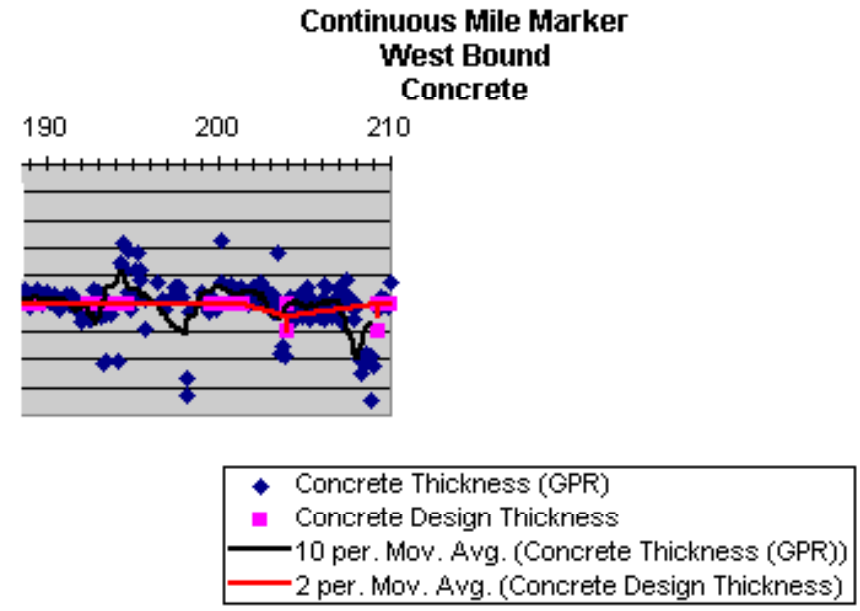

Figure 2 cont. Westbound pavement layer profiles.

TABLE1a

East Bound I-70

Surface Type

Eastbound

Cont. Mile Mark	Start	End	Surface type	Notes
20	20.000	20.453	pcr	
	20.453	21.606	ac	
	21.606	21.612	ppcn	
	21.612	21.646	br	
	21.646	21.655	ppcn	
	21.655	24.000	ac	
24	24.000	24.396	ac	
	24.396	24.405	pcn	
	24.405	24.432	br	
	24.432	24.437	pcn	
	24.437	25.181	ac	
	25.181	25.189	pcn	
	25.189	25.289	br	
	25.289	25.292	pcn	
	25.292	26.627	ac	
	26.627	26.633	un	PPCN?
	26.633	28.001	ac	
28	28.000	29.311	ac	
	29.311	29.322	pcn	
	29.322	29.355	br	
	29.355	29.361	pcn	
	29.361	29.493	ac	
	29.493	29.509	pcn	
	29.509	29.543	br	
	29.543	29.552	pcn	
	29.552	32.002	ac	
32	32.000	33.451	ac	
	33.451	33.493	br	
	33.493	33.519	un	ppcn? , vpd
	33.519	36.000	ac	vpd
36	36.000	37.984	ac	
	37.984	37.991	pcn	
	37.991	38.034	br	
	38.034	38.040	pcn	
	38.040	39.759	ac	
	39.759	39.859	ppcn	?
	39.859	40.033	ac	
40	40.000	41.101	ac	vpd
	41.101	41.107	ppcn	vpd

	41.107	41.148	ac	vpd
	41.148	41.159	pcn	vpd
	41.159	41.177	br	vpd
	41.177	41.187	pcn	vpd
	41.187	42.208	ac	vpd
	42.208	42.212	ppcn	vpd
	42.212	43.998	ac	vpd
44	44.000	44.008	ac	
	44.008	44.053	ppcn	
	44.053	44.544	ac	
	44.544	44.547	ppcn	
	44.547	45.327	ac	
	45.327	45.331	ppcn	
	45.331	45.339	ac	
	45.339	45.416	ppcn	
	45.416	46.380	ac	
	46.380	46.385	ppcn	
	46.385	47.459	ac	
	47.459	47.462	ppcn	
	47.462	47.632	ac	
	47.632	47.634	ppcn	
	47.634	48.000	ac	
48	48.000	48.011	ac	vpd
	48.011	48.015	ppcn	vpd
	48.015	50.403	ac	vpd
	50.403	50.408	ppcn	vpd
	50.408	50.455	br	vpd
	50.455	50.464	ppcn	vpd
	50.464	52.000	ac	vpd
52	52.000	52.938	ac	
	52.938	52.944	ppcn	
	52.944	54.252	ac	
	54.252	54.285	ppcn	
	54.285	54.323	ac	
	54.323	54.327	ppcn	
	54.327	54.348	br	
	54.348	54.352	ppcn	
	54.352	56.000	ac	
56	56.000	56.235	ac	
	56.235	56.268	ppcn	
	56.268	56.281	ac	
	56.281	56.318	ppcn	
	56.318	56.411	ac	
	56.411	56.418	ppcn	
	56.418	56.472	ac	
	56.472	56.512	ppcn	

	56.512	56.989	ac	
	56.989	56.994	ppcn	
	56.994	56.997	ac	
	56.997	57.012	ppcn	
	57.012	57.096	ac	
	57.096	57.108	ppcn	
	57.108	60.000	ac	
60	60.000	61.784	ac	pd
	61.784	61.788	ppcn	pd
	61.788	63.568	ac	pd
	63.568	63.584	ppcr	pd
	63.584	64.002	ac	pd
64	64.000	64.867	ac	pd
	64.867	64.871	ppcn	pd
	64.871	65.655	ac	pd
	65.655	65.662	ppcn	pd
	65.662	65.748	br	pd
	65.748	65.784	ppcn	pd
	65.784	67.999	ac	pd
68	68.000	89.299	ac	pd
	70.130	70.138	ppcr	pd
	70.138	70.192	ac	pd
	70.192	70.197	ppcn	pd
	70.197	70.907	ac	pd
	70.907	70.911	ppcn	pd
	70.911	72.000	ac	pd
72	72.000	76.000	ac	
76	76.000	77.062	ac	pd
	77.062	77.066	ppcn	pd
	77.066	77.198	br	pd
	77.198	77.204	ppcn	pd
	77.204	78.120	ac	pd
	78.120	78.122	ppcn	pd
	78.122	78.167	br	pd
	78.167	78.172	ppcn	pd
	78.172	80.000	ac	pd
80	80.000	84.000	ac	pd
84	84.000	86.746	ac	pd
	86.746	86.749	ppcn	pd
	86.749	87.757	ac	pd
	87.757	87.761	ppcn	pd
	87.761	88.000	ac	pd
88	88.000	92.000	ac	
92	92.000	92.810	ac	
	92.810	92.813	ppcn	
	92.813	92.959	br	

	92.959	92.965	ppcn
	92.965	94.746	ac
	94.746	95.097	pcr
	95.097	95.103	ppcn
	95.103	95.156	br
	95.156	95.161	ppcn
	95.161	95.380	pcr
	95.380	96.000	ac
96	96.000	96.338	ac
	96.338	96.698	pcr
	96.698	97.903	ac
	97.903	98.184	pcr
	98.184	99.367	ac
	99.367	99.364	ppcn
	99.364	99.487	ac
	99.487	99.492	ppcn
	99.492	99.665	ac
	99.665	99.945	pcr
	99.945	100.000	ac
100	100.000	103.999	ac
104	104.000	107.965	ac
	107.965	107.971	ppcn
	107.971	107.997	ac
108	108.000	111.999	ac
112	112.000	113.111	ac
	113.111	113.115	ppcn
	113.115	113.144	br
	113.144	113.153	ppcn
	113.153	114.350	ac
	114.350	114.361	ppcn
	114.361	114.934	br
	114.934	114.942	ppcn
	114.942	116.000	ac
116	116.000	117.726	ac
	117.726	117.732	ppcn
	117.732	117.754	br
	117.754	117.759	ppcn
	117.759	119.990	ac
120	120.000	122.227	ac
	122.227	122.234	ppcr
	122.234	122.369	br
	122.369	122.376	ppcn
	122.376	123.080	ac
	123.080	123.087	ppcn
	123.087	124.000	ac
124	124.000	124.325	ac

	124.325	124.329	ppcn
	124.329	128.000	ac
128	128.000	128.714	ac
	128.714	128.720	ppcn
	128.720	128.761	br
	128.761	128.767	ppcn
	128.767	130.897	ac
	130.897	131.170	pcr
	131.170	132.000	ac
132	132.000	134.771	ac
	134.771	134.796	br
	134.796	136.000	ac
136	136.000	136.610	ac
	136.610	136.623	pcn
	136.623	136.675	br
	136.675	136.687	ppcn
	136.687	140.000	ac
140	140.000	144.000	ac
144	144.000	148.000	ac
148	148.000	152.000	ac
152	152.000	153.354	ac
	153.354	153.366	ppcn
	153.366	153.437	br
	153.437	153.454	ppcn
	153.454	154.638	ac
	154.638	154.810	pcr
	154.810	156.000	ac
156	156.000	158.948	ac
	158.948	160.000	pcr
160	160.000	164.000	pcr
164	164.000	164.887	pcr
	164.887	167.665	ac
	167.665	167.682	br
	167.682	168.000	ac
168	168.000	172.000	ac
172	172.000	176.000	ac
176	176.000	177.049	ac
	177.049	177.061	ppcn
	177.061	178.578	ac
	178.578	178.600	ppcn
	178.600	180.000	ac
180	180.000	184.000	ac
184	184.000	188.000	ac
188	188.000	192.000	ac
192	192.000	192.874	ac
	192.874	192.881	ppcn

	192.881	196.000	ac
196	196.000	197.136	ac
	197.102	197.144	ppcr
	197.144	197.158	ac
	197.158	197.163	ppcn
	197.163	197.166	ac
	197.166	197.170	ppcn
	197.170	200.000	ac
200	200.000	204.000	ac
204	204.000	205.579	ac
	205.579	205.583	ppcn
	205.583	208.000	ac
208	208.000	208.897	ac
	208.897	208.902	ppcn
	208.902	208.904	ac
	208.904	208.908	ppcn
	208.908	208.910	ac
	208.910	208.913	ppcn
	208.913	209.470	ac
	209.470	209.517	ppcn
	209.517	209.546	br
	209.546	209.607	ppcr
210	209.607	210.000	ac

Pavement type codes

ac	asphalt
pcr	reinforced concrete
ppcr	reinforced concrete patch
pcn	non-reinforced concrete
ppcn	non-reinforced concrete patch
br	bridge
un	unknown

Note codes

pd	poor data
vpd	very poor data

TABLE1b

West Bound I-70

Surface Type

Westbound

Cont. Mile Mark	Start	End	Surface type	Notes
	24	21.652	ac	
	21.65221	21.643	ppcn	
	21.6433	21.608	br	
	21.60766	21.599	ppcn	
	21.59933	21.588	ac	
	21.5877	21.581	ppcn	
	21.58073	20.427	ac	
	20.42679	20.400	ppcn	
	20.40005	20.371	br	
	20.37138	20.340	ppcn	
	20.3402	20.000	ac	
	28	25.283	ac	pd
	25.28277	25.179	br	
	25.17869	25.158	ppcn	
	25.15779	24.427	ac	
	24.42668	24.422	ppcn	
	24.42204	24.395	br	
	24.39476	24.373	ppcn	
	24.37329	24.000	ac	
	32	29.571	ac	pd
	29.5714	29.567	ppcn	
	29.56724	29.545	br	
	29.54488	29.374	ac	
	29.3739	29.346	br	
	29.3456	29.334	ppcn	
	29.33372	28.000	ac	
	36	33.562	ac	vpd
	33.56204	33.552	ppcn	
	33.55177	33.511	br	
	33.51109	33.501	ppcn	
	33.50083	32.000	ac	
	40	38.061	ac	vpd
	38.06092	37.719	un	
	37.71941	36.000	ac	
	44	40.000	ac	pd
	48	47.180	ac	pd
	47.17977	47.176	ppcn	

47.17648	47.099	ac
47.09867	47.096	ppcn
47.09577	47.087	ac
47.0865	47.083	ppcn
47.08284	46.830	ac
46.8297	46.816	ppcn
46.81618	45.516	ac
45.51632	45.512	ppcn
45.51207	45.439	ac
45.4387	45.432	ppcn
45.43233	45.418	ac
45.41804	45.410	ppcn
45.40993	45.385	ac
45.38463	45.367	ppcn
45.36726	45.336	ac
45.33598	45.332	ppcn
45.33154	45.325	ac
45.32458	45.320	ppcn
45.31976	45.288	ac
45.2879	45.276	ppcn
45.27612	45.038	ac
45.03804	45.035	ppcn
45.03495	44.830	ac
44.8297	44.826	ppcn
44.82584	44.643	ac
44.6426	44.640	ppcn
44.6399	44.294	ac
44.29369	44.290	ppcn
44.28983	44.282	ac
44.28191	44.278	ppcn
44.27844	44.000	ac
52	50.460	ac
50.45993	50.413	br
50.41315	49.502	ac
49.50239	49.412	ppcr
49.41155	49.372	br
49.37195	49.262	ppcr
49.26208	48.821	ac
48.82087	48.818	ppcn
48.81776	48.811	ac
48.81058	48.807	ppcn
48.80709	48.000	ac
56	54.350	ac
54.35035	54.346	ppcn
54.34609	54.325	br
54.32537	54.321	ppcn

54.32131	52.801	ac	
52.80059	52.795	ppcn	
52.79498	52.000	ac	
60	59.470	ac	
59.46973	59.465	ppcn	
59.46451	55.998	ac	
64	62.589	ac	pd
62.58925	62.576	ppcn	
62.57589	62.295	ac	
62.29537	62.293	ppcn	
62.29265	60.800	ac	
60.79982	61.956	ppcn	
61.9556	61.725	ac	
61.72464	61.712	ppcn	
61.71167	60.003	ac	
68	65.730	ac	pd
65.72967	65.644	br	
65.64449	64.760	ac	
64.76032	64.757	ppcn	
64.75664	64.010	ac	
64.00994	64.005	ppcn	
64.0051	64.004	ac	
72	69.130	ac	
69.13043	69.125	ppcn	
69.12461	69.108	ac	
69.10753	69.101	ppcn	
69.10074	68.426	ac	
68.42628	68.422	ppcn	
68.42201	68.000	ac	
76	72.795	ac	
72.79457	72.780	ppcr	
72.78019	72.000	ac	
80	78.245	ac	
78.24474	79.994	ppcn	
79.99395	79.985	ac	
79.98465	79.980	ppcn	
79.98038	79.933	br	
79.9327	79.926	ppcn	
79.9263	78.990	ac	
78.98964	78.853	br	
78.85279	77.757	ac	
84	80.002	ac	
88	87.795	ac	
87.79481	87.792	ppcn	
87.79209	87.579	ac	
87.57893	87.567	ppcn	

87.5669	87.548	ac
87.54768	87.543	ppcn
87.54341	87.689	ac
87.68901	87.547	pcr
87.54749	87.543	ppcn
87.54321	86.746	pcr
86.74612	84.677	ac
84.67671	84.674	ppcn
84.6738	84.657	ac
84.6571	84.654	ppcn
84.6538	84.000	ac
92	88.000	ac
96	95.370	ac
95.36989	95.162	pcr
95.16196	95.144	ppcn
95.14422	95.091	br
95.091	95.070	ppcn
95.06952	94.737	pcr
94.73702	92.942	ac
92.94229	92.933	ppcr
92.93342	92.788	br
92.78777	92.000	ac
100	99.940	ac
99.94027	99.659	pcn
99.65925	99.534	ac
99.53358	99.528	ppcn
99.52834	99.418	ac
99.41818	99.415	ppcn
99.41488	98.637	ac
98.6368	98.634	ppcn
98.6337	98.381	ac
98.38138	98.377	ppcn
98.37673	98.354	ac
98.35384	98.347	ppcn
98.34744	98.176	ac
98.17639	97.895	pcn
97.89498	96.690	ac
96.69004	96.330	pcr
96.3297	96.000	ac
104	102.733	ac
102.7331	102.730	ppcn
102.7298	100.000	ac
108	104.000	ac
112	108.299	ac
108.2989	108.293	ppcn
108.2931	108.000	ac

116	114.841	ac	
114.8406	114.348	br	
114.348	113.129	ac	
113.1289	113.099	br	
113.0994	112.000	ac	
120	117.757	ac	
117.7575	117.736	br	
117.7358	116.000	ac	
124	122.700	ac	
122.6997	122.695	ppcn	
122.6953	122.569	ac	
122.5688	122.566	ppcn	
122.5655	122.368	ac	
122.3676	122.355	ppcn	
122.3554	122.224	br	
122.2241	122.213	ppcn	
122.2135	121.226	ac	
121.226	121.198	br	
121.1983	120.000	ac	
128	127.091	ac	vpd
127.0909	127.061	br	
127.0607	126.943	ac	
126.9425	126.338	br	
126.3376	125.618	ac	
125.6182	125.602	ppcn	
125.6019	125.562	br	
125.5616	125.551	ppcn	
125.5508	124.503	ac	
124.503	124.444	ppcn	
124.4445	124.025	ac	
124.0249	124.020	ppcn	
124.0197	124.000	ac	
132	130.343	ac	pd
130.343	130.297	br	
130.2971	128.769	ac	
128.7693	128.732	br	
128.7317	128.012	ac	
136	134.784	ac	pd
134.7844	134.760	br	
134.7598	132.000	ac	
140	138.432	ac	
138.432	138.428	ppcn	
138.4281	138.420	ac	
138.4201	138.414	ppcn	
138.4145	138.257	ac	
138.2572	138.253	ppcr	

138.2533	136.685	ac	
136.6853	136.632	br	
136.6319	136.000	ac	
144	140.000	ac	
148	144.000	ac	
152	150.354	ac	
150.3539	150.347	ppcn	
150.3475	149.806	ac	
149.806	149.798	ppcn	
149.7984	149.001	ac	
149.0007	148.994	ppcn	
148.9944	148.000	ac	
156	153.480	ac	
153.4796	153.410	br	
153.4096	151.995	ac	
151.995	156.000	ac	
164	160.000	ac	
168	164.000	ac	
172	168.191	ac	
168.1909	168.121	br	
168.1209	168.000	ac	
176	172.000	ac	
180	179.237	ac	
179.2369	179.233	ppcn	
179.2328	179.153	ac	
179.1529	179.148	ppcn	
179.1478	176.000	ac	
184	181.595	ac	
181.5952	181.443	pcr	
181.4428	180.000	ac	
188	185.372	ac	
185.3722	185.351	ppcn	
185.3506	185.115	ac	
185.115	185.107	ppcn	
185.1075	184.906	ac	
184.9057	184.899	ppcn	
184.8991	184.000	ac	
192	188.000	ac	
196	193.104	ac	
193.1042	193.101	ppcn	
193.1007	192.869	ac	
192.8692	192.866	ppcn	
192.8662	192.000	ac	
191.9998	196.000	ac	pd
195.9999	200.000	ac	pd
199.9999	204.000	ac	

210	209.602	ac
209.602	209.543	ppcr
209.5429	209.516	br
209.5156	209.465	ppcr
209.4653	208.301	ac
208.3014	208.297	ppcn
208.2973	208.000	ac

Pavement type codes

ac	asphalt
pcr	reinforced concrete
ppcr	reinforced concrete patch
pcn	non-reinforced concrete
ppcn	non-reinforced concrete patch
br	bridge
un	unknown

Note codes

pd	poor data
vpd	very poor data

TABLE 2a

East Bound I-70

Radar Anomalies

Eastbound Anomalies

Mile Marker from	Mile Marker to	type	Notes
23.230	23.240	wo	
26.627	26.633	daac	Patch?
27.310	27.359	rs	
29.500	29.509	iapcn,dcpcn	
30.668	30.686	tnac	
31.356	31.462	tnac	
37.170	37.176	iasb	
38.265	38.273	iaac	
42.651	42.654	dcac, iaac	
43.036	43.061	rsac	
43.443	43.494	dcac, iaac	
43.573	43.693	dcac, iaac	
43.983	43.994	rsac	
44.001	44.008	rsac	
46.078	46.100	thac,darn	
49.327	49.353	dcac	
49.537	49.548	dcsb	
50.118	50.135	rsac	
50.600	50.616	rsac	
52.429	52.541	daac, dcac,rsac	
52.580	52.588	iaac	
52.746	52.736	rsac	
52.887	52.939	rsac, dcac	
54.229	54.272	rsac,rsppcn,dcac	
54.376	54.420	dcac,rsac	
54.401	54.409	iasb	
55.324	55.492	dcas,rsac	
55.728	55.907	rsac	
56.096	56.137	daac	
56.235	56.270	iasb	
56.480	56.512	iasb	
56.989	56.994	iasb	
56.997	57.012	iasb	
57.096	57.108	rsppcn	
58.566	58.594	iarn	
59.069	59.081	dcac	

59.398	59.424	daac	ppca?
64.582	64.853	rsac	
64.878	65.148	ppcn	multiple small patches
66.827	66.832	thac	
69.967	69.981	rsac, daac	
72.578	72.583	wosb	
74.265	74.273	daac,rsac	
74.652	74.558	iaac	
74.625	74.655	rsac	
76.258	76.318	dcac	
81.524	81.783	tnac	
90.721	90.758	iasb	
92.509	92.554	dcrn, iarn	
95.919	93.964	wosb	
98.326	98.351	dcac	
98.649	98.654	iaac	
103.493	103.521	dcac	
103.684	103.698	dcac	
113.951	113.960	wosb	
115.214	115.232	iapcr	
117.674	117.693	thac, rsac	
120.546	120.464	wosb, iappcr	
123.271	123.285	wosb, iappcr	
123.757	123.765	wosb, iappcr	
124.164	124.184	wosb	
124.472	124.542	rsac	
125.599	125.630	iarn	
127.065	127.083	rsac	?
128.442	128.702	thac	
135.912	135.924	iasb, rsac	
136.168	136.212	iasb, wosb?	
137.249	137.266	iasb	
137.288	137.318	iasb	
139.872	139.893	wosb	
140.195	140.213	wosb	
140.390	140.425	wosb	
142.803	142.844	wosb	
147.761	147.773	wosb	
147.820	147.846	wosb	
169.366	169.426	thac	
176.648	176.672	wosb	
178.992	179.208	thac	
180.918	181.228	thac	
185.058	185.066	wosb	
185.547	185.555	wosb, iasb	

206.104	206.475	daac
208.854	208.965	tnac

Anomaly code		**Interface suffix code**	
wo	washout	sb	base coarse
ia	increase amplitude	ac	asphalt
da	decrease amplitude	pcn	nonreinforced concrete
th	thickening	pcr	reinforced concrete
tn	thinning	rn	reinforcement
dc	discontinuous		
rs	very rough surface		

TABLE2b

West Bound I-70

Radar Anomalies

Westbound Anomalies

Mile Marker from	Mile Marker to	type	Notes
29.55788	29.33312	thac	
38.35111	38.28608	tnac	
43.9594	43.92821	thac	
49.59029	49.58697	iarn	
49.60896	49.60434	iarn	
50.22413	50.21415	wosb	
58.64805	58.62173	iarn	
59.49225	59.48725	iasb	mult-diffraction
61.82464	61.81224	iasb	
62.05101	62.04545	iasb	
62.37029	62.3677	iasb	
62.64903	62.63811	iasb	
64.25323	64.23602	daac	
64.63951	64.51014	dcac	
66.47486	66.23184	dcac	
66.47912	66.46302	rsac	
70.23084	70.19849	iaac	
73.33718	73.32721	tnac	
76.95675	76.94713	wosb	
80.33408	80.3091	iaac	
81.05631	81.04928	daac (Rn)	
81.95378	81.7258	tnac	
85.93265	85.7403	tnac	
87.8023	87.79731	iarn	
88.09122	88.07919	rsac	
88.95336	88.94734	iasb	
94.32918	94.32135	iarn	
97.43517	97.32346	dcac	
97.88514	97.8402	dcac	
99.17385	98.94766	mult-patches	
100.6227	100.6003	iaac	
100.9732	100.9682	iasb	
101.0111	101.0033	wosb (iasb)	
102.9055	102.8835	dcac	

103.2549	103.2066	dcac
105.9358	105.8515	iapcr base
108.9096	108.8997	iaac
111.1879	111.179	wosb
117.8282	117.8156	iarn
117.9288	117.9201	ia-pcn
120.7302	120.7216	wosb
122.0723	122.0544	wosb
122.5861	122.5798	wopcr base
123.017	123.0057	woac (pcr)
131.204	130.976	tnac
132.7331	132.7253	iapcr base
132.852	132.8219	thac
137.0673	137.0607	wosb
137.8254	137.8121	wosb
137.8528	137.8415	wosb
140.4037	140.3884	iasb
145.7696	145.7094	rsac (thac)
145.9867	145.9484	rsac
149.9547	149.9384	thac
155.6473	155.4827	tnac
161.7786	161.7732	thac
166.1633	166.1528	thac
167.7181	167.6989	iarn (rs at ends)
169.9395	169.9242	wosb
170.1219	170.1102	wosb (iapcr)
171.8365	171.8265	iapcr (wosb)
172.2815	172.2672	wosb
172.6534	172.6382	wosb
173.3262	173.2905	wosb
173.7897	173.7736	wosb
174.02	174.0002	wosb
174.2654	174.2526	wosb
176.7845	176.7671	wosb
179.8302	179.8206	wosb
180.7118	180.6974	wosb
180.7468	180.7355	wosb
181.9371	181.8785	thac
182.5097	182.3899	tnac
184.1968	184.186	iarcr
184.8411	184.8213	daac
185.0076	184.8655	mult-patches
185.5761	185.4858	mult-patches
186.8315	186.8267	iasb
196.4254	196.4169	iaac

196.8694	196.853	dcac
198.1918	198.1824	dcac
208.8515	208.7555	thac

Anomaly code	
wo	washout
ia	increase amplitude
da	decrease amplitude
th	thickening
tn	thinning
dc	discontinuous
rs	very rough surface

Interface suffix code	
sb	base coarse
ac	asphalt
pcn	nonreinforced concrete
pcr	reinforced concrete
rn	reinforcement

TABLE 3a

Eastbound

Tenth Mile Anomalies

Mile Marker from	to	type	Notes
29.5		iapcn,dcpcn	
43.6		dcac, iaac	
44.0		rsac	
46.1		thac,darn	
50.6		rsac	
52.5		daac, dcac,rsac	
52.9		rsac, dcac	
54.4		dcac,rsac	
55.4		dcas,rsac	
55.8	55.9	rsac	
56.1		daac	
56.5		iasb	
57.0		iasb	
57.1		rsppcn	
59.4		daac	ppca?
64.6	64.8	rsac	
64.9	65.1	ppcn	multiple small patches
76.3		dcac	
81.5	81.7	tnac	
94.0	95.9	wosb	
103.5		dcac	
103.7		dcac	
120.5		wosb, iappcr	
124.5		rsac	
125.6		iarn	
128.5	128.7	thac	
137.3		iasb	
140.2		wosb	
140.4		wosb	
169.4		thac	
179.0	179.2	thac	
181.0	181.2	thac	
206.2	206.4	daac	
208.9		tnac	

Anomaly code		Interface suffix code	
wo	washout	sb	base coarse
ia	increase amplitude	ac	asphalt
da	decrease amplitude	pcn	nonreinforced concrete
th	thickening	pcr	reinforced concrete
tn	thinning	rn	reinforcement
dc	discontinuous		
rs	very rough surface		

TABLE 3b

Westbound

Tenth Mile Anomalies

Mile Marker from	to	type	Notes
29.4	29.5	thac	
38.3		tnac	
64.6		dcac	
66.3	66.4	dcac	
70.2		iaac	
81.8	81.9	tnac	
85.8	85.9	tnac	
87.8		iarn	
97.4		dcac	
99	99.1	mult-patches	
100.6		iaac	
102.9		dcac	
105.9		iapcr base	
108.9		iaac	
131	131.2	tnac	
155.6	155.6	tnac	
167.7		iarn (rs at ends)	
173.3		wosb	
174		wosb	
180.7		wosb	
181.9		thac	
182.4	182.5	tnac	
184.9	185	mult-patches	
185.5		mult-patches	
208.8		thac	

Anomaly code	
wo	washout
ia	increase amplitude
da	decrease amplitude
th	thickening
tn	thinning
dc	discontinuous
rs	very rough surface

Interface suffix code	
sb	base coarse
ac	asphalt
pcn	nonreinforced concrete
pcr	reinforced concrete
rn	reinforcement

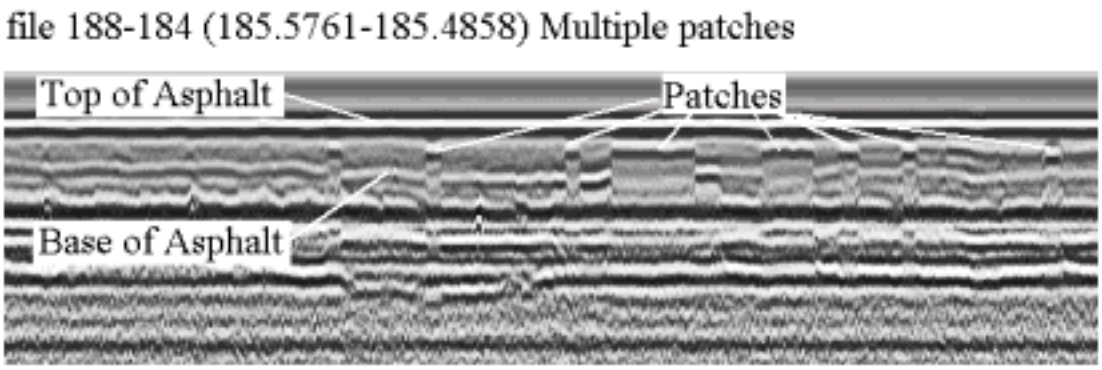

Figure 3. Example GPR profile at 185.5 mile westbound showing radar signature of multiple patches in the pavement.

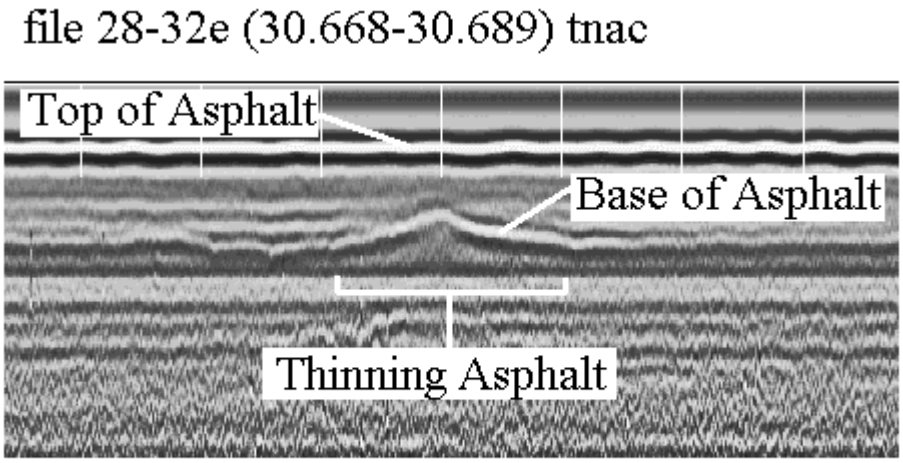

Figure 4. Example GPR profile at 30.7 mile eastbound showing radar signature of anomalously thin area in asphalt pavement.

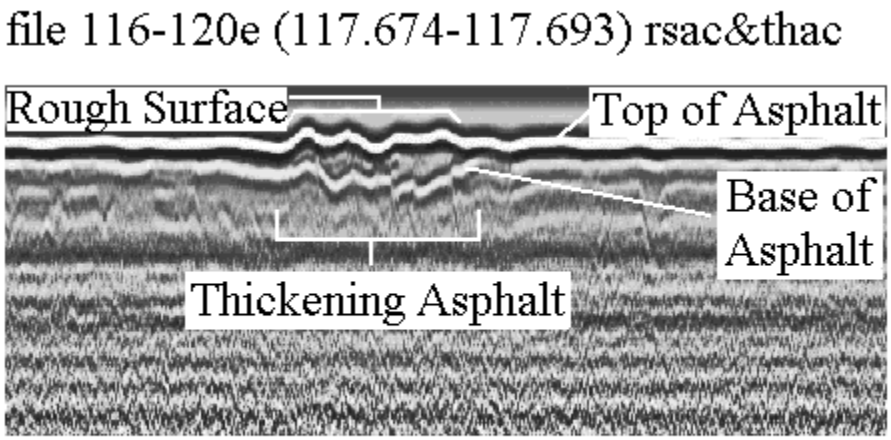

Figure 5. Example GPR profile at 117.7 mile eastbound showing radar signature of anomalously thick area in asphalt pavement, here associated with very rough pavement surface.

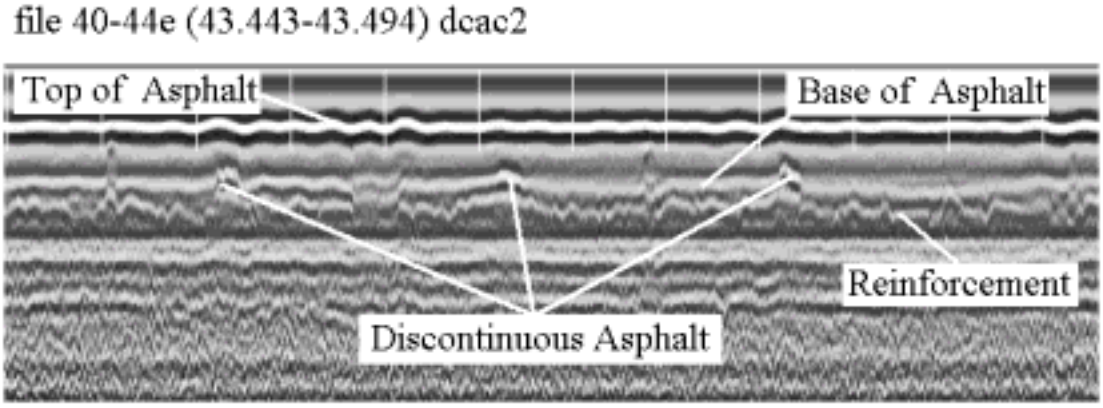

Figure 6. Example GPR profile at 43.5 mile eastbound showing radar signature of discontinuous area in asphalt pavement.

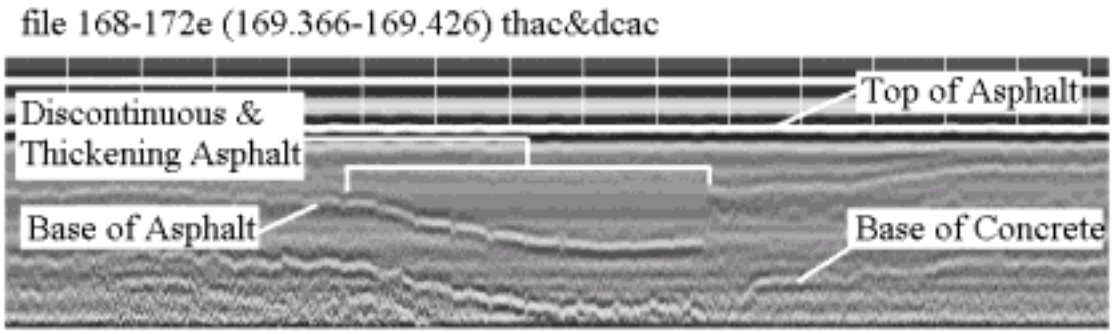

Figure 7. Example GPR profile at 169.4 mile eastbound showing radar signature of thickening asphalt pavement area associated here with a discontinuity in the asphalt layer.

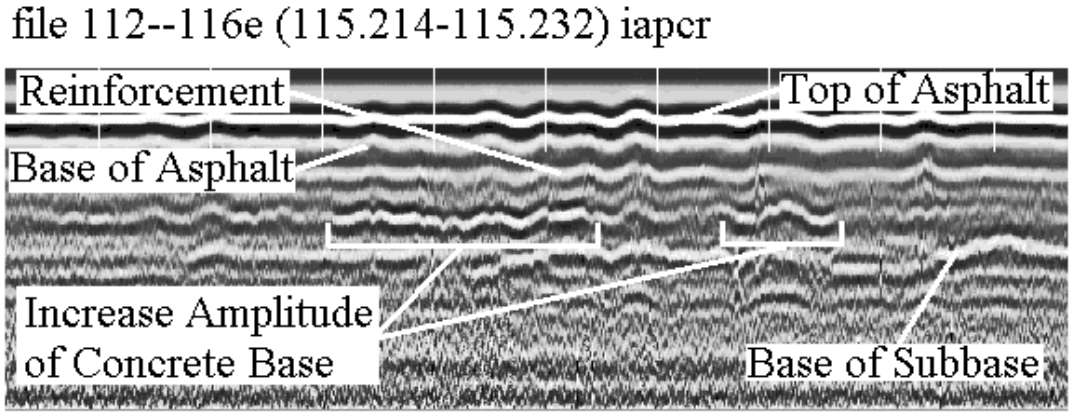

Figure 8. Example GPR profile at 115.2 mile eastbound showing increased amplitude radar signature at base of concrete interface.

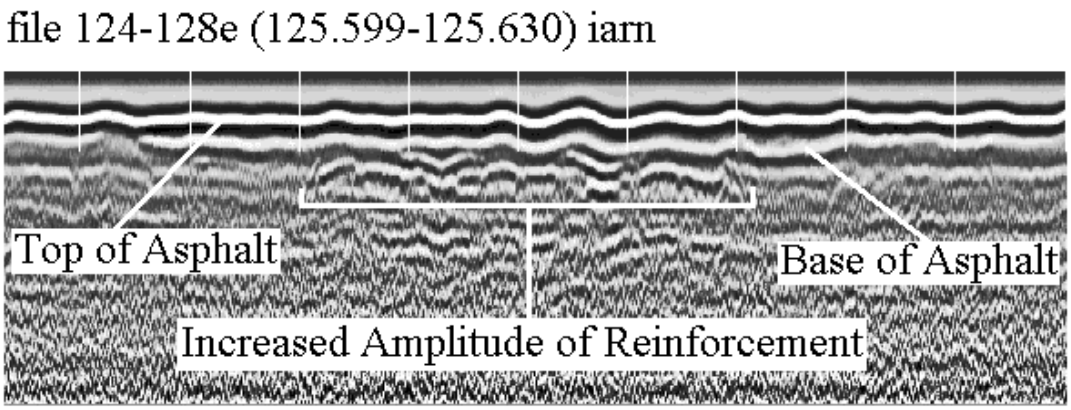

Figure 9. Example GPR profile at 125.6 mile eastbound showing increased amplitude radar signature of concrete reinforcement.

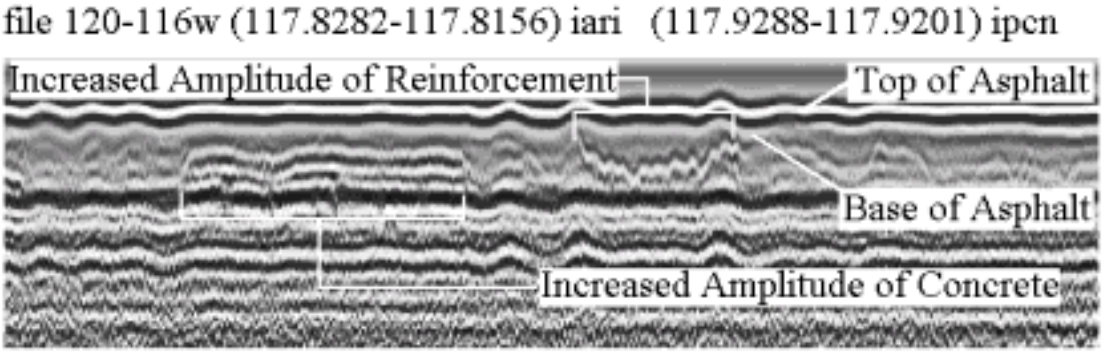

Figure 10. Example GPR profile at 117.8 mile westbound showing increased amplitude radar signature of both the concrete reinforcement and base of concrete interface.

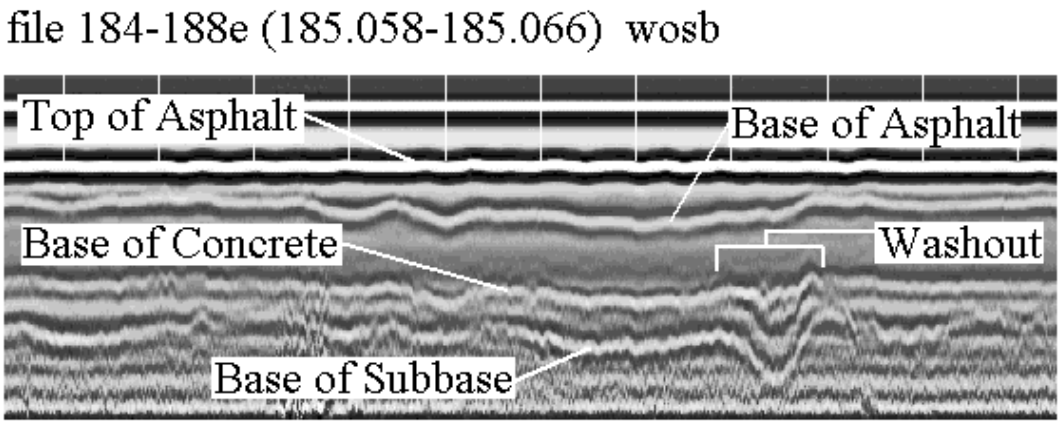

Figure 11. Example GPR profile at 185 mile eastbound showing radar signature of possible washout in base course affecting also the base of concrete reflection.

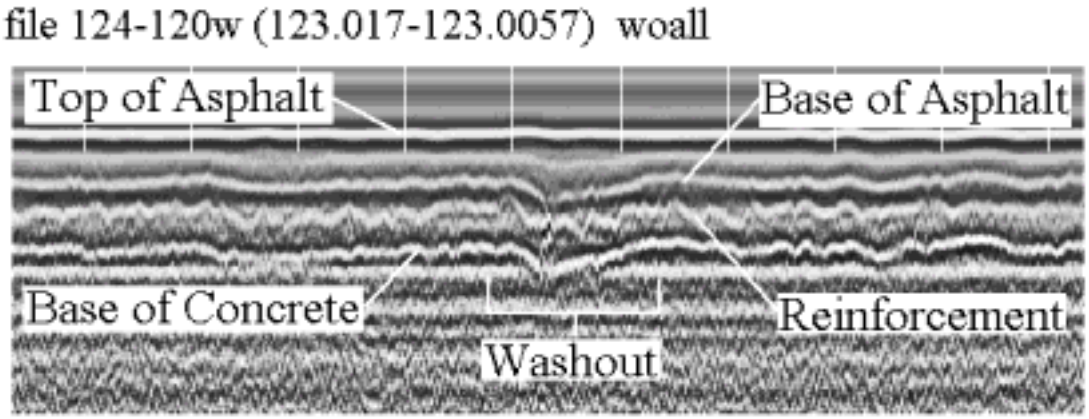

Figure 12. Example GPR profile at 123 mile westbound showing radar signature of possible washout affecting all pavement layers (base of concrete, concrete reinforcement and asphalt overlay).

SUGGESTIONS FOR FUTURE WORK

1) Get core information from various anomalous regions and correlate findings with radar signatures to aid in future automatic identification of problem areas. This core information could be obtained at areas where previous geotechnical ground truth were acquired (e.g., falling weight deflectometer) for further comparison.
2) Re-survey area of I70 currently being resurfaced for comparison with previous profile. In addition, get information on pavement layers that were stripped prior to resurfacing (during milling process or other) for correlation with radar profile in this report.
3) Get core information from various points along the I70 corridor in order to adjust dielectric constants along the length of the surveyed portion of I70.
4) Collect data over a small portion of the previously surveyed area (in area untouched by MoDOT maintenance) in which good and bad areas exist (areas easy to interpret and areas more difficult to interpret). With an associated calibration file carefully acquired, compare results of automated technique (desired) and interpreter-based technique (as used in this study) for more definitive investigation of when/where the automated technique breaks down.

CONCLUSIONS

In this report we have applied the ground penetrating radar technique to high resolution roadway pavement analysis along 380 miles of Interstate 70 across Missouri. Through a comparison with history information, we have demonstrated the utility of the tool for determining pavement layer thickness estimates in a rapid fashion and across a large portion of

roadway. We have produced pavement layer profiles based on the GPR data which can be used to revise and update design history information. In addition, we have delineated areas of anomalous radar signals, which may be indicative of roadway problems and can be further investigated. Because completely automated techniques need to be used carefully, in particular when reflections from specific layers (e.g., concrete to base coarse) are not clearly defined, interpreter input is necessary to help guide the analysis and keep it as accurate as possible when faced with such a large quantity of data covering such widely variable roadway surface.

REFERENCES CITED

ASTM Designation D 4748 - 87 (1995), Standard Test Method for Determining the Thickness of Bound Pavement Layers Using Short-Pulse Radar.

Cardimona, S., M. Roark, D. J. Webb and T. Lippincott, 1998. Ground penetrating radar, *Highway Applications of Engineering Geophysics with an Emphasis on Previously Mined Ground,* pp. 41-56.

Daniels, D., 1996. Surface-penetrating radar, Inst. Electr. Eng.

Ground Penetrating Radar Surveys of

Select Test Pavements in Missouri

Steve Cardimona[*], Brent Willeford[*], John Wenzlick[+], Neil Anderson[*]

[*]The University of Missouri-Rolla, Department of Geology and Geophysics

[+]The Missouri Department of Transportation

Section 3

EXECUTIVE SUMMARY

Ground penetrating radar (GPR) instrumentation and techniques applied to roadway pavement analysis offers a methodology to perform detailed assessment of layering in roadways. This study summarizes current methodologies for pavement assessment using GPR, and applies the techniques to 35 test pavements of the Strategic Highways Research Program Long Term Pavement Performance sites across the state of Missouri. The result is a correlation of GPR reflection character and GPR-derived layer thickness estimates with design information for each test pavement. Asphalt surface layering proved to be the easiest to image, creating a strong signal in the GPR data. Not as consistently clear is the concrete-to-baserock interface where the dielectric contrast between these two media is not always strong enough to create a high amplitude reflected signal. Unbonded concrete overlays proved to be more easy to interpret, with a clear interface at base of overlay. Reinforcement within concrete pavements creates another interface within the pavement layering that is normally quite distinct, and the difference between rebar reinforcement and continuous reinforcement can be noted in the radar data. Test pavements from completely different sites that had similar design show similar radar reflection signatures. This consistency demonstrates that radar can be used to monitor quality of test pavement performance over time, so that variations in the pavement reflection signature for a given pavement type can be interpreted as potential problems in the pavement.

TABLE OF CONTENTS

LIST OF FIGURES

LIST OF TABLES

BACKGROUND AND METHODOLOGY

Ground penetrating radar (Daniels, 1996; Cardimona, et al., 1998) uses a radio wave source to transmit a pulse of electromagnetic energy through the roadway pavement. Reflected energy, originating at interfaces between layers with different dielectric properties or of differing conductivities is received and recorded for analysis of the pavement. GPR data consist of a) changes in reflection strength, b) changes in arrival time of specific reflections, c) source wavelet distortion, and d) signal attenuation. For roadway analysis, these different GPR signatures can be used as discriminants for detecting poor quality pavements (e.g., insufficient asphalt overlay, variable concrete pavement or base coarse).

Various GPR tools and methodologies exist, but most modern antennae for roadway analysis are designed as air-launched horn antennae with nominal peak frequencies of around 1.0GHz, offering the ability to obtain high resolution images of pavement layers. Data can be collected by monostatic antennae, which means the same antennae acts both as transmitter and receiver, or with bistatic antennae where the transmitting and receiving antennae are separate. Horn antennae designed for high speed road pavement imaging are normally mounted behind a truck or van. Collection of this data is fast and not disruptive to traffic patterns, with reasonable collection speeds up to 50mph.

The standard methodology for the automatic interpretation of GPR data over pavements (ASTM D 4748-87) measures reflection amplitudes, scaled with an initial amplitude calibration. The contrast in dielectric constant (relative dielectric) across an interface is what produces the reflection at an interface between two layers, so the reflection amplitudes can be directly related to the dielectric values. Once all layer dielectric constants are determined, the layer thicknesses can be calculated using the radar wave velocities (based also on the dielectric constants) and the measured travel time of each interface reflection. This automatic interpretation must include core

samples for each different pavement along the GPR survey in order to best determine dielectric constants (ASTM D 4748-87).

User guided interpretation uses similar concepts to any automated interpretation scheme, but the amplitude of reflection events is not formally used to measure dielectric constants. Instead, after interface reflections (and their associated travel times) are picked from the data, direct ground truth is used to calibrate the signal. Dielectric constants are determined from this ground truth, and layer thickness estimates along the whole survey are then produced. Often automated interpretation procedures need to be guided by the user, especially when all layer interfaces are not distinct, and thus user guided interpretation can be more robust overall. In the absence of ground truth in the form of core samples, test pavement design information is used for calibration of the radar data, with an associated loss in confidence in the resulting interpretation (Cardimona et al., 1999).

TEST PAVEMENT SITES AND FIELD PROCEDURES

In Fall 1998, the Department of Geology and Geophysics at UMR acquired GPR data along numerous test pavements in Missouri (Table 1), including pavements designated for general pavement studies (GPS test pavements) and pavements designated for specific pavement studies (SPS test pavements) within the Strategic Highways Research Program. All data were collected using in-house, state-of-the-art equipment. Geophysical Survey Systems, Inc manufactures the instruments and the software for analysis of the data. The bulk of these data were acquired using single-channel 1.0GHz air-launched bistatic horn antennae (Geophysical Survey Systems, Incorporated antenna model #4208). Additional data were collected at the Ralls County site (SPS-8A test section) using the 1.5GHz ground-coupled antenna (Geophysical Survey Systems, Incorporated antenna model #5100). In general, data acquisition included lead in sections

adjoining the test pavements. Key acquisition parameters are the scans-per-meter and the time recording length (time window). The scans/m defines the horizontal sampling. The time window determines (with the radar velocity) the maximum depth imaging expected.

All single-channel horn data for the Northwest test pavements (Table 1a) were collected at 5 radar scans/m (1.5 scans /ft) with a 25 ns time recording window. The horn data for the Ralls County test pavement (Table 1b) were collected at 10 scans/m (3.0 scans/ft) with a 20ns time recording window. We used the 1.5GHz ground-coupled antenna to acquire additional data over the concrete portions of test pavement SPS-8A. Five profile lines, spaced 5ft apart, were collected from Station 195 to Station 208 to supplement the air-launched data acquired over the same pavement. The ground-coupled radar data were collected at 10 scans/m (3.0 scans/ft) with a 20ns time recording window.

Table 1a (Northwest Missouri)

Test Section	Date	Location	Length (ft)	Type of Pavement	Notes
295483	10/6	HWY 210	1250	3” ac / 9” rpccp (GPS-7B)	Poor reflection, Low confidence; Asphalt layer not interpreted (4” type III aggr. base)
294036	10/6	Hwy 435	1250	10” rpccp (GPS-4)	Poor reflection, Low confidence (4” type III aggregate base)
294069	10/6	Hwy 635	1250	3” ac / 10” rpccp (GPS-7B)	Poor reflection, Low confidence; Asphalt layer not interpreted (6” sand soil base)
295000	10/7	Hwy 35-N	1000	9” rpccp (GPS-4)	Poor reflection, Low confidence (4” type III aggr. base)
295058	10/7	Hwy 35-N	950	9” rpccp (GPS-4)	Poor reflection, Low confidence (4” bituminous base)
295081	10/7	Hwy 35-N	1125	9” rpccp (GPS-4)	Poor reflection, Low confidence (4” open graded bituminous base)
295091	10/7	Hwy 35-N	1050	9” rpccp (GPS-4)	Poor data **(File Not interpreted)** (4” cement treated aggregate base)
290607	10/7	Hwy 35-N	500	4”ac / 6” pccp (SPS-6)	
290659	10/7	Hwy 35-N	500	4”ac / 9” pccp (SPS-6)	
290660	10/7	Hwy 35-N	500	8”ac / 9” rpccp (SPS-6)	
290608	10/7	Hwy 35-N	500	8”ac / 9” rpccp (SPS-6)	
290662	10/7	Hwy 35-N	500	8”ac / rpccp (SPS-6)	Base of concrete not picked.
290664	10/7	Hwy 35-N	500	8”ac / rpccp (SPS-6)	Base of concrete not picked.
290663	10/7	Hwy 35-N	500	12”ac / rpccp (SPS-6)	Asphalt / concrete interface not clear. Base of concrete not picked.
290661	10/7	Hwy 35-N	500	12”ac / rpccp (SPS-6)	Base of concrete not picked.
290605	10/7	Hwy 35-N	1000	9” rpccp (SPS-6)	Poor data (multiple reflections) **(File Not interpreted)**

Test Section	Date	Location	Length (ft)	Type of Pavement	Notes
290601	10/7	Hwy 35-N	500	9” rpccp (SPS-6)	SPS-Control Section
290602	10/7	Hwy 35-N	1000	9” rpccp (SPS-6)	Discontinuous Reflections (medium Confidence)
290604	10/7	Hwy 35-N	500	4”ac / 9” rpccp (SPS-6)	
290603	10/7	Hwy 35-N	500	4”ac / 9” rpccp (SPS-6)	
290606	10/7	Hwy 35-N	500	4”ac / 9” rpccp (SPS-6)	
290666	10/7	Hwy 35-N	500	9” rpccp (SPS-6)	Poor reflection, Low confidence
290665	10/7	Hwy 35-N	500	5”ac / 9” rpccp (SPS-6)	
	10/7	Hwy 29 S Mound City	5 miles	4.75”ac/ 10” rpccp	
	10/7	Hwy 29 N Mound City	5 miles	5.75-6.75”ac/ 10” rpccp	
	10/8	Hwy 29 S Rock Port	See Fig. 1	Fiber-reinforced unbonded pccp	See Figure 1 for design

Table 1b (Ralls County)

Test Section	Date	Location	Length (ft)	Type of Pavement	Notes
SPS-8A	2/11	W. Service Rd Route 61	Stations 177-208	Varies	See Figure 2 for design

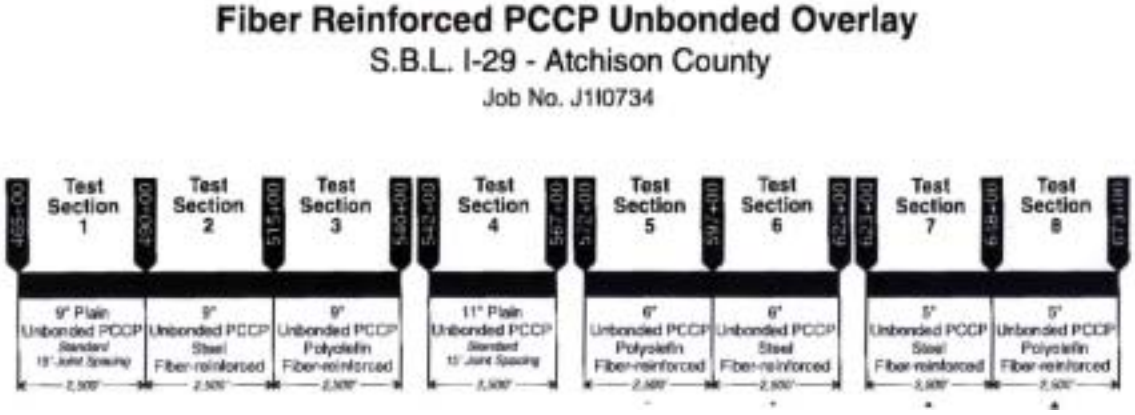

Figure 1. Design specs for test pavements on Highway 29, near Rockport, MO.

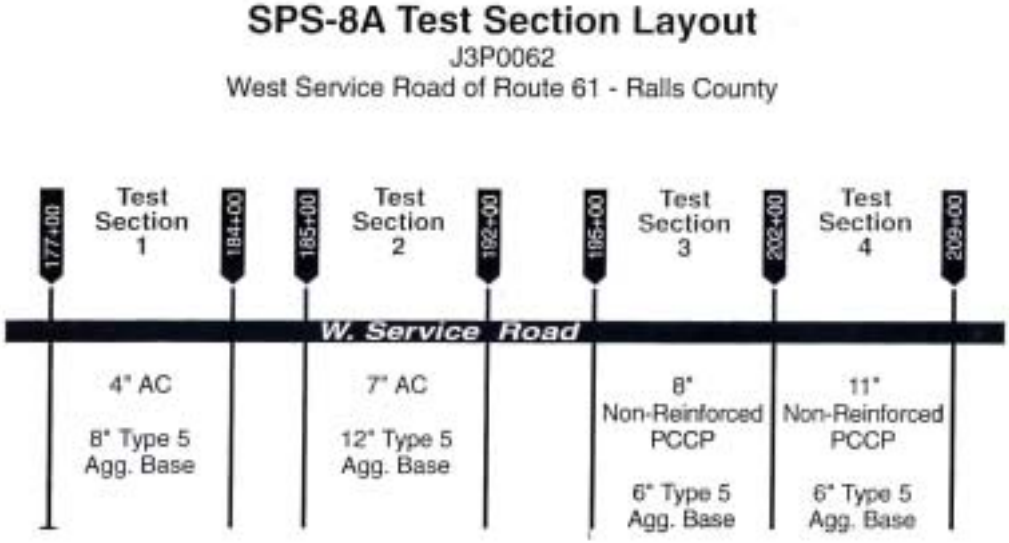

Figure 2. Design specs for test pavements on W. Service Rd., Highway 61, Ralls County.

PROCESSING AND INTERPRETATION

User guided interpretation procedures were chosen for this study. After interface reflections (and their associated travel times) are picked from the data, ground truth is used to calibrate the signal. Dielectric constants are determined from this ground truth, and layer thickness estimates along the whole survey are then produced. In the absence of ground truth in the form of core samples, test pavement design information (Table 1) was used for calibration of the radar data before layer thicknesses were interpreted. Where thickness of concrete was unspecified, a design of 9 inches was assumed. Where type of concrete (reinforced versus non-reinforced) was unspecified, reinforced concrete was assumed. Specific processing steps included:

1) **Filtering** applied to enhance signal/noise ratio in poor quality data (high and low frequencies cut off) -- Northwest mostly
2) **Stacking** applied to enhance signal/noise ratio in poor quality data (10 scan stack to enhance reflection events) -- Northwest mostly
3) **Layer** interpretation and **picking**
4) **Import** layer data **into spreadsheet**
5) **Two-way travel time** determined (time thickness)
6) **Estimate dielectric constants** using available ground truth
    - core data for W. Service Road, Hwy 61 Ralls County
    - core data for Hwy 29 Atchison County
    - design specs for the rest
7) **Estimate thickness** throughout section using dielectric values and two-way travel times
8) **Sorting**, averaging (over 10ft sections) and plotting data
    - 5ft intervals most northwest data
    - 15ft intervals Hwy 29, Atchison County
    - 25ft intervals in Ralls County

SUMMARY OF RESULTS

Figures 3-15 show example data from each different type of test pavement (Table 1). Labeled in each case are the interpreted layer interfaces. Appendix A includes an example of the data with all thickness information in tabular form for Site 295483. (Because of the large amount of data, the complete set of data for all sites is included in an Addendum to this report and can be obtained by special request.) Ten-foot sections were used to create the average thickness estimates in Appendix A. As already noted, having actual core data associated specifically with each GPR survey line is necessary for the most accurate dielectric estimates. Ideally, one would have a clear GPR marker below the surface for accurate correlation of the radar signal with depth. Without that, design thickness can be used (as done in this study), but will result in determination of dielectric values with lower confidence. Where estimated dielectric values appear low, the thickness of the layer may be incorrectly assumed (e.g., concrete layer thinner than design suggests). Estimated dielectric values that appear high may also be indicative of incorrect assumed thickness of the layer (e.g., asphalt layer thicker than design suggests). Dielectric values are also sensitive to data picks. When an interface is hard to pick because the reflection event is not clear, the associated dielectric calculated may be in error relative to the poor data quality and travel time pick.

Northwest

Figures 3-11 show example data from each different type of test pavement from the Northwest survey collection (Table 1a). Labeled in each case are the interpreted layer interfaces horizontal scale is the same in all at 16.4 ft/mark. Appendix A includes all thickness information

in tabular form. There are a couple noticeable inconsistencies in the GPR-derived dielectric values for some of these LTPP sites:

1) On very thin asphalt overlays (3 in, test pavements 294069 and 295483), the asphalt-concrete interface was not interpreted (e.g., Figure 4). The interpretation of a thin surface layer is more difficult because the surface reflection has the largest dominant wavelength (due to complete travel in air). This large wavelength makes the waveform in the radar signal longer and thus it would mask any reflection from the base of a thin surface layer.

2) On thin asphalt overlays (4 in, test pavements 290607, 290659, 290604, 290603 and 290606), our interpretation resulted in the determination of high asphalt dielectric values because the asphalt interface is hard to pick as separate from the surface reflection (Figure 5). As with note (1) above, the interpretation of a thin surface layer is more difficult because the surface reflection has the largest dominant wavelength, and so resolution of the first layer is more difficult.

3) Low concrete dielectrics determined (test pavements 295483, 294036 and 290602) could be due to incorrect time pick due to difficulty in interpretation of some base-of-concrete interfaces, but may also likely be due to different thickness (thinner) pavement than design specification suggests.

4) Unbonded overlays with Polyolefin fiber reinforcement within the concrete pavement yield a very strong reflection event (cf. Figure 1 and Figure 11). The Polyolefin is not as disruptive to radar investigation as steel reinforcement, which makes the base of concrete interface difficult to interpret even on unbonded overlays (cf. Figure 1 and Figure 11).

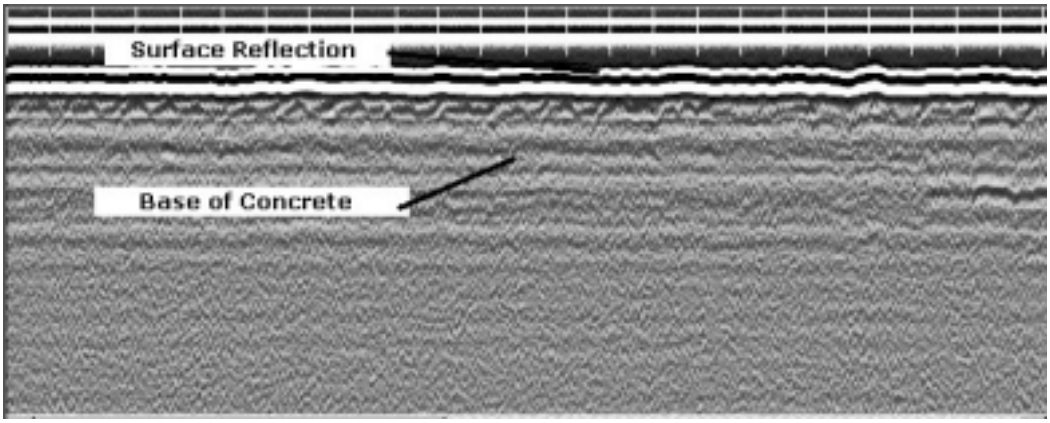

Figure 3. Portion of data from Hwy 35N, GPS-4 test pavement #295058, 9” reinforced Portland Concrete Cement Pavement over bituminous base. Concrete dielectric 8.2. Horizontal scale is 16.4ft/mark.

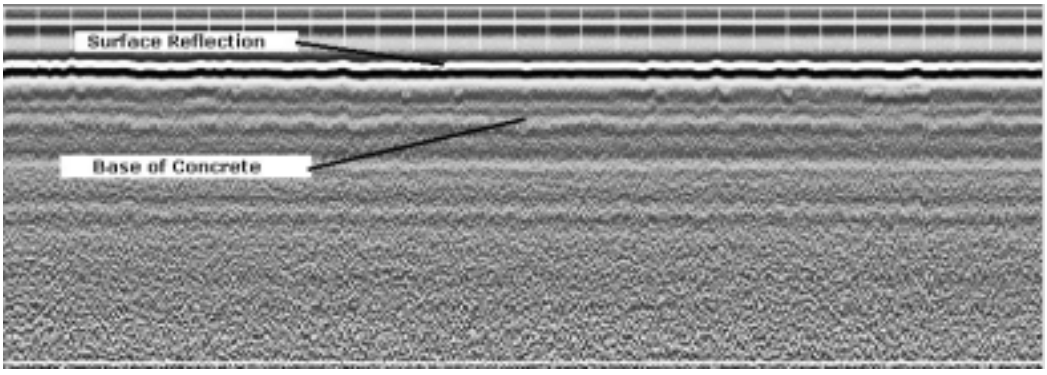

Figure 4. Portion of data from Hwy 635, GPS-7B test pavement #294069, 10” reinforced Portland Concrete Cement Pavement over sand soil base. Concrete dielectric 9.6. Three inch asphalt overlay not apparent (and not interpreted) due to overlap with waveform of surface reflection. Horizontal scale is 16.4ft/mark.

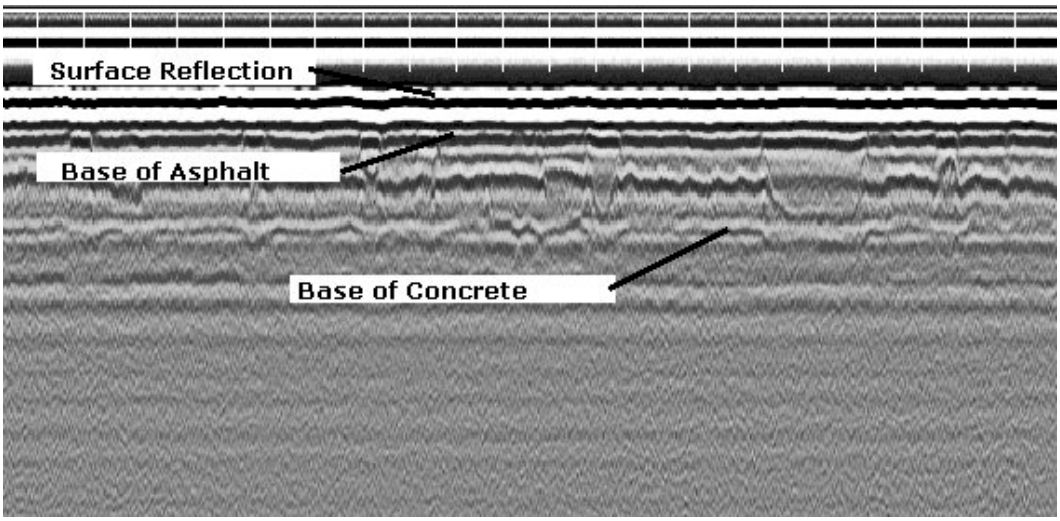

Figure 5. Portion of data from Hwy 35N, SPS-6 test pavement #290606, 4" Asphalt Concrete over 9" reinforced Portland Concrete Cement Pavement. Asphalt dielectric 8.3 (high), concrete dielectric 9.3. Horizontal scale is 16.4ft/mark.

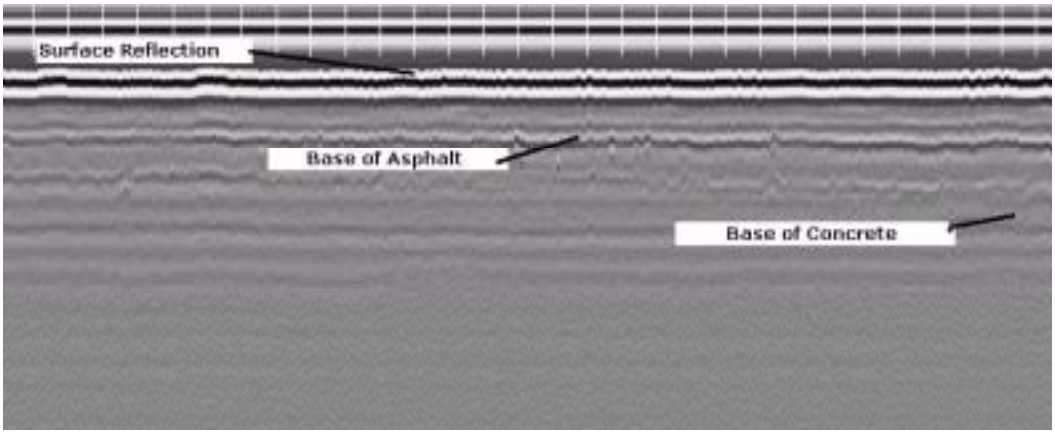

Figure 6. Portion of data from Hwy 35N, SPS-6 test pavement #290608, 8" Asphalt Concrete over 9" reinforced Portland Concrete Cement Pavement. Asphalt dielectric 6.5, concrete dielectric 13.9. Horizontal scale is 16.4ft/mark.

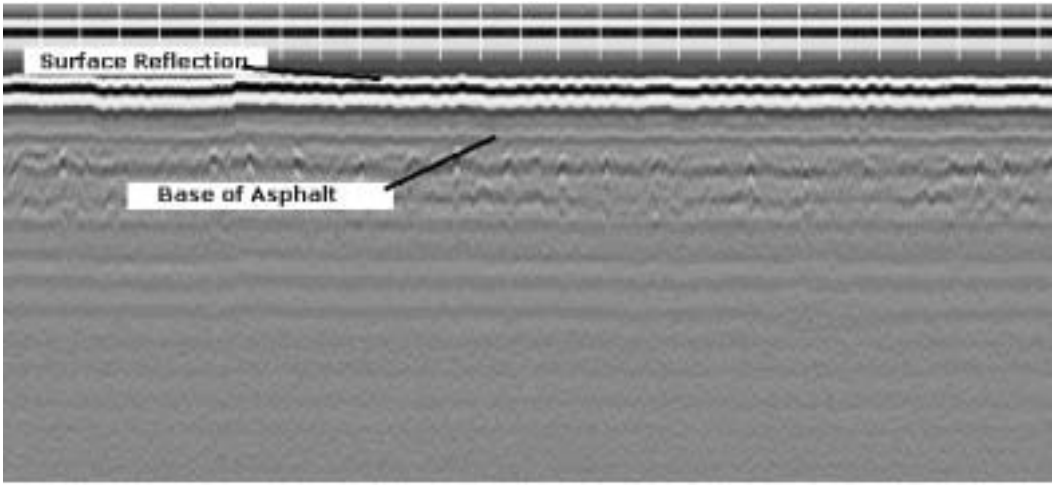

Figure 7. Portion of data from Hwy 35N, SPS-6 test pavement #290662, 8” Asphalt Concrete over rubblized Portland Concrete Cement Pavement. Asphalt dielectric 3.8. Horizontal scale is 16.4ft/mark.

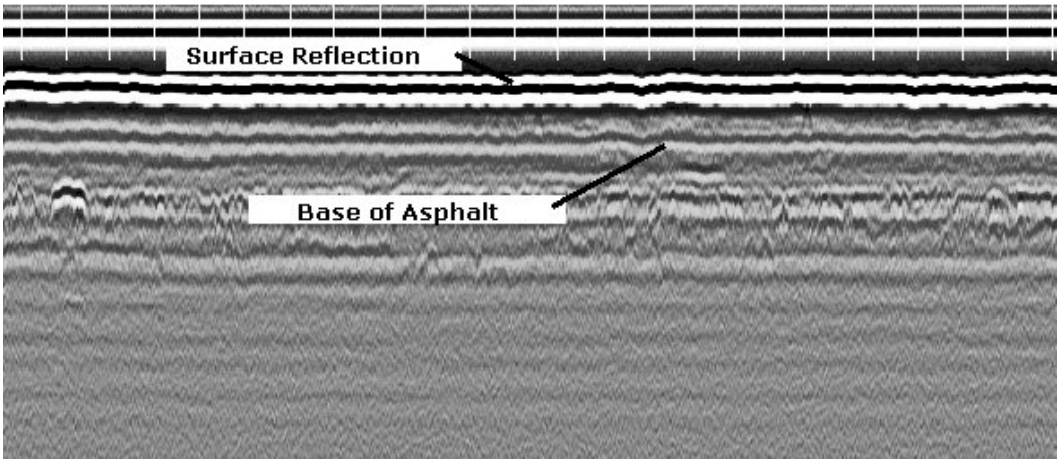

Figure 8. Portion of data from Hwy 35N, SPS-6 test pavement #290661, 12” Asphalt Concrete over rubblized Portland Concrete Cement Pavement. Asphalt dielectric 5.8. Horizontal scale is 16.4ft/mark.

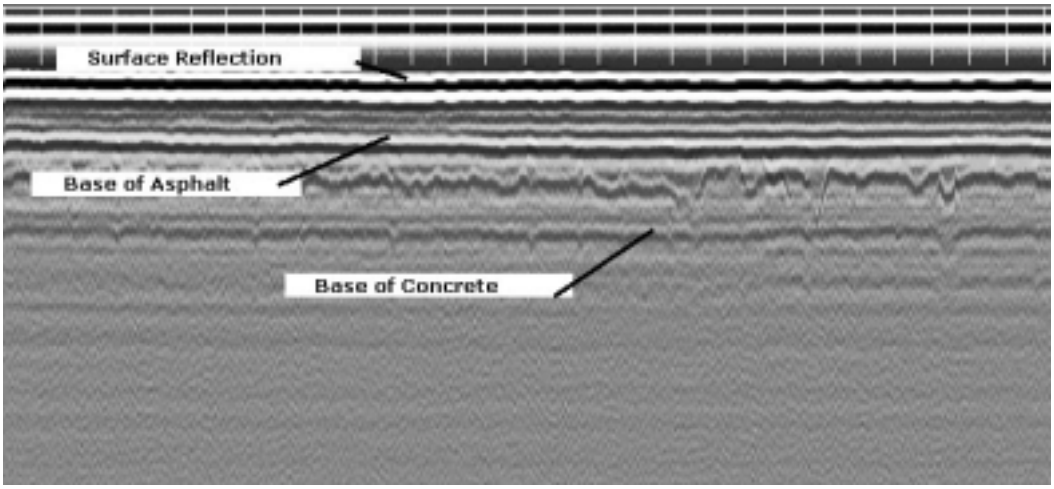

Figure 9. Portion of data from Hwy 29N, showing 7” asphalt over 10” reinforced concrete. Asphalt dielectric was 6.2 (high-suggesting actually thicker layer than 7” design), concrete dielectric 6.8. Horizontal scale is 16.4ft/mark.

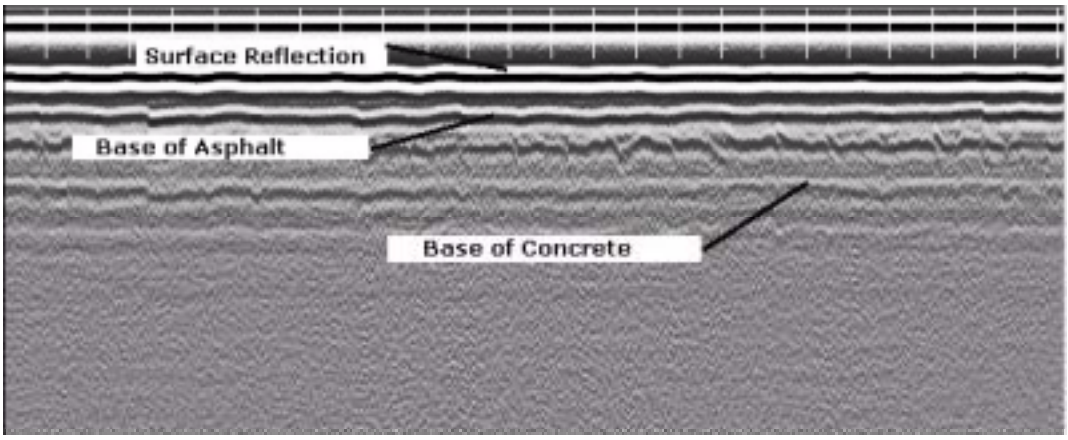

Figure 10. Portion of data from Hwy 29S, showing 7” asphalt over 10” reinforced concrete. Toward the end of the survey over this portion of Hwy 29 South, the base of concrete interface became un-interpretable (not shown, but cf. Appendix A). Asphalt dielectric was 4, concrete dielectric 7.1. Horizontal scale is 16.4ft/mark.

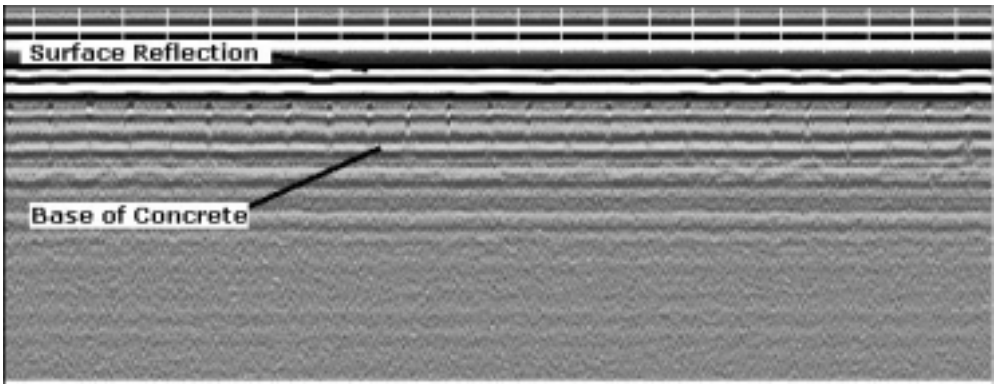

Figure 11a. Portion of data from Hwy 29, Atchison County (Test Section 1, Figure 1), with 9" plain unbonded PCCP overlay. The standard 15' joint spacing is clear. Horizontal scale is 16.4ft/mark.

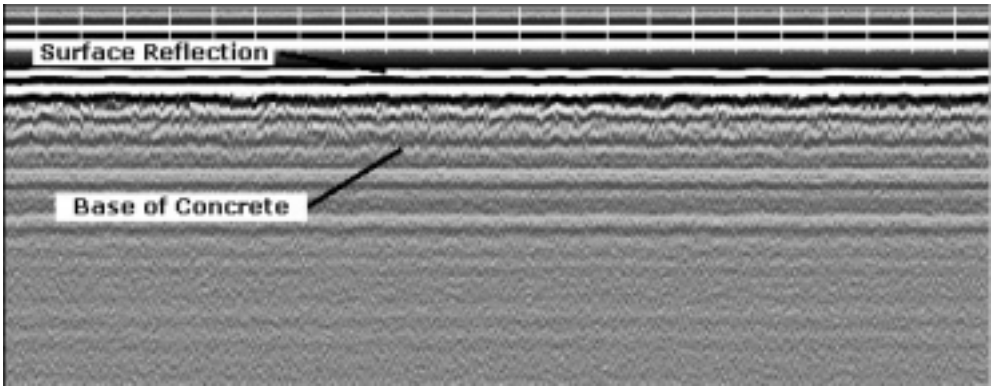

Figure 11b. Portion of data from Hwy 29, Atchison County (Test Section 2, Figure 1), with 9" unbonded PCCP overlay having steel fiber-reinforcement. Base of concrete difficult to interpret. Horizontal scale is 16.4ft/mark.

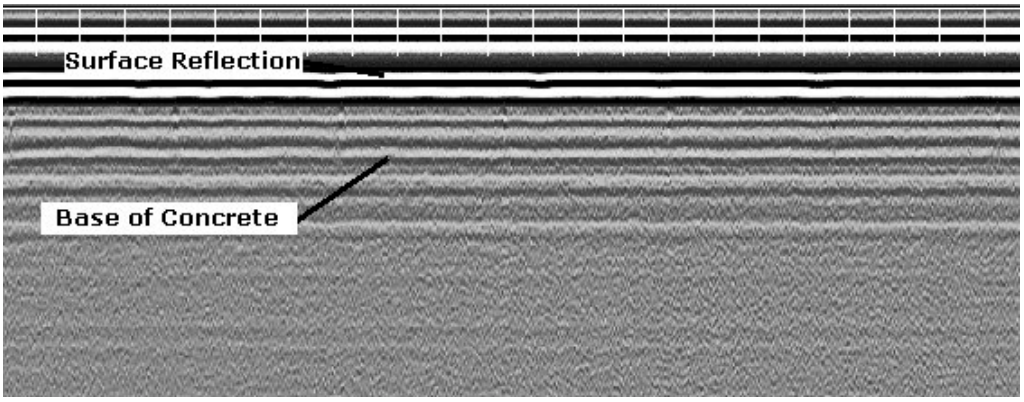

Figure 11c. Portion of data from Hwy 29, Atchison County (Test Section 3, Figure 1), with 9” unbonded PCCP overlay having polyolefin fiber-reinforcement. Horizontal scale is 16.4ft/mark.

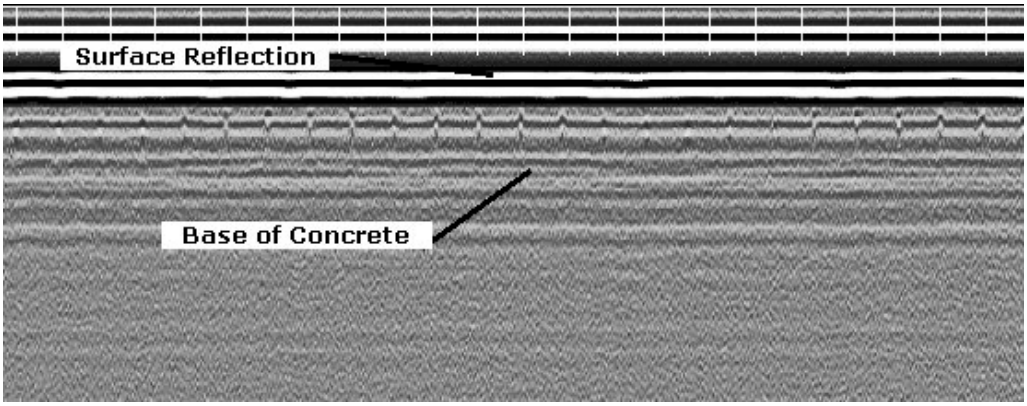

Figure 11d. Portion of data from Hwy 29, Atchison County (Test Section 4, Figure 1), with 11” plain unbonded PCCP overlay. The standard 15’ joint spacing is clear. Horizontal scale is 16.4ft/mark.

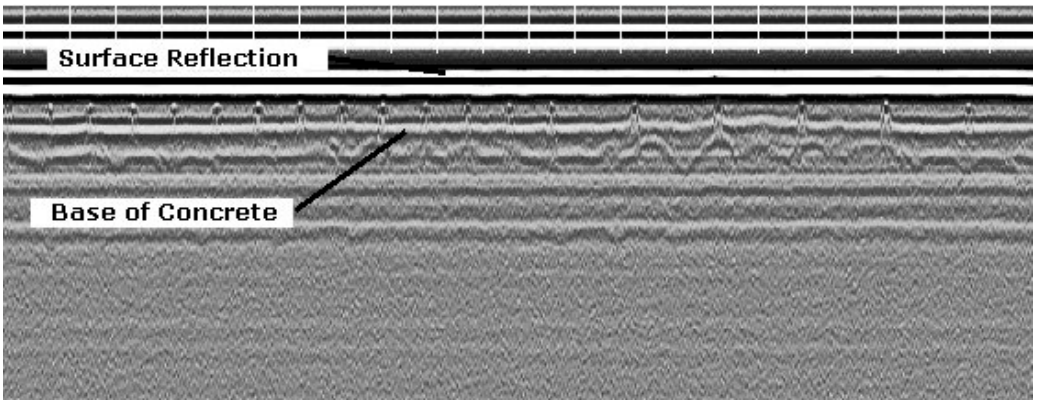

Figure 11e. Portion of data from Hwy 29, Atchison County (Test Section 5, Figure 1), with 6” unbonded PCCP overlay having polyolefin fiber reinforcement. Horizontal scale is 16.4ft/mark.

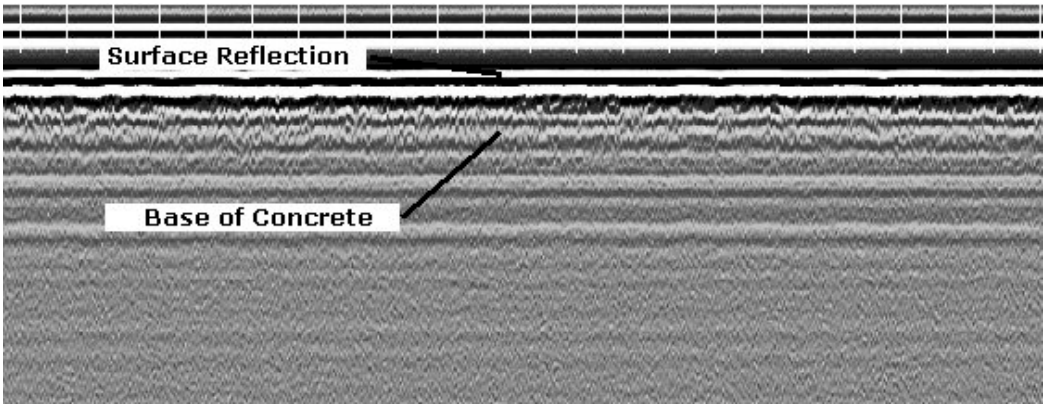

Figure 11f. Portion of data from Hwy 29, Atchison County (Test Section 6, Figure 1), with 6” unbonded PCCP overlay having steel fiber reinforcement. Base of concrete difficult to interpret. Horizontal scale is 16.4ft/mark.

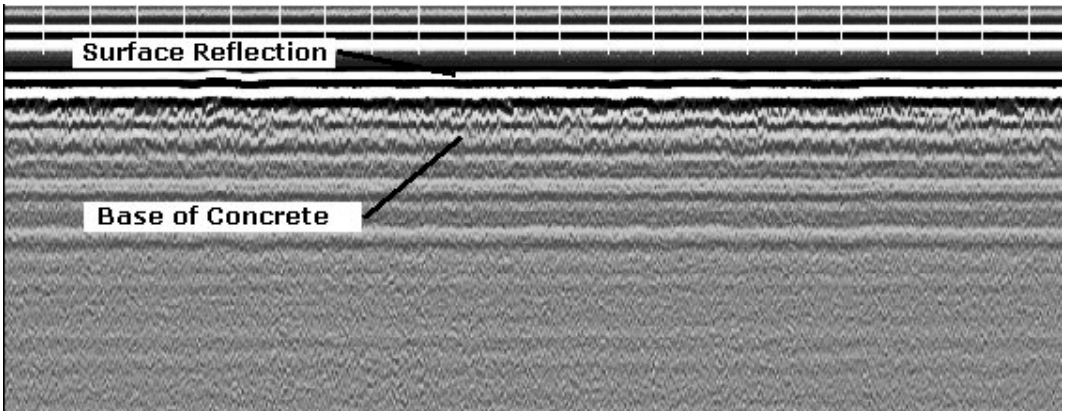

Figure 11g. Portion of data from Hwy 29, Atchison County (Test Section 7, Figure 1), with 5" unbonded PCCP overlay having steel fiber reinforcement. Base of concrete difficult to interpret. Horizontal scale is 16.4ft/mark.

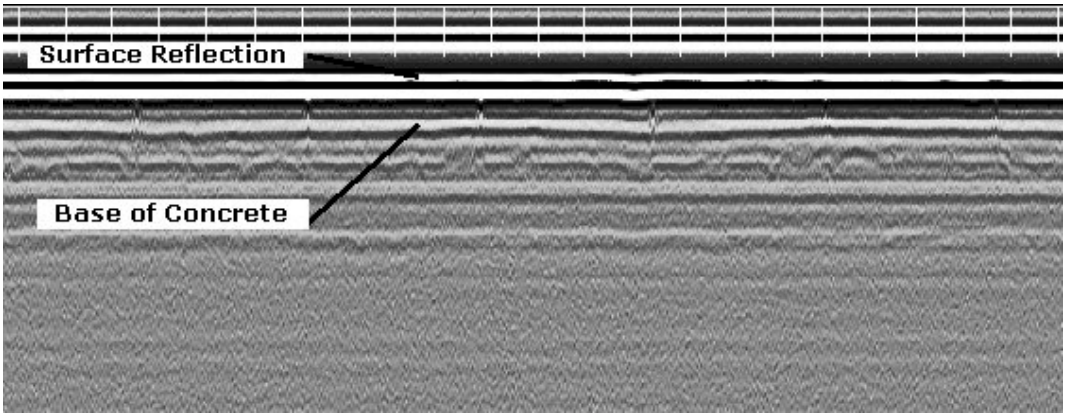

Figure 11h. Portion of data from Hwy 29, Atchison County (Test Section 8, Figure 1), with 5" unbonded PCCP overlay having polyolefin fiber reinforcement. Horizontal scale is 16.4ft/mark.

Frankford

Figure 12 shows data from asphalt pavement over type 5 aggregate base coarse, showing clearly the transition from 4 inch to 7 inch pavement (cf. Table 1b and Figure 2). In this ideal case, the reflection from the interface between the pavement and the baserock is clear throughout, as is the reflection from the base of the baserock.

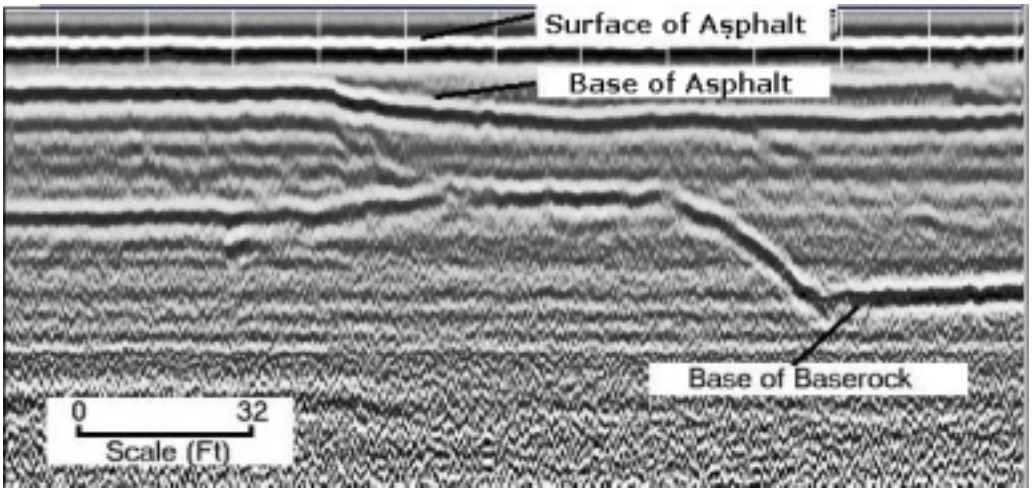

Figure 12. Asphalt pavement over type 5 aggregate baserock. Image shows transition from 4 inch asphalt over 8 inch base to 7 inch asphalt over 12 inch base. Horizontal scale is 16.4ft/mark.

Figure 13 shows the transition from asphalt pavement to concrete pavement, each over the same type 5 aggregate base coarse. In this case, the reflection from the base of concrete is lost; however, note that the base coarse reflection (interface between base coarse and subgrade) is evident throughout the transition. Figure 14 shows a transition from 8in concrete to 11in concrete over type 5 aggregate base (cf. Figure 2). These examples show that the dielectric contrast between the gravel base coarse and the concrete is not large enough to yield a reflection, but the radar signal does indeed penetrate through the concrete. Here is an important example of when automated picking algorithms might break down. Any automated methodology to determine layer thicknesses requires that the interface between all layers be distinctly represented in the GPR reflection signatures. If this is not the case, the algorithm will not be accurate.

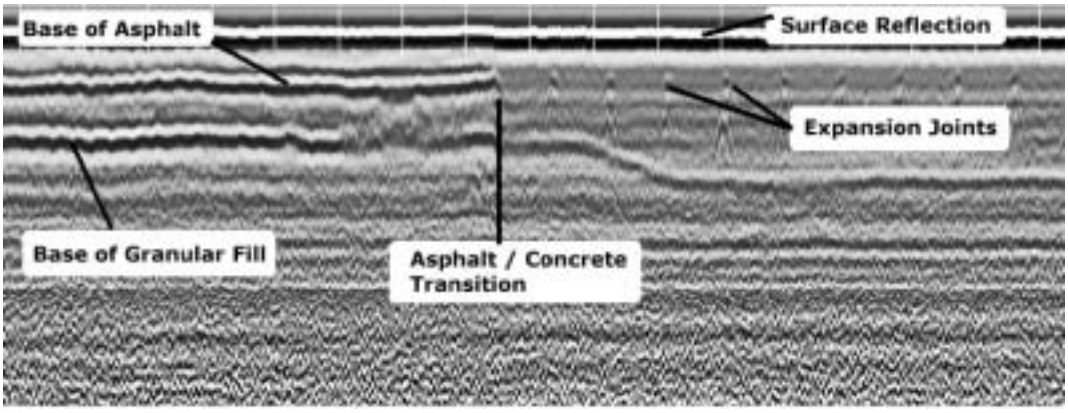

Figure 13. Asphalt and concrete pavements over type 5 aggregate baserock. Image shows transition from 4 inch asphalt over 8 inch base to 8 inch non-reinforced concrete over 6 inch base. Although the expansion joints within the concrete are clear, the reflection from the base of concrete is not. The radar signal does penetrate through the concrete, however, since the reflection from the base rock is clear across the transition from asphalt to concrete. Horizontal scale is 16.4ft/mark.

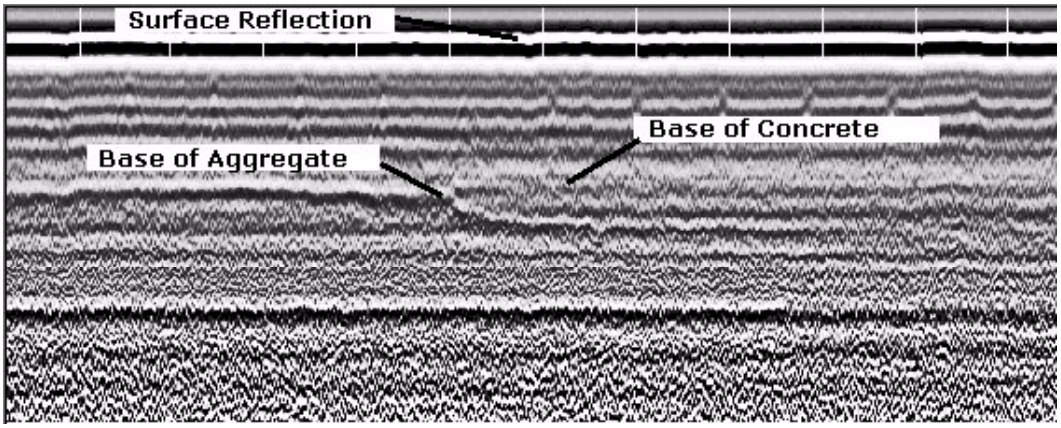

Figure 14. Concrete pavements over 6” of type 5 aggregate baserock. Image shows transition from 8 inch non-reinforced concrete to 11 inch non-reinforced concrete. The radar signal does penetrate through the concrete. Horizontal scale is 16.4ft/mark.

Figure 15 shows the detail possible in pavement imaging using ground-coupled, 1.5GHz radar antennae. Rebar reinforcement is easily detected. The smaller nominal wavelength, and being ground-coupled instead of air-launched, offers the increased resolution necessary to see such detail in the reinforcement within the concrete. Appendix B includes an example of the data with all thickness information in tabular form for File 1 of the ground-coupled data along with a graph all five concrete thickness profiles taken using the 1.5 GHz ground-coupled antenna. (Because of the large amount of data, the complete set of data for both ground-coupled and air-launched antenna data is included in an Addendum to this report and can be obtained by special request.)

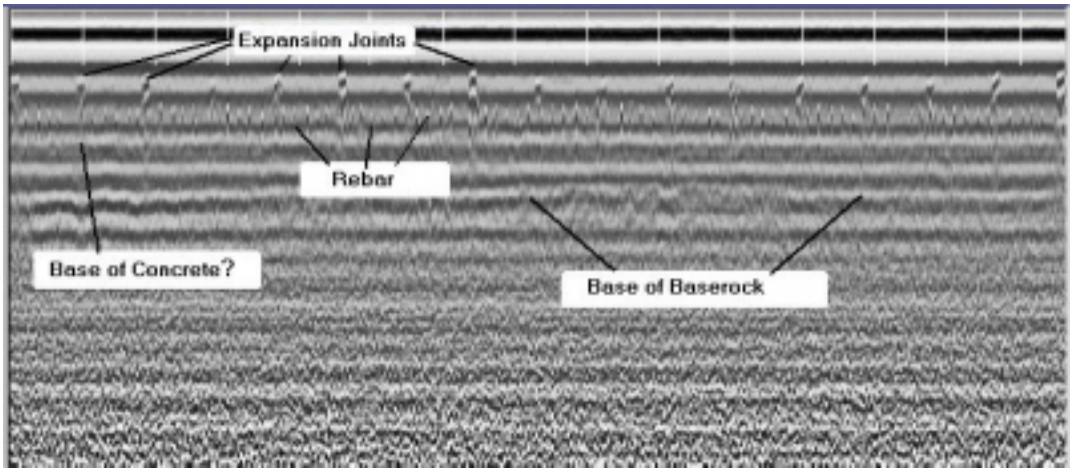

Figure 15. Eight inches concrete over 6 inches type 5 aggregate baserock. Data collected with 1.5 GHz ground-coupled antennae. As in Figure 13, the concrete-to-baserock interface is not clearly defined; however, the smaller wavelength than for the 1.0 GHz air-launched horn antennae offers increased resolution necessary to see the detail in the rebar-reinforcement within the concrete layer. Horizontal scale is 16.4ft/mark.

FUTURE WORK

1) Core select test pavements and re-survey over cores for more clear correlation of GPR with test pavements (for this project, mostly just design thickness information was used). Ideally, have aluminum foil put in bottom of core holes before they are plugged back up, then scan for foil target using both 1.5GHz ground-coupled and 1.0GHz horn antennae.

2) Resurvey select test pavement locations using the 1.5GHz ground-coupled antennae to see if we can improve the vertical resolution of thin surface asphalt layers (<4in thick).

3) Catalogue test pavement and base coarse type, and sub-grade if known, along with GPR reflection character signatures for each. Identify pavement types that are most successfully imaged by GPR and those that pose more of an interpretation challenge. Note, this would be especially useful if coupled with (1) above.

CONCLUSIONS

In this report we have applied ground penetrating radar techniques to high resolution roadway pavement analysis along numerous test pavements in Missouri. The range of test pavement types successfully surveyed in this study clearly shows the utility of GPR for determining pavement and sub-pavement layer thickness estimates. Interpretation can become more difficult over concrete pavements because the interface between the concrete and the base coarse is often indistinct. This is not because the radar signal will not penetrate through the concrete. The examples in this report demonstrate that the GPR signal does image the interface between the base rock and the sub-base. Although automated techniques need to be used carefully, interpreter input can help guide the analysis and keep it as accurate as possible when faced with low signal-to-noise scenarios. No matter what interpretation method is used, accurate

core samples associated directly with GPR survey locations are important. Ideally, a subsurface target at a known depth will be available for most accurate correlation of the GPR signal with a core sample. In addition to using GPR to estimate pavement layer thickness, the consistency of the radar reflection signature from similar test pavements demonstrates that radar can be used to monitor test pavement performance over time. Variations in the pavement reflection signature for a given pavement type can be interpreted in terms of potential problems in the pavement.

REFERENCES CITED

ASTM Designation D 4748 - 87 (1995), Standard Test Method for Determining the Thickness of Bound Pavement Layers Using Short-Pulse Radar.

Cardimona, S., M. Roark, D. J. Webb and T. Lippincott, 1998. Ground penetrating radar, *Highway Applications of Engineering Geophysics with an Emphasis on Previously Mined Ground*, pp. 41-56.

Cardimona, S., B. Willeford, J. Wenzlick, N. Anderson, 1999. Ground penetrating radar applied to pavement studies: Case examples from select test pavements in Missouri, report for the Missouri Department of Transportation, UMR Department of Geology and Geophysics contribution May 1999.

Daniels, D., 1996. Surface-penetrating radar, Inst. Electr. Eng.

APPENDIX A

Thickness Data for all Pavement Section 295483 listed in Table 1

NOTE: (Because of the large amount of data, the complete set of data for all sites is included in an Addendum to this report and can be obtained by special request.)

Site: 295483
10/6/1998

	Distance (ft)	Concrete Thickness (in)	Average Thickness (in)
1	0.66	9.46	9.03
1	5.90	9.00	9.15
1	13.77	9.00	9.13
1	20.98	8.54	8.85
1	30.16	9.00	8.93
1	37.37	8.29	8.82
1	45.24	8.78	8.81
1	52.46	8.78	8.95
1	60.32	9.00	9.00
1	64.91	9.00	8.98
1	71.47	8.75	9.13
1	78.03	9.22	9.20
1	84.58	8.78	8.98
1	89.83	9.22	8.89
1	95.73	8.75	8.94
1	102.29	9.22	9.04
1	108.19	9.00	8.99
1	113.44	8.54	8.80
1	120.65	8.78	8.94
1	126.55	8.78	8.90
1	132.45	9.24	8.86
1	138.35	9.22	8.94
1	145.56	9.24	8.83
1	150.81	9.46	9.00
1	156.06	9.46	9.19
1	161.96	8.75	9.17
1	168.51	8.78	8.86
1	175.73	9.46	8.95
1	182.94	9.46	9.05
1	189.50	9.22	9.16
1	196.71	9.22	9.05
1	205.23	8.75	9.04
1	212.45	9.22	9.04
1	217.03	9.00	9.06
1	226.21	9.00	8.98
1	232.77	8.78	8.77
1	238.02	8.54	8.80
1	243.26	9.00	8.94
1	253.10	8.78	8.98
1	259.66	9.00	8.98
1	269.49	9.00	8.89
1	274.74	9.00	8.82
1	282.60	8.78	8.74
1	291.78	9.00	8.79

Site: 295483
10/6/1998

	Distance (ft)	Concrete Thickness (in)	Average Thickness (in)
1	301.62	8.78	9.08
1	308.18	8.78	8.99
1	315.39	9.00	8.98
1	327.85	8.75	8.73
1	335.06	8.75	8.67
1	344.90	9.00	8.87
1	361.94	9.24	8.90
1	370.47	9.24	8.89
1	379.65	9.00	8.82
1	386.86	9.00	8.75
1	393.42	8.78	8.71
1	399.32	9.24	8.92
1	406.53	9.22	8.91
1	413.74	9.00	9.08
1	420.96	8.75	9.20
1	426.20	9.00	9.12
1	432.10	8.78	8.83
1	436.69	9.00	9.00
1	443.91	9.46	9.04
1	450.46	9.24	9.05
1	456.36	8.54	9.02
1	461.61	9.00	8.93
1	469.48	8.54	8.80
1	476.69	9.24	9.11
1	481.94	9.46	9.18
1	492.43	9.00	9.05
1	499.64	9.46	9.09
1	506.85	8.78	9.10
1	512.75	9.22	9.08
1	518.65	9.24	9.06
1	525.21	9.46	9.08
1	533.08	9.24	9.03
1	538.98	9.46	9.03
1	543.57	9.24	9.11
1	551.44	8.75	9.07
1	559.96	9.22	9.03
1	566.52	8.75	9.12
1	572.42	8.78	9.00
1	579.63	9.00	8.79
1	585.54	8.78	8.80
1	590.78	8.78	8.93
1	597.34	8.78	8.81
1	605.21	8.78	8.99
1	614.39	9.00	8.97

Site: 295483
10/6/1998

	Distance (ft)	Concrete Thickness (in)	Average Thickness (in)
1	620.29	9.00	8.86
1	626.19	9.24	9.05
1	632.09	8.78	9.05
1	640.61	9.00	9.18
1	645.86	9.46	9.30
1	651.10	8.78	9.11
1	659.63	9.00	8.88
1	666.19	9.00	8.92
1	676.02	9.00	8.88
1	682.58	9.24	8.80
1	689.14	9.00	8.85
1	695.04	9.24	8.91
1	702.90	9.46	9.07
1	708.15	9.00	9.16
1	715.36	8.29	8.89
1	723.89	8.78	8.91
1	731.10	8.05	8.82
1	737.66	9.24	8.97
1	744.87	9.24	9.03
1	750.77	9.24	8.89
1	756.02	9.00	8.95
1	761.26	9.00	8.95
1	769.13	8.05	8.79
1	780.93	8.54	8.77
1	786.83	9.00	8.84
1	791.42	8.78	8.93
1	799.29	8.29	8.73
1	804.54	9.46	8.80
1	809.78	8.29	8.82
1	817.65	9.22	9.09
1	828.14	9.00	8.99
1	834.04	9.00	8.77
1	842.57	8.54	8.86
1	848.47	8.78	8.75
1	854.37	8.29	8.73
1	859.62	8.29	8.73
1	865.52	9.24	8.92
1	870.11	9.00	8.93
1	876.01	9.24	9.00
1	881.91	8.78	8.91
1	890.43	9.00	9.03
1	898.30	8.54	8.90
1	906.17	8.78	8.90
1	912.73	9.00	8.91

Site: 295483
10/6/1998

	Distance (ft)	Concrete Thickness (in)	Average Thickness (in)
1	925.19	8.78	8.72
1	929.78	9.46	8.91
1	936.33	8.29	8.83
1	942.23	8.78	8.82
1	947.48	9.00	8.72
1	952.07	9.00	8.75
1	959.28	8.29	8.71
1	964.53	8.78	8.81
1	970.43	9.24	8.95
1	976.33	9.24	8.91
1	982.89	8.54	8.73
1	988.79	9.24	8.84
1	994.69	9.24	8.84
1	1001.25	9.00	8.84
1	1007.80	8.78	8.93
1	1015.02	9.00	8.99
1	1020.26	8.78	8.97
1	1028.13	9.00	9.06
1	1037.96	8.78	8.97
1	1044.52	9.00	8.73
1	1049.77	9.24	8.94
1	1056.32	8.54	8.91
1	1062.88	9.24	8.90
1	1070.09	9.24	8.90
1	1079.93	8.29	8.86
1	1084.52	8.29	8.73
1	1090.42	9.24	8.84
1	1098.29	8.78	8.88
1	1104.19	8.78	8.90
1	1108.78	8.54	8.80
1	1114.68	8.51	8.81
1	1119.93	8.78	8.83
1	1127.79	9.00	8.66
1	1133.04	8.54	8.71
1	1139.60	8.54	8.75
1	1149.43	9.22	8.91
1	1154.68	9.24	8.89
1	1159.27	8.78	8.95
1	1165.83	8.78	8.84
1	1171.73	8.54	8.67
1	1177.63	8.54	8.77
1	1182.22	9.24	8.97
1	1188.12	9.24	8.84
1	1194.02	8.29	8.79

Site: 295483
10/6/1998

	Distance (ft)	Concrete Thickness (in)	Average Thickness (in)
1	1199.92	9.00	8.84
1	1205.17	8.78	8.91
1	1211.07	9.00	9.14
1	1216.97	8.75	9.14
1	1222.87	8.78	8.92
1	1227.46	9.24	8.79
1	1235.33	9.22	8.96
1	1243.20	9.00	9.09
1	1251.72	8.78	9.01

APPENDIX B

Frankford Thickness Data

(File 1, Northbound Lane, 1.5 GHz Antenna)

(Concrete Thickness Profiles for all 5 Offsets)

NOTE: (Because of the large amount of data, the complete set of data for all sites is included in an Addendum to this report and can be obtained by special request.)

SPS-8A Test Section
J3P0062
File 1 Data
Northbound Lane
20 Ft. Offset
1.5 Ghz Antenna

	Station No.	Distance (ft)	Concrete Thickness (in)	Average (in)
1	195.04	3.61	8.151	8.6326
1	195.20	20.35	8.766	8.7044
1	195.25	25.27	8.766	8.77216
1	195.30	29.87	8.843	8.7198
1	195.35	34.79	8.689	8.65204
1	195.39	39.39	8.227	8.60584
1	195.44	44.31	8.612	8.65204
1	195.49	48.91	8.535	8.61512
1	195.56	56.46	8.689	8.60588
1	195.61	61.05	8.304	8.5504
1	195.67	66.96	8.535	8.59352
1	195.72	71.56	8.689	8.6736
1	195.76	76.48	8.689	8.6428
1	195.81	81.08	8.535	8.612
1	195.86	86	8.689	8.66128
1	195.91	90.59	8.689	8.66128
1	195.96	95.52	8.689	8.61508
1	196.00	100.11	8.535	8.61816
1	196.05	105.04	8.612	8.60584
1	196.10	109.63	8.612	8.59352
1	196.15	114.56	8.766	8.5812
1	196.19	119.15	8.689	8.59044
1	196.24	124.07	8.535	8.65196
1	196.29	128.67	8.535	8.61816
1	196.34	133.59	8.612	8.63048
1	196.38	138.19	8.689	8.63356
1	196.43	143.11	8.766	8.68592
1	196.48	147.71	8.689	8.66744
1	196.53	152.63	8.689	8.63356
1	196.57	157.23	8.612	8.66128
1	196.62	162.15	8.612	8.63664
1	196.67	167.07	8.612	8.68576
1	196.74	174.3	8.919	8.81504
1	196.80	179.55	8.919	8.8458
1	196.85	184.8	8.766	8.78744
1	196.89	189.39	8.689	8.76592
1	196.94	194.32	8.766	8.7598
1	196.99	198.91	8.766	8.73212
1	197.04	204.17	8.843	8.7198
1	197.09	208.76	8.843	8.74444
1	197.14	213.68	8.689	8.72596
1	197.18	218.28	8.535	8.71052
1	197.24	223.53	8.689	8.79972

SPS-8A Test Section
J3P0062
File 1 Data
Northbound Lane
20 Ft. Offset
1.5 Ghz Antenna

	Station No.	Distance	Concrete Thickness	Average
1	197.28	228.13	8.689	8.82128
1	197.33	233.05	8.766	8.80912
1	197.38	237.65	8.843	8.83672
1	197.43	242.57	8.689	8.80592
1	197.47	247.16	8.689	8.75368
1	197.52	252.09	8.689	8.74752
1	197.57	256.68	8.919	8.7136
1	197.62	261.61	8.612	8.70132
1	197.66	266.2	8.843	8.83368
1	197.71	271.45	8.689	8.7844
1	197.76	276.05	8.843	8.73508
1	197.81	280.97	8.766	8.76892
1	197.86	285.57	8.612	8.769
1	197.90	290.49	8.766	8.75668
1	197.95	295.09	8.612	8.73196
1	198.00	300.01	8.766	8.7228
1	198.05	304.61	8.689	8.66436
1	198.10	309.53	8.612	8.67052
1	198.14	314.45	8.689	8.7598
1	198.19	319.38	8.843	8.83672
1	198.24	323.97	9.535	8.8582
1	198.29	328.9	8.843	8.82136
1	198.33	333.49	8.689	8.76908
1	198.39	338.74	8.689	8.75984
1	198.43	343.34	8.689	8.81832
1	198.48	348.26	8.843	8.85824
1	198.53	352.86	8.689	8.8366
1	198.58	357.78	8.304	8.67044
1	198.62	362.38	8.689	8.71976
1	198.67	367.3	8.612	8.73208
1	198.72	371.9	8.689	8.69512
1	198.77	376.82	8.766	8.8212
1	198.81	381.42	8.535	8.84272
1	198.87	386.67	8.535	8.82736
1	198.91	391.26	8.689	8.82128
1	198.96	396.19	8.766	8.87664
1	199.01	400.78	8.766	8.92276
1	199.06	405.7	8.766	8.8244
1	199.10	410.3	8.689	8.87056
1	199.15	415.22	8.766	8.83356
1	199.20	419.82	9.612	8.9228
1	199.25	424.74	9.227	8.972
1	199.29	429.34	9.612	8.94736

SPS-8A Test Section
J3P0062
File 1 Data
Northbound Lane
20 Ft. Offset
1.5 Ghz Antenna

	Station No.	Distance	Concrete Thickness	Average
1	199.34	434.26	8.689	8.75972
1	199.39	438.86	8.766	8.76592
1	199.44	443.78	8.843	8.77208
1	199.48	448.38	9.227	8.75972
1	199.53	453.3	9.304	8.81504
1	199.58	457.89	9.304	8.7812
1	199.63	462.82	8.843	8.80892
1	199.67	467.41	9.227	8.8612
1	199.72	472.34	9.227	8.91044
1	199.77	476.93	8.535	8.72272
1	199.82	481.86	8.535	8.5688
1	199.87	486.78	8.843	8.58416
1	199.92	492.03	8.535	8.6272
1	199.97	496.96	8.535	8.68264
1	200.04	503.52	8.304	8.65804
1	200.09	508.77	8.535	8.63348
1	200.14	513.7	8.689	8.74728
1	200.18	518.29	9.227	8.6888
1	200.23	523.21	9.074	8.66108
1	200.28	527.81	8.304	8.57796
1	200.33	532.73	9.304	8.6426
1	200.37	537.33	8.304	8.52572
1	200.42	542.25	8.535	8.54424
1	200.47	546.85	9.227	8.61496
1	200.52	551.77	8.766	8.62736
1	200.56	556.37	8.689	8.689
1	200.61	561.29	8.689	8.78436
1	200.66	565.89	8.689	8.76892
1	200.71	570.81	8.535	8.66432
1	200.75	575.4	9.227	8.78732
1	200.80	580.33	8.612	8.6796
1	200.85	584.92	8.689	8.59044
1	200.90	589.85	8.535	8.6458
1	200.94	594.44	8.689	8.71656
1	200.99	599.37	8.535	8.74416
1	201.04	603.96	8.612	8.77188
1	201.09	608.89	9.304	8.80576
1	201.13	613.48	8.535	8.7196
1	201.18	618.4	8.612	8.695
1	201.23	623	8.612	8.65812
1	201.28	627.92	8.535	8.612
1	201.33	632.52	8.766	8.7074
1	201.37	637.44	9.535	8.83048
1	201.42	642.04	8.689	8.69812

1	201.47	646.96	8.689	8.63664

SPS-8A Test Section
J3P0062
File 1 Data
Northbound Lane
20 Ft. Offset
1.5 Ghz Antenna

	Station No.	Distance	Concrete Thickness	Average
1	201.52	651.56	9.227	8.71964
1	201.56	656.48	8.689	8.6704
1	201.61	661.08	8.304	8.47956
1	201.66	666	9.535	8.65184
1	201.71	670.59	8.535	8.6796
1	201.76	675.52	8.304	8.53804
1	201.80	680.11	8.304	8.59036
1	201.85	685.04	8.535	8.98408
1	202.00	700.14	11.457	10.50036
1	202.05	705.06	11.457	11.32456
1	202.10	709.66	11.226	11.25988
1	202.15	714.58	11.457	11.32148
1	202.19	719.17	11.457	11.34616
1	202.24	724.1	11.996	11.40776
1	202.29	728.69	11.38	11.48772
1	202.34	733.62	11.457	11.6078
1	202.38	738.21	11.457	11.53392
1	202.43	743.14	11.688	11.59856
1	202.48	747.73	11.457	11.57084
1	202.53	752.65	11.149	11.59228
1	202.57	757.25	11.457	11.62628
1	202.62	762.17	11.457	11.5678
1	202.67	766.77	11.457	11.49696
1	202.72	771.69	11.226	11.39856
1	202.76	776.29	11.688	11.52476
1	202.81	781.21	11.457	11.5246
1	202.86	785.81	11.149	11.44148
1	202.91	790.73	12.457	11.8754
1	202.95	795.33	12.149	11.66316
1	203.00	800.25	12.226	11.37692
1	203.05	804.84	11.149	11.3738
1	203.10	809.77	11.457	11.36464
1	203.14	814.36	11.226	11.46616
1	203.19	819.29	11.149	11.463
1	203.24	823.88	11.534	11.40768
1	203.29	828.81	11.611	11.62328
1	203.33	833.4	11.073	11.4602
1	203.38	838.33	11.072	11.32784
1	203.43	842.92	12.534	11.5248
1	203.50	850.14	11.611	11.60172
1	203.55	854.74	11.611	11.65092
1	203.60	859.66	11.149	11.56776
1	203.64	864.26	11.149	11.58624

SPS-8A Test Section
J3P0062
File 1 Data
Northbound Lane
20 Ft. Offset
1.5 Ghz Antenna

	Station No.	Distance	Concrete Thickness	Average
1	203.69	869.18	12.149	11.6478
1	203.74	873.78	11.688	11.6602
1	203.79	878.7	11.765	11.76484
1	203.83	883.29	11.611	11.73408
1	203.88	888.22	11.457	11.52168
1	203.93	892.81	11.765	11.46632
1	203.98	897.74	11.457	11.4694
1	204.02	902.33	11.765	11.66936
1	204.07	907.26	11.688	11.54008
1	204.12	911.85	11.457	11.52164
1	204.17	916.77	11.534	11.54632
1	204.21	921.37	11.688	11.64172
1	204.26	926.29	11.226	11.51852
1	204.31	930.89	11.611	11.48776
1	204.36	936.14	11.688	11.58628
1	204.41	940.74	11.149	11.55548
1	204.46	945.66	11.226	11.45696
1	204.50	950.26	11.149	11.4846
1	204.55	955.18	11.611	11.50928
1	204.60	959.77	11.149	11.31536
1	204.65	964.7	11.226	11.24756
1	204.69	969.29	11.457	11.31532
1	204.74	974.22	11.226	11.28456
1	204.79	978.81	11.226	11.17068
1	204.84	983.74	11.226	11.22304
1	204.88	988.33	11.149	11.34616
1	204.93	993.25	11.534	11.37076
1	204.98	997.85	11.226	11.38916
1	205.03	1002.77	11.457	11.50308
1	205.07	1007.37	11.534	11.50008
1	205.12	1012.29	11.611	11.50932
1	205.17	1016.89	11.534	11.56472
1	205.22	1021.81	11.457	11.50312
1	205.26	1026.41	11.457	11.4108
1	205.31	1031.33	11.611	11.43236
1	205.36	1035.93	11.457	11.42928
1	205.41	1040.85	11.765	11.6294
1	205.45	1045.44	11.303	11.5956
1	205.50	1050.37	11.457	11.50944
1	205.55	1054.96	11.149	11.37084
1	205.60	1059.89	11.611	11.38928
1	205.64	1064.48	11.611	11.5432
1	205.69	1069.41	11.149	11.45076

SPS-8A Test Section
J3P0062
File 1 Data
Northbound Lane
20 Ft. Offset
1.5 Ghz Antenna

	Station No.	Distance	Concrete Thickness	Average
1	205.74	1074	11.457	11.48472
1	205.79	1078.93	11.227	11.51872
1	205.84	1083.52	11.765	11.56484
1	205.88	1088.44	12.072	11.59548
1	205.93	1093.04	11.457	11.51844
1	205.98	1097.96	11.227	11.64156
1	206.03	1102.56	11.226	11.62308
1	206.07	1107.48	11.226	11.3738
1	206.12	1112.08	11.226	11.31528
1	206.17	1117	11.226	11.32764
1	206.22	1121.6	11.073	11.26928
1	206.27	1126.52	11.457	11.4416
1	206.31	1131.12	11.38	11.50624
1	206.36	1136.04	11.226	11.33692
1	206.41	1140.63	11.227	11.29076
1	206.46	1145.56	11.226	11.24764
1	206.50	1150.15	11.226	11.32772
1	206.55	1155.08	11.226	11.50924
1	206.60	1159.67	11.149	11.45684
1	206.65	1164.6	11.457	11.44152
1	206.69	1169.19	11.226	11.30304
1	206.74	1174.11	11.996	11.24152
1	206.79	1178.71	11.149	11.33996
1	206.84	1183.63	11.611	11.48472
1	206.88	1188.23	11.457	11.46932
1	206.93	1193.15	11.303	11.42628
1	206.98	1197.75	11.227	11.30348
1	207.03	1202.67	11.073	11.14972
1	207.07	1207.27	10.996	11.09128
1	207.12	1212.19	10.688	11.06352
1	207.17	1216.79	11.227	11.14336
1	207.22	1221.71	11.073	11.13708
1	207.26	1226.31	11.073	11.18948
1	207.31	1231.23	10.996	11.21736
1	207.36	1235.82	10.996	11.1098
1	207.41	1240.75	11.611	11.25408
1	207.45	1245.34	11.611	11.35544
1	207.50	1250.27	11.457	11.47548
1	207.55	1254.86	11.534	11.37112
1	207.60	1259.79	11.073	11.18036
1	207.64	1264.38	11.073	11.162
1	207.69	1269.3	11.919	11.17148
1	207.74	1273.9	11.149	11.20184
1	207.79	1278.82	11.227	11.22932

SPS-8A Test Section
J3P0062
File 1 Data
Northbound Lane
20 Ft. Offset
1.5 Ghz Antenna

	Station No.	Distance	Concrete Thickness	Average
1	207.83	1283.42	11.073	11.18336
1	207.88	1288.34	11.38	11.2664
1	207.93	1292.94	11.149	11.32776
1	207.98	1297.86	11.457	11.31844
1	208.02	1302.46	11.457	11.32456
1	208.07	1307.38	11.303	11.36772
1	208.12	1311.98	11.149	11.2816
1	208.17	1316.9	11.226	11.28472
1	208.21	1321.49	11.226	11.26628
1	208.26	1326.42	12.072	11.20484
1	208.31	1331.01	11.457	11.28784
1	208.47	1347.1	11.303	11.40152
1	208.75	1374.67	11.611	11.43129

Final Report

RI98-002B

Automated Pavement Analysis of Collector Routes Using Ground Penetrating Radar

MISSOURI DEPARTMENT OF TRANSPORTATION
RESEARCH, DEVELOPMENT AND TECHNOLOGY

BY: Steve Cardimona, Shane Hickman

The University of Missouri-Rolla, Department of Geology and Geophysics

JEFFERSON CITY, MISSOURI
DATE SUBMITTED: April 2000

EXECUTIVE SUMMARY

Ground penetrating radar (GPR) surveys have been performed over 42 miles of secondary highways to determine the thickness of the asphalt pavement, which isn't known for many of theses pavement sections, and also to determine if indications of potential maintenance problem areas could be identified. Results of this work suggest that GPR will yield good estimates of pavement thickness by determining an average dielectric constant from a minimum amount of cores. It also established a range of 4 -7 as the dielectric constant (or conductivity) for this type of AC pavement. It was also determined by correlation of GPR data and coring that anomalous areas could be characterized, especially to recognize pavement where the asphaltic cement was stripping from the aggregate. This study demonstrates GPR would be an effective tool to inventory the structure of MoDOT's secondary road system to provide good preventative maintenance data.

TABLE OF CONTENTS

LIST OF FIGURES

LIST OF TABLES

PHASE I SURVEY OVERVIEW

The data for Phase I was collected in December of 1999 over a site that consisted of Route T from I-44 to the junction with Route M and Route M from the junction with Route T to Highway 63. Routes T and M are two lane, state roads that are lightly traveled and consist of an asphalt layer with a gravel or clay base. For the most part, the routes are located in rural areas with a small section of Route T running through the small community of Doolittle, the only area of significant development along the survey site. The purpose of Phase I of this study was to get an estimate of asphalt thickness across the site, identify and categorize common anomalies, and to provide a basis for collection of data for Phase II. An important goal at this site was to find a relationship between stripped asphalt and an anomalous feature in the GPR data. Asphalt becomes stripped when it loses oil content and the aggregate becomes unconsolidated. Data was collected with only one antenna and it was mounted on the driver's side of the survey vehicle. Data was collected in both driving directions with the data files being broken into four mile (6.4 km) sections. The total length of the study site was approximately 42 miles (68 km). The data was collected with a range of 20ns and a scan was collected every 8 inches (20 cm). During acquisition, a two point gain function was applied along with a 2,000 MHz low-pass filter and a 250 MHz high-pass filter.

The goal in the Phase I study was to provide pavement thickness data every tenth mile across the entire site. There was no previous history information to use for estimating the dielectric constant (or conductivity) of the asphalt or to compare with the thickness data calculated from the GPR data. (Normally a known dielectric constant is used along with the travel time of the radar pulse to figure a pavement layer thickness.)

Instead, six cores were drilled before the Phase I data was collected. At the same time that the Phase I data was collected, GPR data was also collected over each core location. (If a good dialectic constant is not known, cores are taken, and if they show a good homogeneous asphalt mix, they are accurately measured and using this dimension and the travel time a dielectric constant is back calculated.) Table 1 shows the core measurements, the GPR travel times, and the resulting dielectric constants of the asphalt at each location. Only core locations one and two were used to determine a dielectric constant for determining asphalt thickness because cores three and four contained stripped asphalt (dielectric constants greater than normal indicate the presence of moisture in the system and dielectric constants lower than normal indicate the presence of excessive air voids) and cores five and six exhibited anomalously high dielectric constants (dielectric constants greater than 16 indicate layers saturated with water). (See Appendix B for a list of normal dielectric values for various different pavement layers.)

The first step to determine pavement thickness was to average the data over 5.5 feet (1.7 m) in order to reduce file size and increase signal to noise ratio. The second step was to implement a semi-automated layer picking process for the surface and the base of asphalt reflections. Once the layer picking was complete, the information was then exported to a spreadsheet. This data was then sorted into tenth mile intervals. Then all data within 20 feet (6.1 m) of each tenth mile marker were stacked to get an average asphalt thickness. The final step was to graph this data for ease in viewing. An average dielectric of 6.45 was used for the asphalt in order to estimate asphalt thickness across the entire site. This value was determined from the data acquired at two of the six control points collected at this site (Table 1). Only data from cores 1 and 2 were found to be

suitable for use as control points. Figure 1 shows the pavement plots for both lanes created for this study site.

Table 1. Core thickness, GPR travel times, and calculated dielectric constants of control data from Phase I on Routes T and M.

Core Location (miles from I-44)	Core Thickness	GPR Travel Time	Dielectric Constant
Core 1 (.5)	4 in.	1.68 ns	6.15
Core 2 (.5)	4.25 in.	1.87 ns	6.75
Core 3 (3)	4 in. (stripped)	2.19 ns	10.45
Core 4 (3)	3.75 in. (stripped)	1.52 ns	5.73
Core 5 (18)	6.5 in.	3.48 ns	10
Core 6 (18)	6 in.	4.45 ns	19.18

There were five major types of anomalies found throughout the data collected on Routes T and M. One type of anomaly found throughout the data consisted of the base of asphalt reflection having a very low amplitude or disappearing altogether (Figure 2). This suggests that there is a change in the contrast of the dielectric constants between the asphalt and the base. The most likely cause for this would be the loss of oil content in the asphalt layer. If the asphalt became stripped then the contrast in dielectric constant between the asphalt layer and a gravel base might be diminished or disappear altogether depending on the severity of the stripping. It is expected that any asphalt layer with a normal amount of oil present will create a strong reflection with a clean gravel base. It is unclear though, how stripped asphalt would affect the GPR data when a clay base is present.

A second type of anomaly found was the presence of diffraction points at depth (Figure 3). Above these points, the base of asphalt reflection is generally offset from the

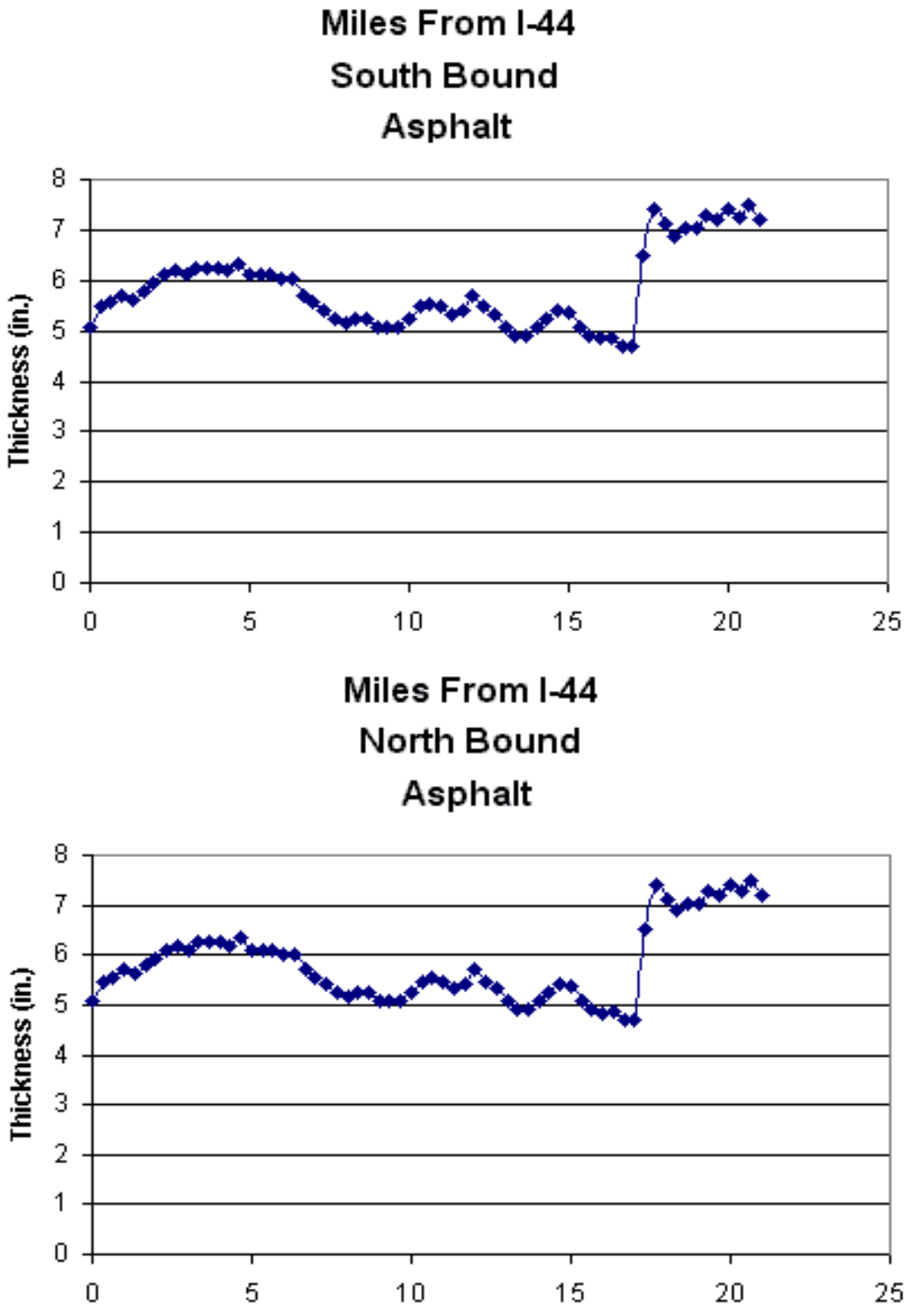

Figure 1. Pavement thickness plots from Routes T and M after Phase I study.

surrounding area. This suggests that the diffractions are most likely some type of utility that was installed after the road was paved and the asphalt layer used to fill in the trench is not the same thickness as the surrounding area.

A third type of anomaly found was associated with areas where a reflector dips down from the base of asphalt reflection and then meets back up with the base of asphalt reflection a short distance later (Figure 4). It is thought that these features may be caused by topography. They may occur in areas where there were topographic lows before the road was constructed and they were filled in before the road was built. These features show a relatively normal base of asphalt reflection, but also show a much deeper third reflection and sometimes other structure is present in the GPR data between this deep reflection and the base of asphalt reflection.

A fourth type of anomaly found was related to sections of data that exhibit a very noisy character (Figure 5). These areas usually occur for short distances and seem to affect the entire length of the scan in a random pattern. This noise is thought to be caused by cell phones, which operate on some of the same frequencies that is recorded when collecting GPR data.

The fifth type of anomaly found was an apparent “washout” feature occurring as very localized increases in layer thickness (Figure 6). Initial interpretation was that these anomalies were caused by increased water content.

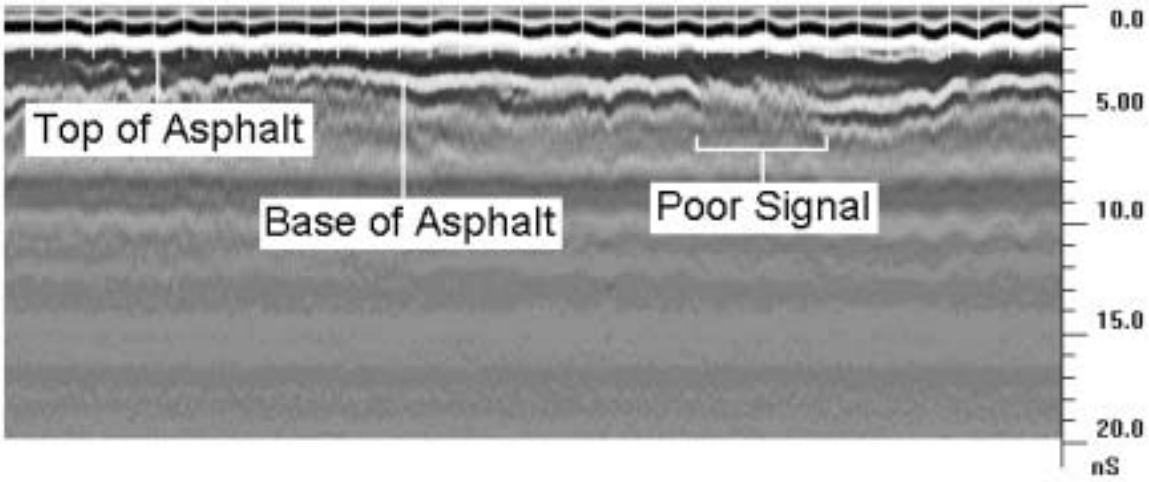

Figure 2. An example of a weak reflection from the base of asphalt. Scale: 1in=76 ft (2 cm=18 m)

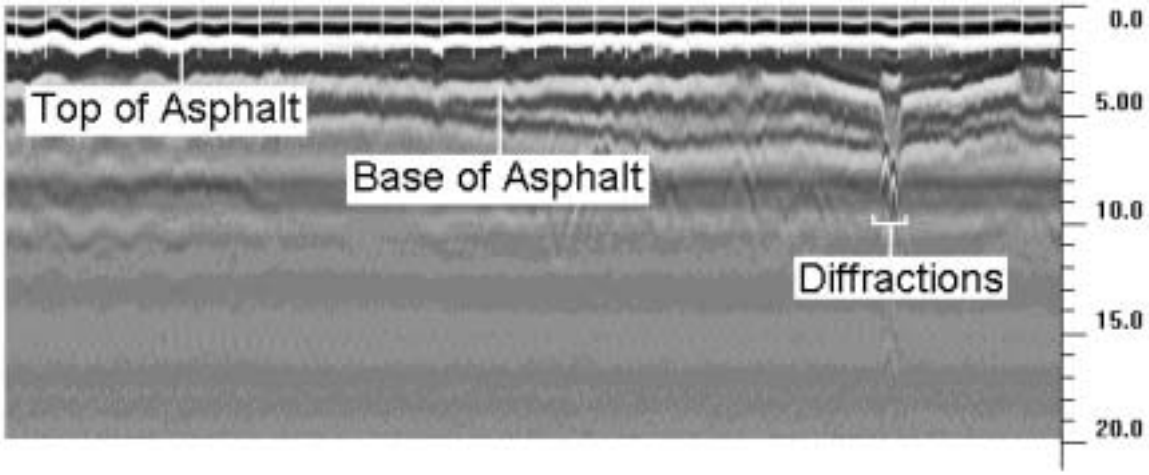

Figure 3. An example of diffractions below the base of asphalt. Scale: 1in=76 ft (2 cm=18 m)

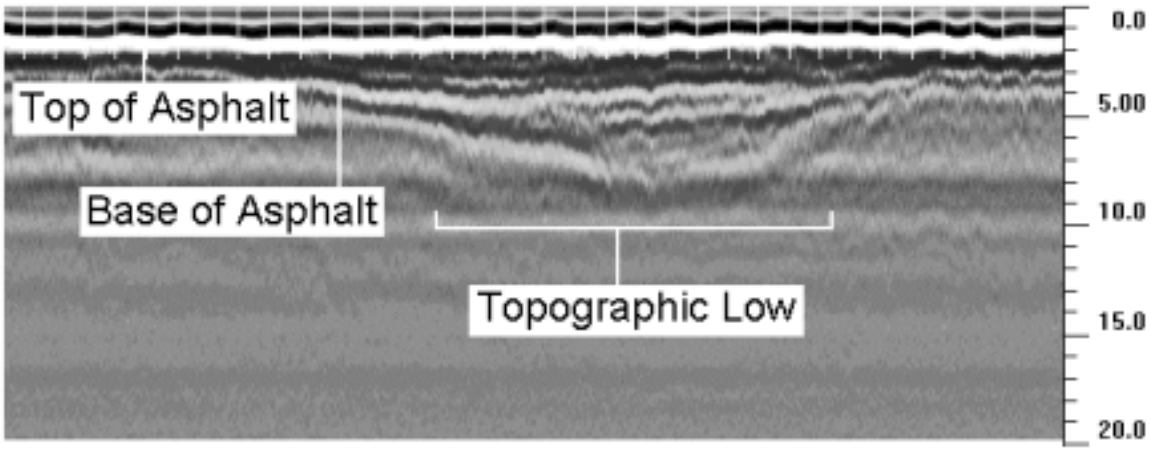

Figure 4. An example of plunging reflector, thought to be related to topographic lows prior to roadway construction. Scale: 1in=76 ft (2 cm=18 m)

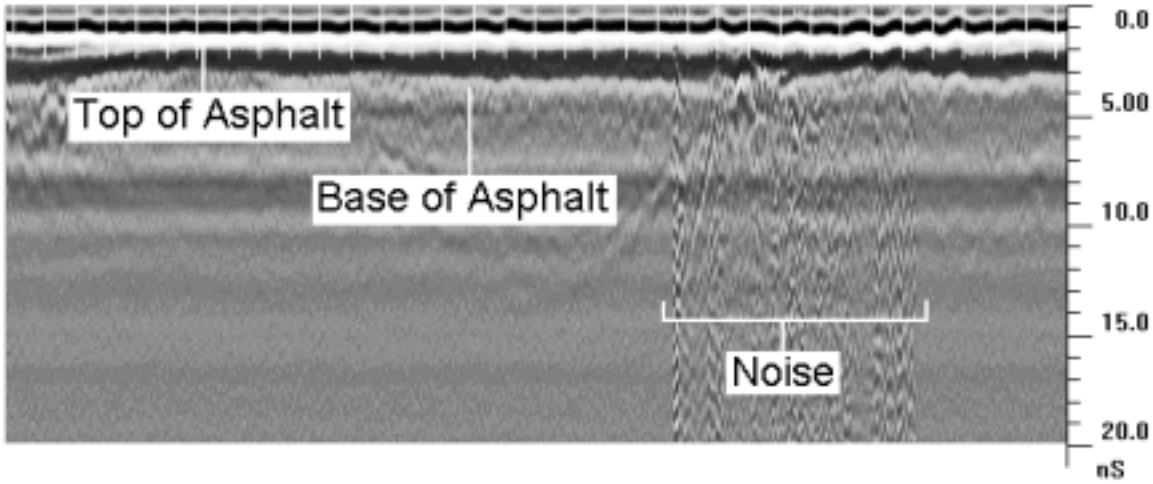

Figure 5. An example of signal that displays a noisy character. Scale: 1in=76 ft (2 cm=18 m)

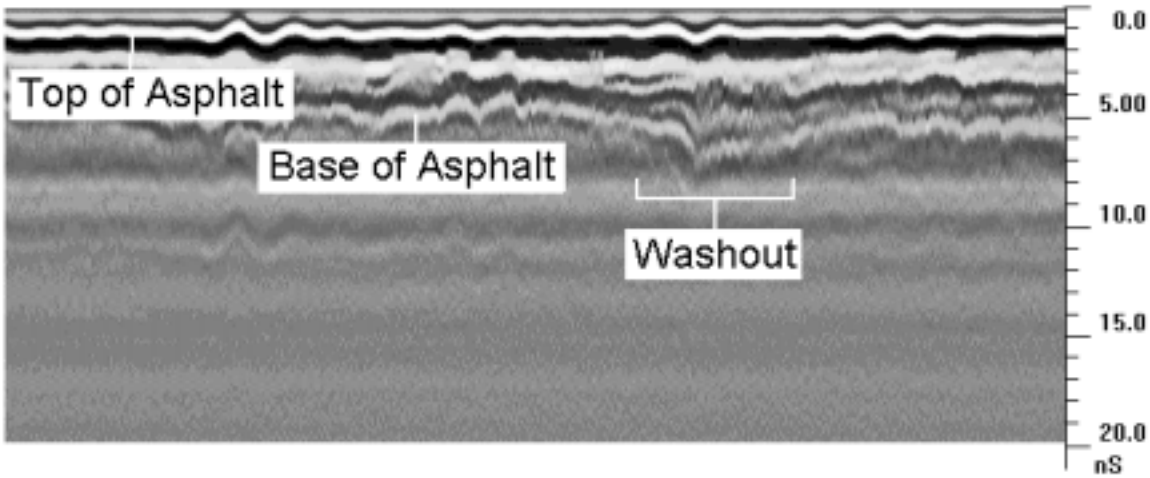

Figure 6. An example of an apparent "washout" feature. Scale: 1in=76 ft (2 cm=18 m)

PHASE II SURVEY OVERVIEW

Data for Phase II was collected in April 2000 in areas along the southbound lane associated with anomalies in the radar record determined in Phase I. In the first day of Phase II, seventy areas were resurveyed and 6 of these chosen for coring. Two days were then spent collecting 15 cores associated with the 6 areas (Table 2).

Table 2

Area number	Miles from I44	Type of anomaly studied
1	10.9-11.1	weak reflection
2	11.1-11.2	weak reflection
3	11.9-12.1	change in reflection width
4	18.5-18.6	very localized depression
5	19.1-19.25	topographic low
5	19.1-19.25	very localized depression
6	19.4-19.5	weak reflection

Ground penetrating radar (GPR) surveys have been performed over 42 miles of secondary highways to determine the thickness of the asphalt pavement, which isn't known for many of theses pavement sections, and also to determine if indications of potential maintenance problem areas could be identified. Results of this work suggest that GPR will yield good estimates of pavement thickness by determining an average dielectric constant from a minimum amount of cores. It also established a range of 4 -7 as the dielectric constant for this type of AC pavement. It was also determined by correlation of GPR data and coring that anomalous areas could be characterized, especially to recognize pavement where the asphaltic cement was stripping from the aggregate. This study demonstrates GPR would be an effective tool to inventory the structure of MoDOT's secondary road system to provide good preventative maintenance data.

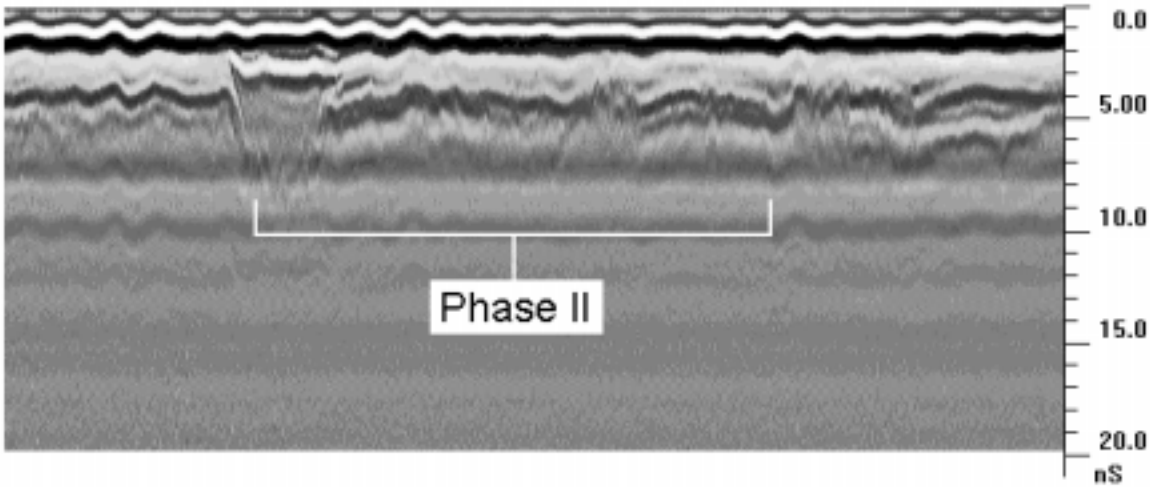

Figure 7a. An example of an apparent “washout” feature. Scale: 1in=76 ft (2 cm=18 m)

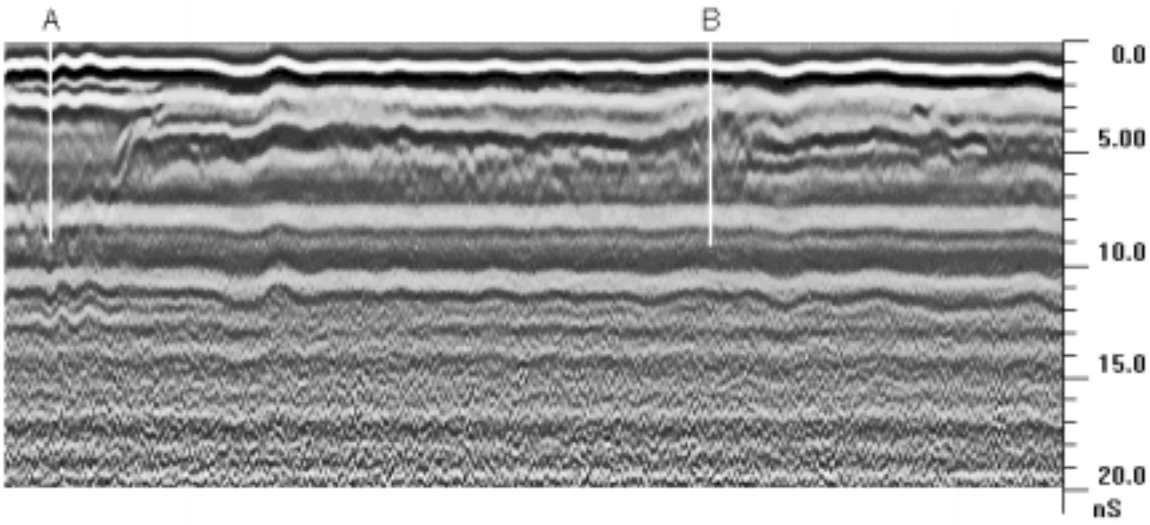

Figure 7b. Data collected during Phase II over area 1 with core locations indicated. Cores were drilled to find a relationship between stripped asphalt and weak reflections at the base of asphalt. Scale: 1in=38 ft (2 cm=9 m)

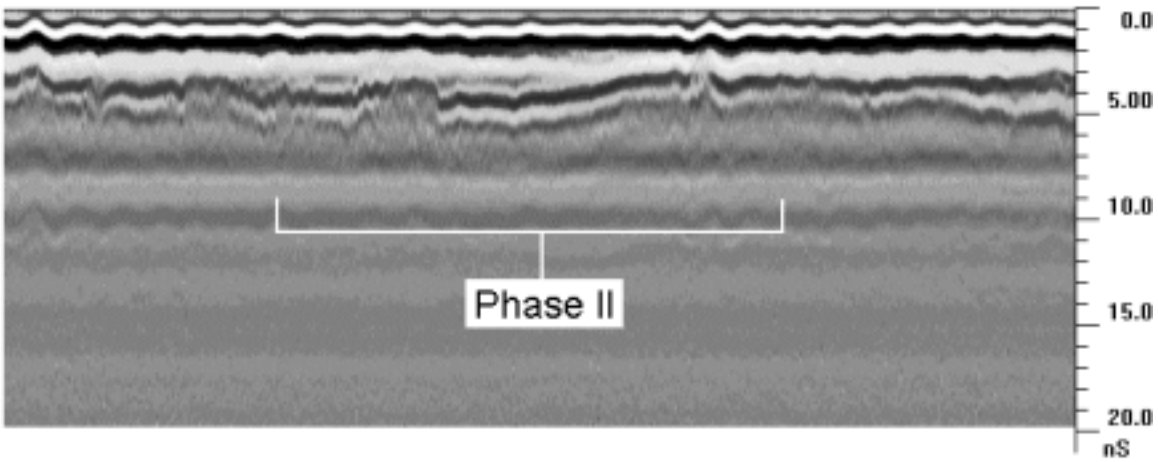

Figure 8a. Data collected during Phase I over area 1. Scale: 1in=76 ft (2 cm=18 m)

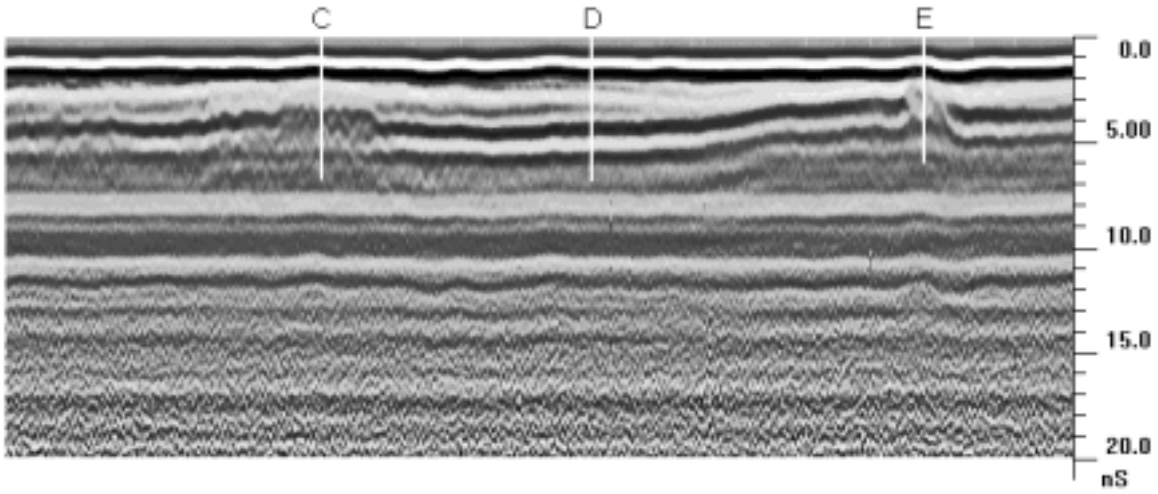

Figure 8b. Data collected during Phase II over area 1 with core locations indicated. Cores were drilled to find a relationship between stripped asphalt and weak reflections at the base of asphalt. Scale: 1in=38 ft (2 cm=9 m)

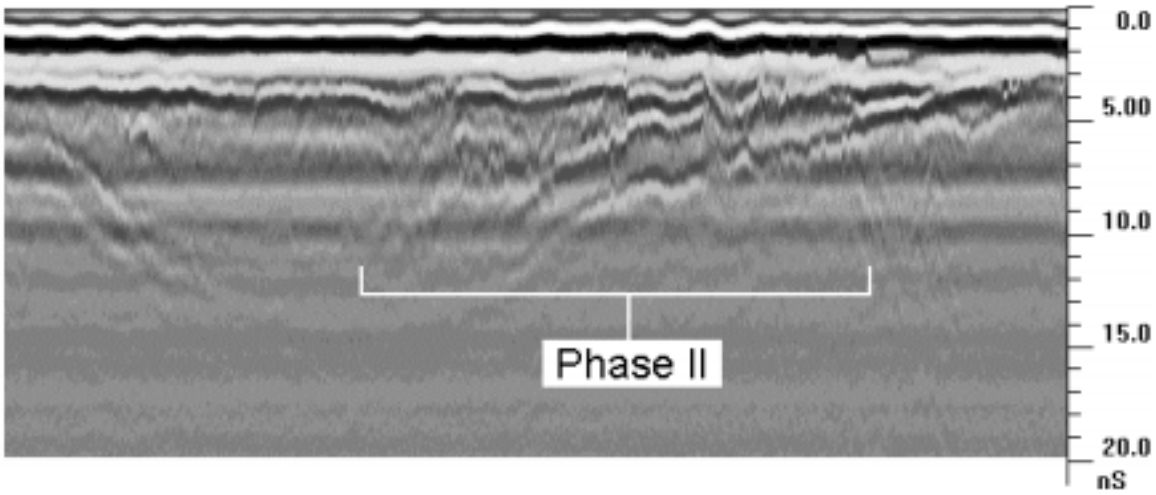

Figure 9a. Data collected during Phase I over area 6. Scale: 1in=76 ft (2 cm=18 m)

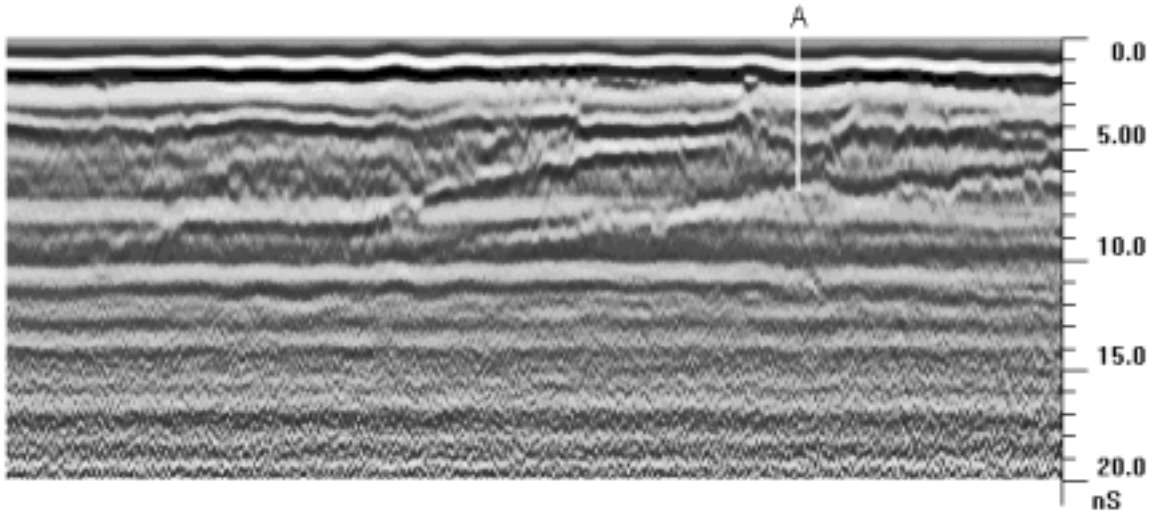

Figure 9b. Data collected during Phase II over area 6 with core locations indicated. Cores were drilled to find a relationship between stripped asphalt and weak reflections at the base of asphalt. Scale: 1in=38 ft (2 cm=9 m)

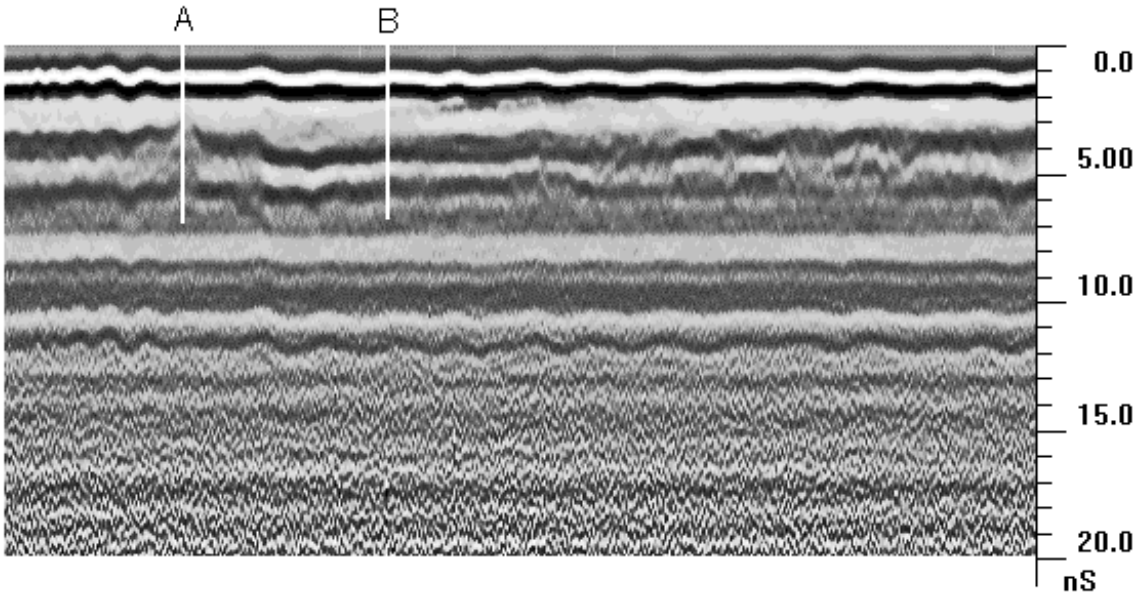

Figure 10. Data collected during Phase II over area 2 with core locations indicated. Cores were drilled to find a relationship between stripped asphalt and weak reflections at the base of asphalt. Scale: 1in=38 ft (2 cm=9 m). (Note: no Phase I data available.)

Table 3

Core location	Core thickness (in)	GPR dielectric constant
Core A, area 1	4.25	5.45
Core B, area 1	7.25 (stripped)	6.34
Core C, area 1	5 (stripped)	10.7
Core D, area 1	6	6.8
Core A, area 2	5.5	6.31
Core B, area 2	7	6.28
Core A, area 3	6.5	4.37
Core B, area 3	6.5	4.22
Core A, area 4	5.5 (stripped)	14.2
Core B, area 4	5.5	5.33
Core A, area 5	7.25	6.34
Core B, area 5	4.75 (stripped)	38.6
Core C, area 5	5.75	4.52
Core A, area 6	8 (unconsolidated)	5.72

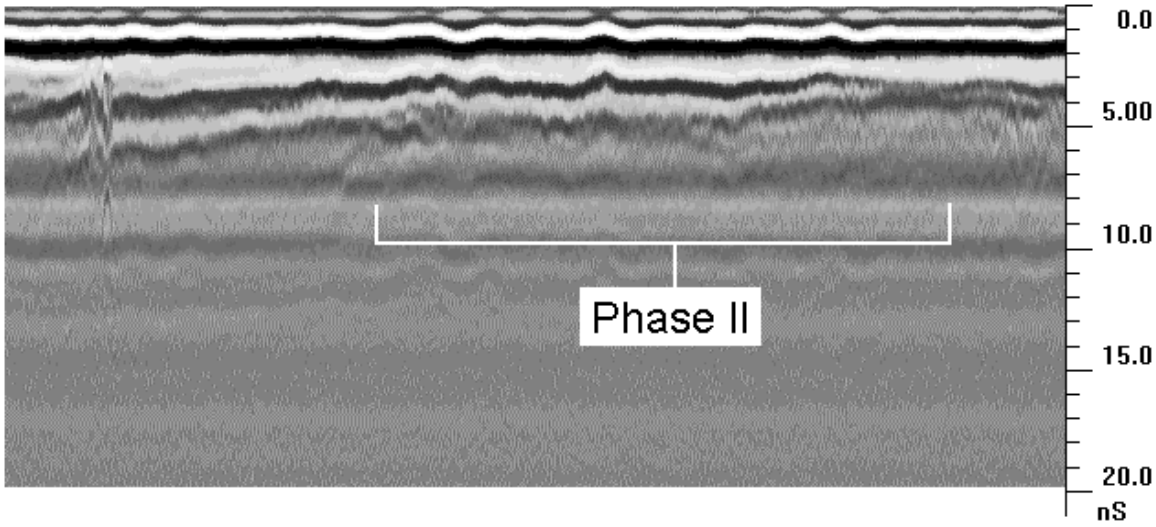

Figure 11a. Data collected during Phase I over area 3. Scale: 1in=76 ft (2 cm=18 m)

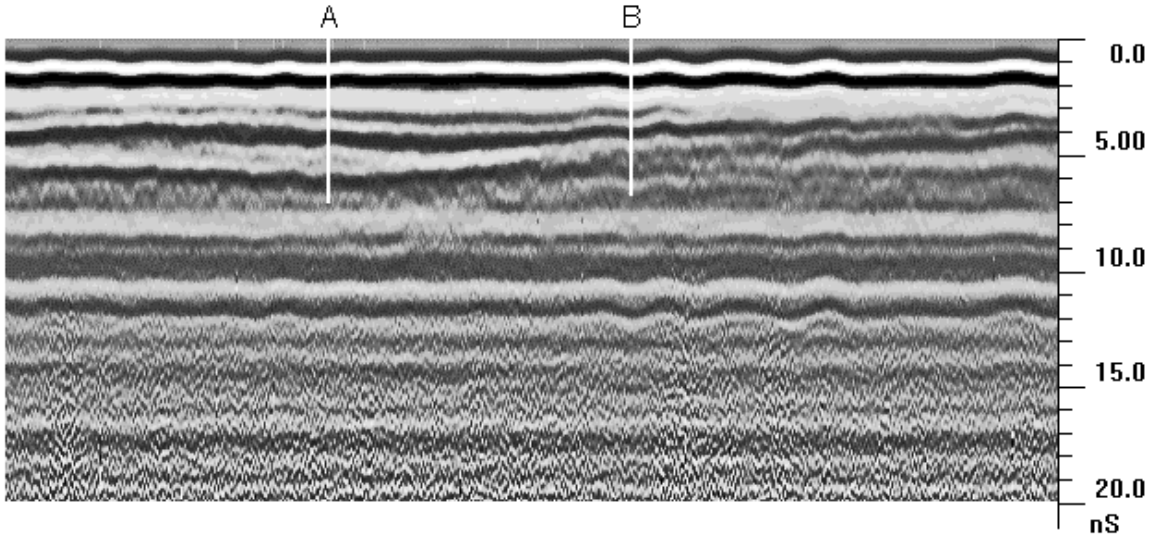

Figure 11b. Data collected during Phase II over area 3 with core locations indicated. Cores were located to determine cause of change in width of the base of asphalt reflection. Scale: 1in=38 ft (2 cm=9 m)

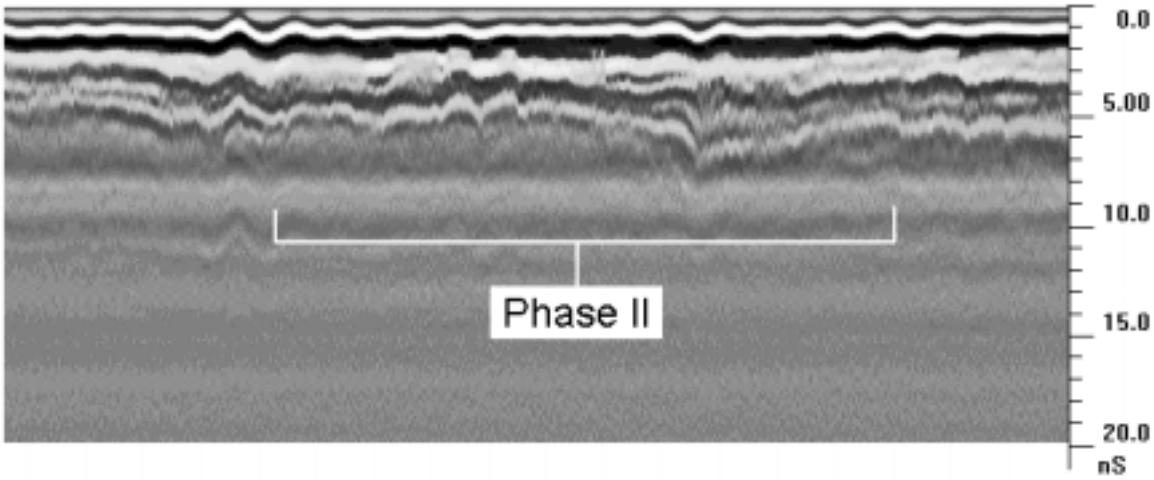

Figure 12a. Data collected during Phase I over area 4. Scale: 1in=76 ft (2 cm=18 m)

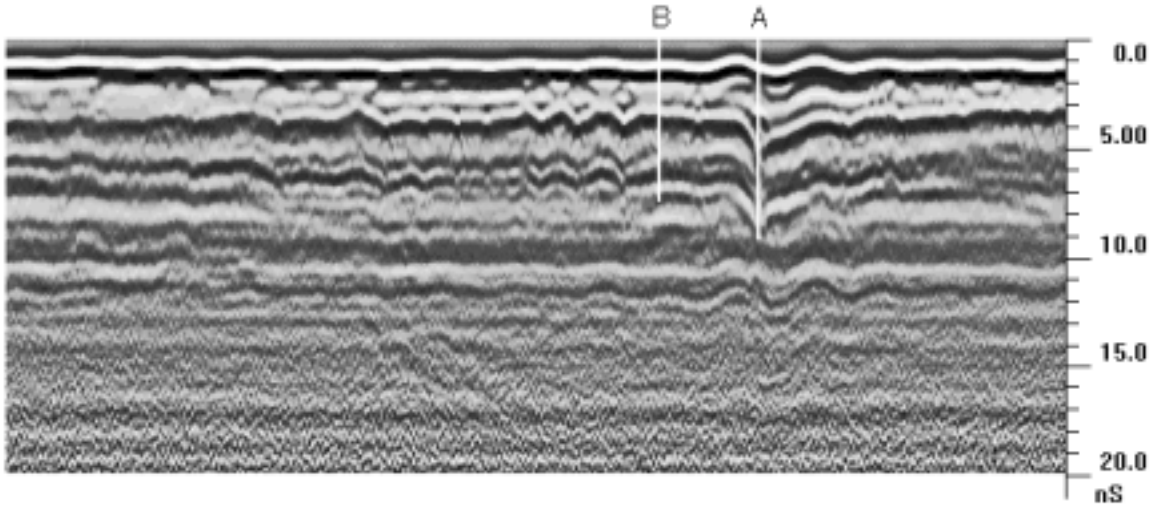

Figure 12b. Data collected during Phase II over area 4 with core locations indicated. Cores located to determine cause of localized depression in GPR reflection. Scale: 1in=38 ft (2 cm=9 m)

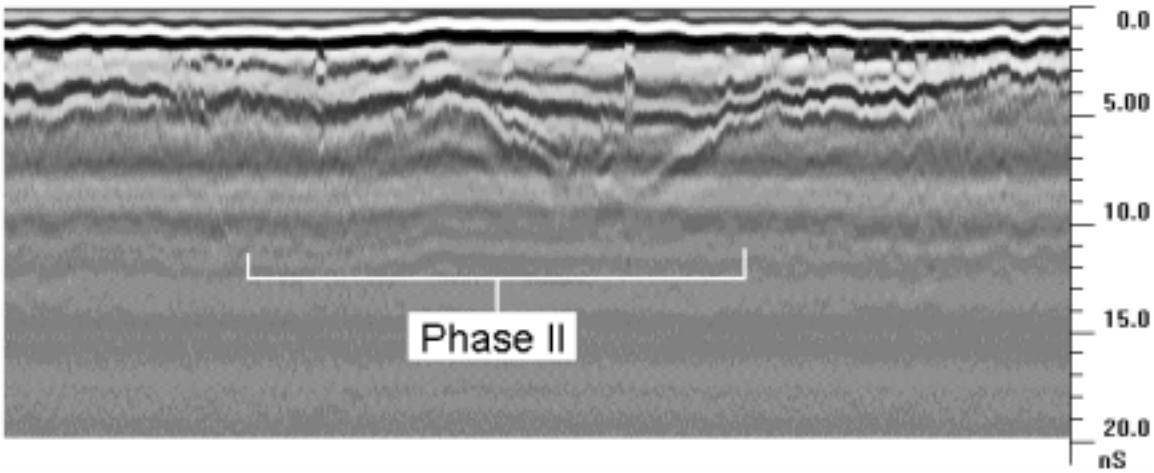

Figure 13a. Data collected during Phase I over area 5. Scale: 1in=76 ft (2 cm=18 m)

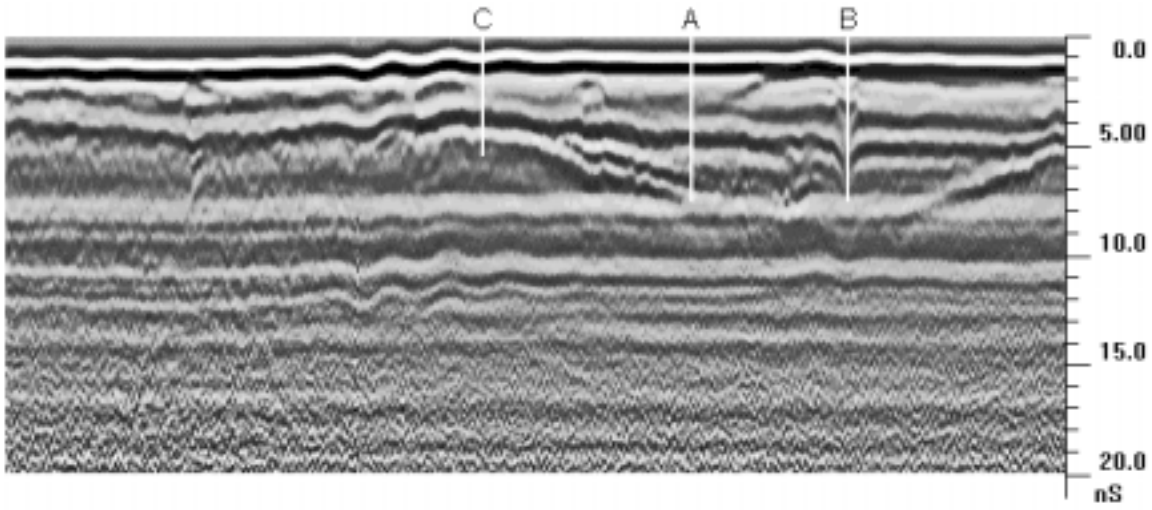

Figure 13b. Data collected during Phase II over area 5 with core location indicated. Cores located to determine cause of localized depression in GPR reflection and topographic feature. Scale: 1in=38 ft (2 cm=9 m)

DISCUSSION OF RESULTS

The average dielectric constant calculated in Phase II was 5.51, which was calculated using only the cores that contained asphalt that was in good condition. The dielectric constant determined from Phase I was 6.45, which is significantly higher than the average calculated in Phase II. In Phase II it was found that the dielectric could vary greatly at this site. The available core data suggests a range for the dielectric constant from 4 to 7 over this site. This range of dielectric constants is likely caused by variances in the asphalt content and condition. It would be impossible to get enough control in order to get accurate dielectric constants for pavement thickness data over the entire site because it varies even over short distances. The most reasonable method for calculating pavement thickness in an area such as Routes T and M would be to take the average dielectric constant calculated in Phase II and revise the pavement thickness data to take into account as much core control as possible. Appendix A has the revised pavement thickness plots using a dielectric constant of 5.51. The correction is not dramatic.

Since the base of the T & M roadways is gravel and sand in most areas, it was hypothesized that if the asphalt was stripped of its oil content, the base of the asphalt reflection in the GPR data would be very weak if present at all. The core information (Table 3) indicated that the asphalt was indeed stripped when the radar reflection amplitude was low at one of the three tested locations (area 1). Another cause for the weak reflection in the radar was unconsolidated asphalt (area 6). At area 2, the weak reflection correlated with thinner asphalt, but no stripping was evident and the asphalt was not unconsolidated.

In both areas 4 and 5, the asphalt was stripped in association with the localized depressions in the radar reflection signal. The core hole at both areas 4 and 5 was several inches deeper than the recovered core itself. In addition, the width of the core holes expanded two or three times in size below the base of the consolidated asphalt. The gravel base at each of these sites was found to be very loosely packed with a very high porosity. Dielectric constants were calculated from core data over both anomalies and the values of 14.2 and 38.6 were much larger than would be expected from asphalt. The stripping and unconsolidated nature of the asphalt in these cores suggests that there could have been a high water content in the asphalt that would result in very high dielectric constants and increased radar travel time. It was impossible to get an accurate measurement of water content of the base material or the asphalt where the cores were drilled because the drill injects water into the hole in order to cool the bit.

Two other types of anomalies in the Routes T and M site data was drilled with inconclusive results. The first of these was the presence of a deeper, dipping third reflection that was thought to be caused by an in-filled topographic low during roadway construction (area 5). Unfortunately the drill used to obtain core samples for this study was inadequate for drilling deep enough to determine the cause of the third reflection directly. One of the cores obtained in an area where the third reflector is not present indicates a clay base. Two cores obtained in areas where the third reflector is present however, indicated that the base consisted of sand and gravel. This might suggest that the third reflector, which separates from the base of asphalt and then rejoins it several feet later, is the result of a sand lens in the surrounding clay base. Without a direct confirmation of this interface from core control however, this is only speculation.

The other anomaly that provided inconclusive results consisted of the period of the reflected radar pulse associated with the base of asphalt reflection changing substantially over a short distance (area 3). The core in the area where the reflection had a longer period showed that the base was clay and the asphalt was not stripped but it was unconsolidated. The core in the area where the reflection had a shorter period showed that there was a thin sand and gravel layer between the clay and asphalt. It also showed that the asphalt layer was slightly stripped but was mostly intact. This suggests that areas where the asphalt is unconsolidated may exhibit a base of asphalt reflection that has a longer period than an area where the asphalt is in good condition. In the areas where the asphalt is unconsolidated, the reflection interface may be less distinct. This may result in the reflected energy from this interface consisting of only lower frequency energy. The areas where the asphalt is in good condition however, should exhibit a sharper boundary and result in a reflection that consists of more high frequency energy giving the reflection a shorter period. Although this could explain the phenomena, more work would need to be done in order to determine any relationship more thoroughly.

CONCLUSIONS

Radar data collected along Routes T and M were clear and offered accurate mapping of pavement thickness. The detailed assessment of the radar signals suggest that stripping of the oil in the asphalt or an unconsolidated asphalt layer will produce an anomaly in the radar data. Either a low amplitude reflection from the base of asphalt or a localized depression (increased travel time) of the reflection is associated with stripping and un-consolidation of the asphalt. The latter seems to be the more effective radar anomaly to indicate problems, as the increased travel time is most likely associated with an increase in water content which would be the cause of the stripping of the asphalt. It may be that an area where the asphalt is unconsolidated could affect the period of the radar reflection energy by eliminating some of the high frequency content. The cause of the topographic anomalies where not directly determined by core data but the data suggests that they were the result of sand lenses in a surrounding clay base layer, probably related to in-fill during the construction of Routes T and M.

The one disadvantage to using GPR in pavement studies is that the types of anomalies encountered and the signal character can vary between road types and geologic (base and sub-base) setting. Ideally, roadways would be grouped by these two characteristics and test data such as that collected in this study could be acquired for each type of road and geologic setting to help form standards for determining pavement thickness, identifying common radar anomalies, and the cause of these anomalies.

APPENDIX A

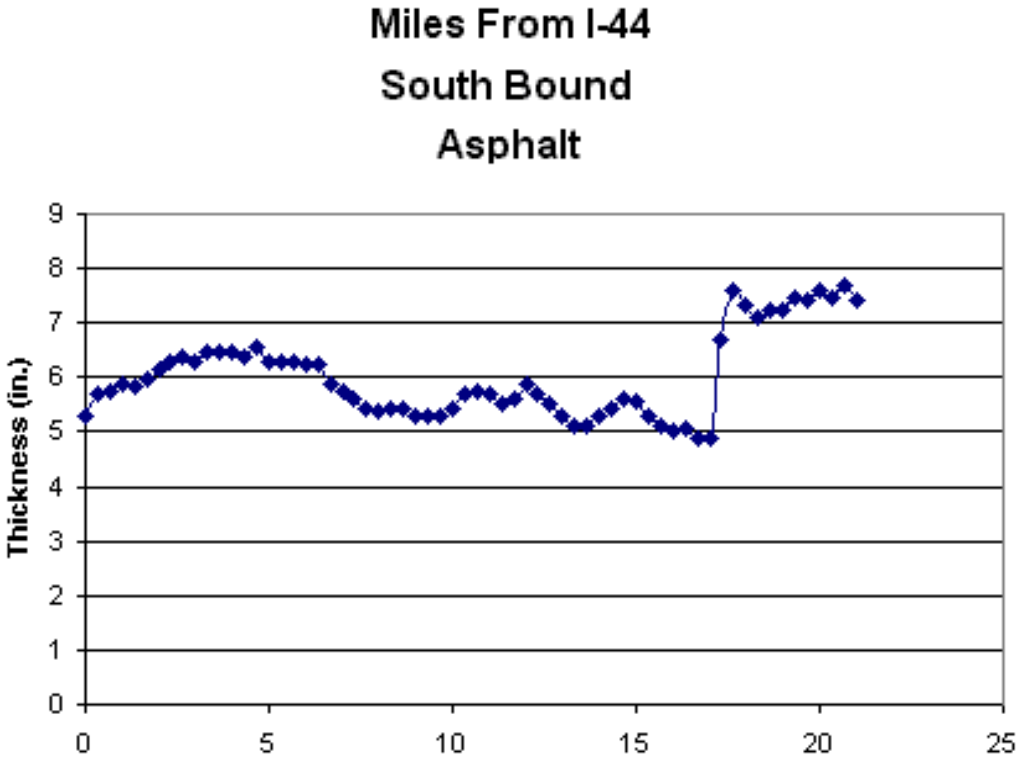

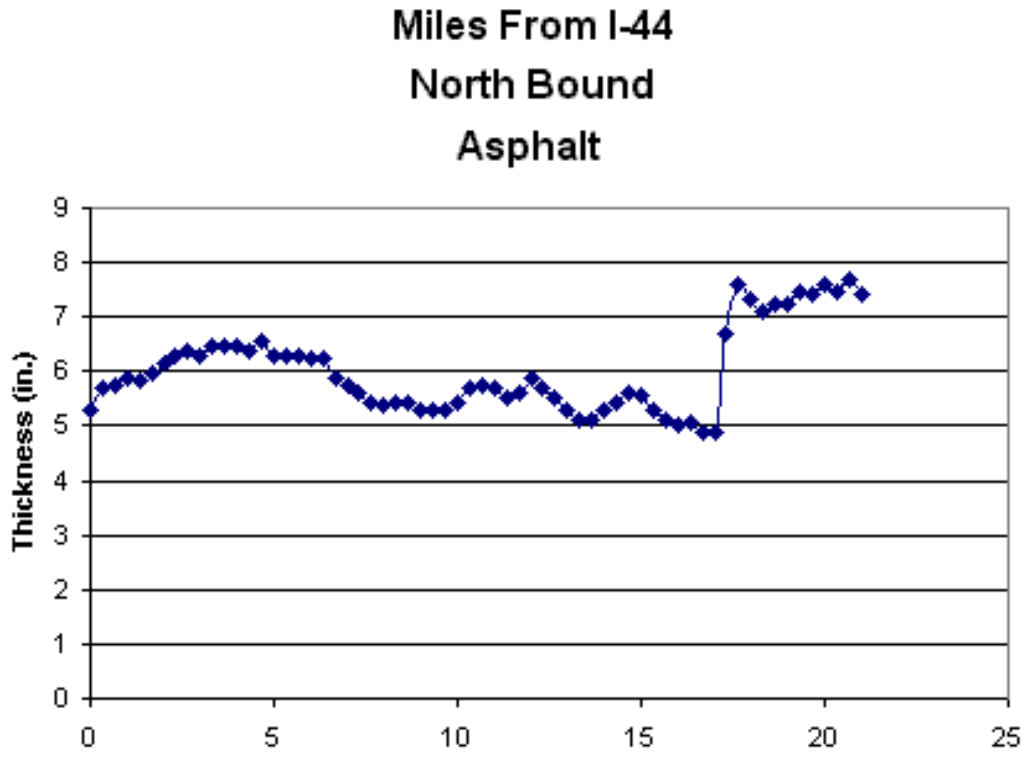

Appendix A. Pavement Thickness plots from Routes T and M after Phase II study.

APPENDIX B

Wimsatt, Scullion, Ragsdale, and Servos

NORMAL DIELECTRIC CONSTANT VALUES FOR VARIOUS PAVEMENT LAYERS

Pavement Type	Dielectric Value Range
Asphalt Concrete Pavement (Normal Aggregate)	5.0 – 6.5
Asphalt Concrete Pavement (Lightweight Aggregate)	3.5 – 4.5
Flexible Base (Granular Base)	7.0 – 10.0
Cement Treated Base	6.0 –8.0
Concrete Pavement	7.0 – 9.0

Dielectric constants greater than those listed indicate the presence of moisture in the system.
Dielectric constants greater than 16 indicate layers saturated with water.
Dielectric constants less than those listed indicate the presence of excessive air voids.
Water has a dielectric constant of 81.